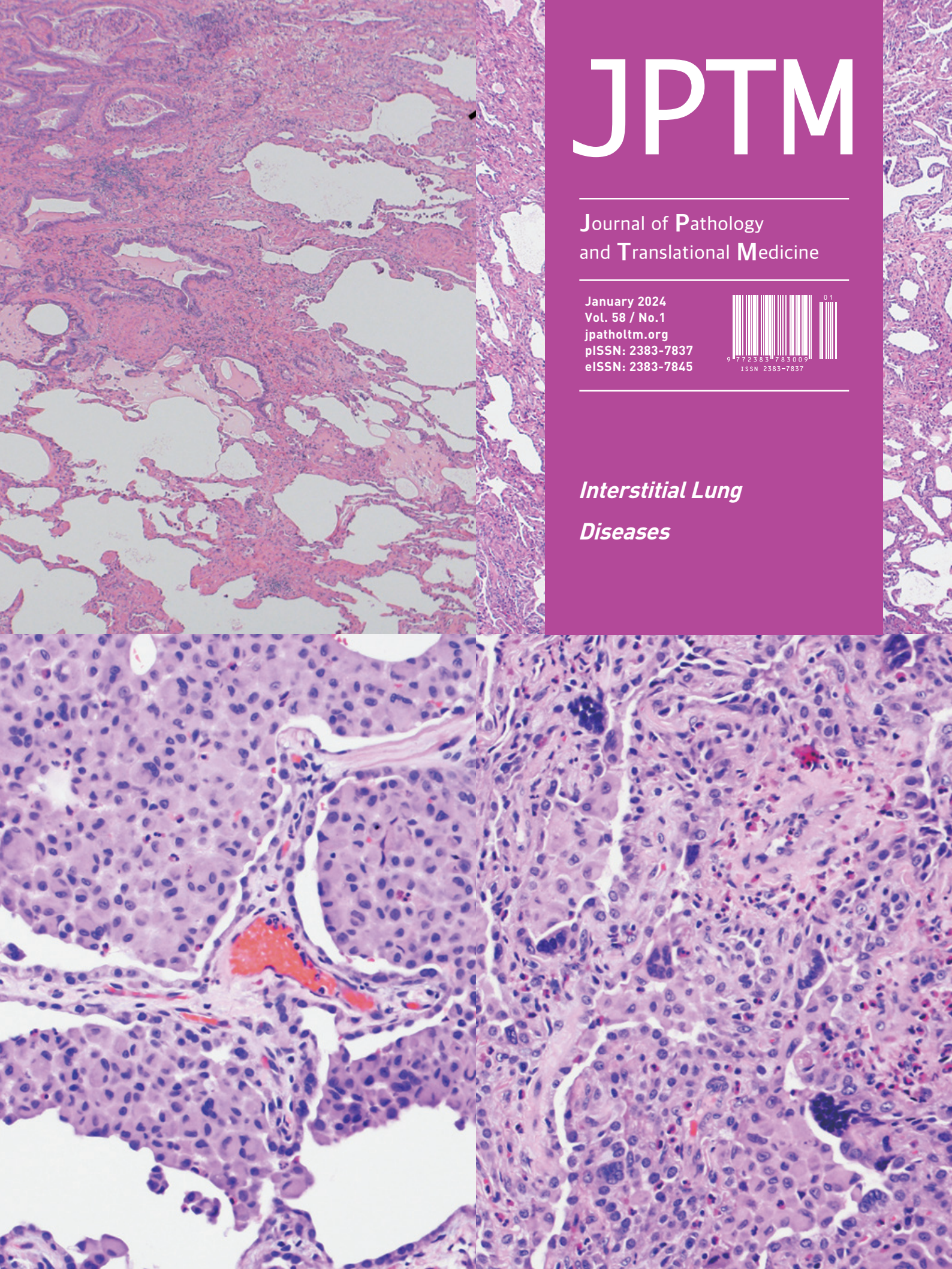

JPTM

Journal of Pathology and Translational Medicine

January 2024
Vol. 58 / No.1
jpatholtm.org
pISSN: 2383-7837
eISSN: 2383-7845

Interstitial Lung Diseases

Journal of Pathology and Translational Medicine

Volume 58 • Number 1 • January 2024 (bimonthly)
Published since 1967
Printed on 11 January 2024 Published on 15 January 2024

J Pathol Transl Med
pISSN: 2383-7837
eISSN: 2383-7845

Aims & Scope

The Journal of Pathology and Translational Medicine is an open venue for the rapid publication of major achievements in various fields of pathology, cytopathology, and biomedical and translational research. The Journal aims to share new insights into the molecular and cellular mechanisms of human diseases and to report major advances in both experimental and clinical medicine, with a particular emphasis on translational research. The investigations of human cells and tissues using high-dimensional biology techniques such as genomics and proteomics will be given a high priority. Articles on stem cell biology are also welcome. The categories of manuscript include original articles, review and perspective articles, case studies, brief case reports, and letters to the editor.

Subscription Information

To subscribe to this journal, please contact the Korean Society of Pathologists/the Korean Society for Cytopathology. Full text PDF files are also available at the official website (https://jpatholtm.org). *Journal of Pathology and Translational Medicine* is indexed by Emerging Sources Citation Index (ESCI), PubMed, PubMed Central, Scopus, KoreaMed, KoMCI, WPRIM, Directory of Open Access Journals (DOAJ), and CrossRef. Circulation number per issue is 50.

Contact the Korean Society of Pathologists/the Korean Society for Cytopathology

Publishers: Choi, Joon Hyuk, MD, Lee, Seung-Sook, MD
Editors-in-Chief: Jung, Chan Kwon, MD, Park, So Yeon, MD
Published by the Korean Society of Pathologists/the Korean Society for Cytopathology

Editorial Office
Room 1209 Gwanghwamun Officia, 92 Saemunan-ro, Jongno-gu, Seoul 03186, Korea
Tel: +82-2-795-3094 Fax: +82-2-790-6635 E-mail: office@jpatholtm.org

#1508 Renaissancetower, 14 Mallijae-ro, Mapo-gu, Seoul 04195, Korea
Tel: +82-2-593-6943 Fax: +82-2-593-6944 E-mail: office@jpatholtm.org

Printed by iMiS Company Co., Ltd. (JMC)
Jungang Bldg. 18-8 Wonhyo-ro 89-gil, Yongsan-gu, Seoul 04314, Korea
Tel: +82-2-717-5511 Fax: +82-2-717-5515 E-mail: ml@smileml.com

Manuscript Editing by InfoLumi Co.
210-202, 421 Pangyo-ro, Bundang-gu, Seongnam 13522, Korea
Tel: +82-70-8839-8800 E-mail: infolumi.chang@gmail.com

Front cover image: Usual interstital pneumonia, nonspecific interstitial pneumonia, desquamative interstitial pneumonia, and giant cell interstitial pneumonia (p2).

This work was supported by the Korean Federation of Science and Technology Societies Grant funded by the Korean Government (Ministry of Education).

Journal of Pathology and Translational Medicine

J Pathol Transl Med
pISSN: 2383-7837
eISSN: 2383-7845

Volume 58, Number 1, January 2024

CONTENTS

JPTM
Journal of Pathology and Translational Medicine 2024; 58: 1-11
https://doi.org/10.4132/jptm.2023.11.17

REVIEW

Diagnosis of interstitial lung diseases: from Averill A. Liebow to artificial intelligence

Eunhee S. Yi[1], Paul Wawryko[2], Jay H. Ryu[3]

[1]Division of Anatomic Pathology, Mayo Clinic Rochester, Rochester, MN;
[2]Division of Anatomic Pathology, Mayo Clinic Arizona, Arizona, FL;
[3]Division of Pulmonary and Critical Medicine, Mayo Clinic Rochester, Rochester, MN, USA

Histopathologic criteria of usual interstitial pneumonia (UIP)/idiopathic pulmonary fibrosis (IPF) were defined over the years and endorsed by leading organizations decades after Dr. Averill A. Liebow first coined the term UIP in the 1960s as a distinct pathologic pattern of fibrotic interstitial lung disease. Novel technology and recent research on interstitial lung diseases with genetic component shed light on molecular pathogenesis of UIP/IPF. Two antifibrotic agents introduced in the mid-2010s opened a new era of therapeutic approaches to UIP/IPF, albeit contentious issues regarding their efficacy, side effects, and costs. Recently, the concept of progressive pulmonary fibrosis was introduced to acknowledge additional types of progressive fibrosing interstitial lung diseases with the clinical and pathologic phenotypes comparable to those of UIP/IPF. Likewise, some authors have proposed a paradigm shift by considering UIP as a stand-alone diagnostic entity to encompass other fibrosing interstitial lung diseases that manifest a relentless progression as in IPF. These trends signal a pendulum moving toward the tendency of lumping diagnoses, which poses a risk of obscuring potentially important information crucial to both clinical and research purposes. Recent advances in whole slide imaging for digital pathology and artificial intelligence technology could offer an unprecedented opportunity to enhance histopathologic evaluation of interstitial lung diseases. However, current clinical practice trends of moving away from surgical lung biopsies in interstitial lung disease patients may become a limiting factor in this endeavor as it would be difficult to build a large histopathologic database with correlative clinical data required for artificial intelligence models.

Key Words: Usual interstitial pneumonia; Idiopathic pulmonary fibrosis; Progressive pulmonary fibrosis; Familial pulmonary fibrosis; Digital pathology; Artificial intelligence

Received: October 23, 2023 **Revised:** November 6, 2023 **Accepted:** November 17, 2023
Corresponding Author: Eunhee S. Yi, MD, Division of Anatomic Pathology, Mayo Clinic Rochester, 200 First Street SW, Rochester, MN 55905, USA
Tel: +1-507-284-2656, Fax: +1-507-266-3771, E-mail: Yi.joanne@mayo.edu

Liebow and Carrington [1] introduced the diagnosis of usual interstitial pneumonia (UIP) over 50 years ago as a type of interstitial pneumonias. The word "usual" in UIP was used because it was the most common and usual type among interstitial pneumonias. In addition to UIP, desquamative interstitial pneumonia (DIP), bronchiolitis obliterans with interstitial pneumonia (BIP), lymphoid interstitial pneumonia (LIP), and giant cell interstitial pneumonia (GIP) were included in their classification of interstitial pneumonias [1]. While UIP, DIP, and LIP are still acknowledged in the current classification of interstitial pneumonias, BIP and GIP have been excluded; a subset of BIP might correspond to organizing pneumonia (OP) and GIP is now regarded as hard metal pneumoconiosis. Characteristic histopathologic features of various types of interstitial lung diseases (ILDs) are illustrated in Fig. 1A–D. Nearly three decades after the term UIP was first introduced, Katzenstein and Myers [2] clarified cardinal histologic features of UIP that became the current histopathologic criteria for diagnosing UIP.

The 2002 American Thoracic Society (ATS)/European Respiratory Society (ERS) statement summarized the consensus from the first international meeting on the diagnosis and treatment of idiopathic interstitial pneumonias (IIPs) [3,4]. This statement established a basic framework of the contemporary classification scheme of IIPs: UIP, nonspecific interstitial pneumonia (NSIP), DIP, OP, acute interstitial pneumonia (AIP), and LIP [4]. This nomenclature for IIP became applicable to other ILDs as patterns,

pISSN 2383-7837
eISSN 2383-7845

which facilitated a clearer communication in the non-idiopathic ILDs with underlying conditions or identifiable causes (such as connective tissue disease [CTD] and hypersensitivity pneumonitis [HP] or other exposure–related conditions, etc.). Some significant modifications have been made over the ensuing years in a few subsequent consensus statements by ATS and other international organizations [5-7]. Novel technologies including omics at different levels (genetic, epigenetic, transcriptional, translational, and metabolic, etc.) advanced the deep understanding in pathogenesis of ILDs and expedited the development of several effective antifibrotic medications that have been U.S. Food and Drug Administration–approved or on active clinical trials.

Pathologic examination has been the gold standard to classify ILDs until high-resolution computed tomography (HRCT) became an acceptable method after the second ATS/ERS statement in 2013, which led to a significant decrease in the frequency of lung biopsies for diagnosing ILDs [5]. Currently, most cases characteristic for UIP on chest HRCT no longer undergo lung biopsies (Fig. 2). Only atypical and complex ones are subject to lung biopsies, posing great challenges to pathologists. Surgical lung biopsy has been the main approach but transbronchial lung cryobiopsy was accepted in the 2022 practice guidelines by ATS/ERS/Japanese Respiratory Society (JRS)/Latin American Thoracic Association (ALAT) as a conditional alternative in the centers with appropriate expertise [7]. Genetic profiling of transbronchial biopsy specimens has been introduced to classify ILDs and it completely bypasses morphologic evaluation [8,9]. No recommendation was made in 2022 guidelines either for or against this

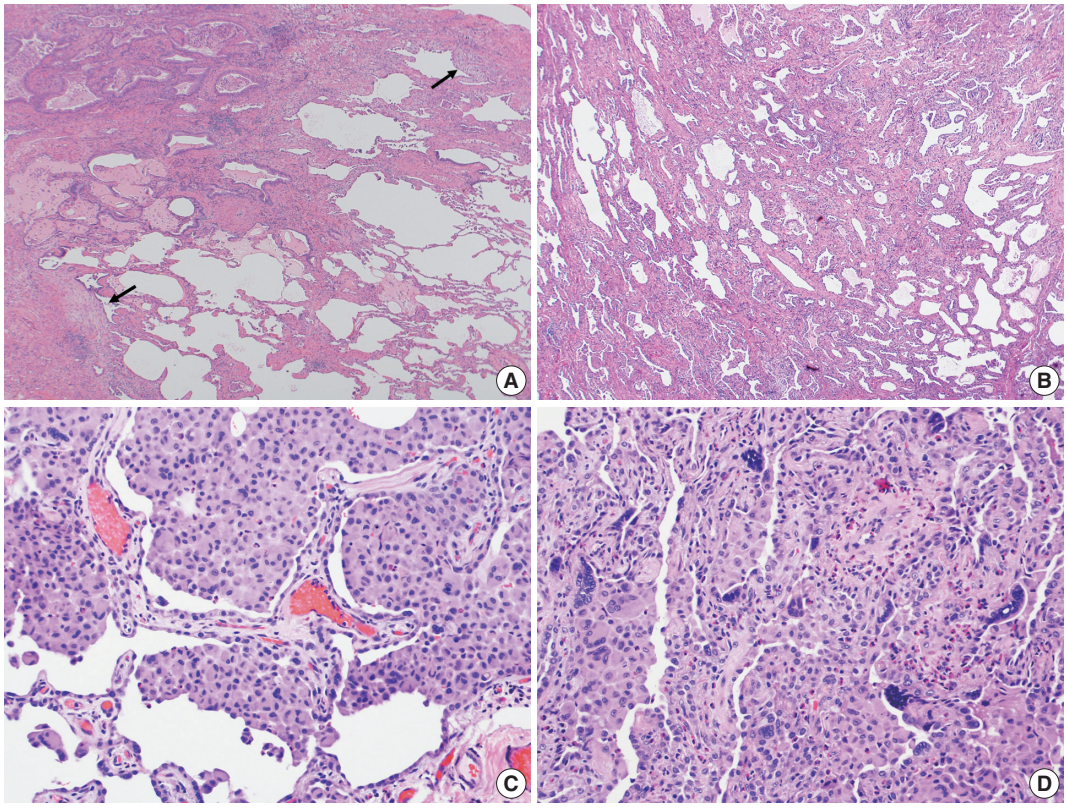

Fig. 1. (A) Usual interstitial pneumonia (UIP), the prototype of interstitial lung disease, showing patchy interstitial fibrosis with subpleural accentuation, marked architectural distortion of alveolar architecture with scarring and microscopic honeycomb changes, and temporal heterogeneity of fibrosis evidenced by scattered fibroblastic foci with dome-shaped myofibroblastic/fibroblastic proliferation over scarred areas (arrows), which likely implies an ongoing acute lung injury in already scarred lung tissue causing progressive clinical course. (B) Nonspecific interstitial pneumonia (NSIP) shows diffuse and uniform fibrous interstitial thickening. In contrast to UIP, NSIP shows relatively well-preserved alveolar architecture without honeycomb changes or fibroblastic foci, which likely explains a more favorable prognosis of NSIP than UIP. (C) Desquamative interstitial pneumonia (DIP) characterized by diffuse collection of pigmented macrophages in the alveolar spaces with mild to moderate interstitial fibrosis. DIP in the original classification by Dr. Liebow is included in the current American Thoracic Society classification. (D) Giant cell interstitial pneumonia (GIP) showing many scattered multinucleated giant cells in the alveolar spaces or septa. GIP was included in the Dr. Liebow's original classification of interstitial lung diseases but dropped in the current idiopathic interstitial pneumonia classification as GIP is now primarily regarded as a hard metal pneumoconiosis (e.g., cobalt).

https://doi.org/10.4132/jptm.2023.11.17

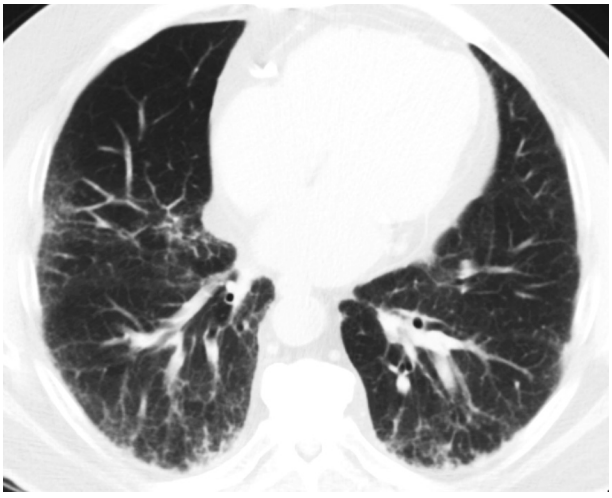

Fig. 2. An axial view of high-resolution computed tomography demonstrates a portion of lower lung fields with classific findings of usual interstitial pneumonia characterized by peripherally accentuated reticular densities and honeycomb changes.

genomic classifier testing, due to the lack of consensus among the committee members [7].

Recent advances in whole slide imaging (WSI) and artificial intelligence (AI) technology, such as deep learning (DL)–based image processing, have opened the door to quantitatively evaluate histopathologic findings. However, relative paucity of database, as compared to radiologic counterpart, is a limiting factor for widespread investigation and advancement to a higher level of interpretation beyond quantitative analysis, thus far.

Several topics that represent milestones in the field of ILD diagnosis are reviewed with emphasis on significant recent changes in concepts and trends relevant to practicing pathologists and pulmonologists.

SELECTED TOPICS

Usual interstitial pneumonia

Evolution of histopathologic criteria for UIP

The histologic classification of interstitial pneumonias evolved in a time when surgical lung biopsies were infrequently performed owing to significant morbidity associated with the surgical techniques of the day. As a result, histologic findings did not inform clinical decision-making in most patients with interstitial pneumonia. Clinicians were left to diagnose and manage patients with ILD primarily based on clinical and radiologic features; clinical concepts did not evolve in concert with the histologic classification. In this background, idiopathic pulmonary fibrosis (IPF) originated as a clinical diagnosis without established histopathologic correlates.

The original histologic description of UIP contained a wide spectrum of findings including acute lung injury in the form of what today would be considered diffuse alveolar damage, as well as chronic fibrosis and end-stage lung [2]. Although the histologic findings considered diagnostic of UIP were refined over time, established diagnostic criteria were still lacking into the 1990s with many investigators simply requiring the presence of inflammation and fibrosis in various proportions as diagnostic of UIP [3]. Many also considered even DIP to represent an early "cellular stage" of UIP [2].

In 1998, Katzenstein and Myers [2] described the crucial histologic features that were reflected in the ATS/ERS international consensus statement and established as the current histopathologic criteria of UIP [2,4]. The most recent 2022 ATS/ERS/JRS/ALAT clinical practice guideline used the same criteria including (1) patchy, dense fibrosis with architectural distortion causing destructive scarring and/or honeycombing, (2) predominantly subpleural and/or paraseptal distribution of fibrosis, (3) temporal heterogeneity of fibrosis characterized by fibroblast foci over scarred lung tissue, and (4) absence of features suggesting an alternate diagnosis (including prominent airway-centered changes, significant degree of OP, granulomas, hyaline membranes, dense lymphoid infiltrates, and marked chronic pleuritis, etc.) [4]. Different levels of confidence such as diagnostic of UIP (meeting all criteria) and probable UIP (having only some of these features) were proposed for pathologic diagnosis categories as in radiologic counterparts. This type of categorization may be useful in the clinical trial setting to recruit patients although it has not been widely applied in routine pathology practice.

In the 2013 ATS/ERS statement, the major IIPs were subdivided into three categories: chronic fibrosing interstitial pneumonias (IPF and NSIP), smoking-related interstitial pneumonias (respiratory bronchiolitis-ILD and DIP), and acute/subacute interstitial pneumonias (cryptogenic OP and AIP) [5]. The classification also includes rare IIPs (idiopathic LIP and idiopathic pleuroparenchymal fibroelastosis) and unclassifiable IIP. Each of the IIPs has an associated radiologic and/or pathologic-morphologic pattern (e.g., UIP for IPF) and is considered a "clinical-radiologic-pathologic diagnosis," emphasizing the multidisciplinary approach to diagnosis.

Recent trends of decreasing lung biopsy use

The role of surgical lung biopsy in the diagnosis of IPF has changed over time. With the original ATS statement on IPF,

surgical lung biopsy was recommended in most patients to establish the diagnosis, especially in those with atypical clinical or radiologic features for IPF [4]. The 2002 ATS/ERS IIP guidelines stated that biopsy was required for a confident diagnosis of UIP/IPF, but also noted that in more than 50% of cases of suspected IPF, the presence of typical clinical and HRCT features of UIP was sufficiently characteristic to allow a confident diagnosis without the need for surgical lung biopsy [4]. In the 2011 ATS statement of IPF, radiologic and pathologic criteria were developed to establish confidence categories for UIP (i.e. UIP pattern, probable UIP pattern, possible UIP pattern); thus, surgical lung biopsy was no longer required for histopathologic confirmation in patients with HRCT showing typical UIP pattern [6]. The only change regarding sampling since that time was the adoption of transbronchial lung cryobiopsy as an acceptable alternative to surgical lung biopsy in patients with ILD of undetermined type based on evidence that there was often diagnostic agreement between transbronchial cryobiopsy and surgical lung biopsy samples [7].

Antifibrotic therapy for patients with IPF and those with UIP due to underlying cause

Patients with IPF undergo a progressive decline in pulmonary function with eventual death from either respiratory failure or a complicating comorbidity, with a median survival of 2 to 3 years from the time of diagnosis [6]. Acute exacerbation may occur with histologic manifestions of diffuse alveolar damage or OP, though less common [10]. Based on the hypothesis that inflammation might be the underlying cause of lung injury and fibrosis, corticosteroids and other immunosuppressive agents have been tried without success. No effective pharmacologic therapy for IPF was available until the early 2010s, when two promising antifibrotic agents emerged. Randomized trials showed in disease progression and rate of forced vital capacity decline in IPF patients treated with nintedanib, a tyrosine kinase inhibitor, or pirfenidone, an inhibitor of transforming growth factor β–associated collagen synthesis [11-14]. These two medications were recommended for use in IPF patients as of the 2015 treatment guidelines [15]. Data from more recent clinical trials led to an expansion of antifibrotic therapy to other types of fibrosing ILD if they show evidence of clinical, physiologic, or radiologic progression [4].

As such, diagnostic paradigm seems to have shifted to categorize the ILDs into two groups: cases to be treated vs. not to be treated with antifibrotics, a transition from the previous paradigm: to give or not to give corticosteroids (or other immunosuppressants). The recent proposal advocating UIP as a stand-alone diagnostic entity regardless of underlying causes is at least partly based on this therapeutic paradigm. However, such a lumping of various fibrosing ILDs might not be entirely justified, given the limited efficacy, significant side effects, and high cost of currently available antifibrotics as well as the risk of losing potentially useful diagnostic granularity. This proposal is reviewed in the section below. Similarly, the recent concept of progressive pulmonary fibrosis (PPF) published in the 2022 ATS guidelines would be in keeping with such a trend of lumping ILD diagnoses (see Concept of PPF: green light for lumping fibrosing ILD diagnoses, as exactly shown in the manuscript).

Recent proposal of UIP as stand-alone entity

UIP is generally regarded as the correlate of IPF. Accordingly, the cases with histopathologic features of other diseases such as fibrotic HP and CTD-related ILD are considered not consistent with UIP [16]. It is not uncommon, however, to have some minor changes associated with HP, CTD-related ILD, or other diseases (e.g., a few poorly formed granulomas, interstitial chronic inflammatory infiltrates, lymphoid hyperplasia, and airway-centered fibrosis, etc.) in the cases otherwise acceptable for UIP. Pathologists are often in a difficult position to determine whether the presence of these minor changes would disqualify the diagnosis of UIP or not. There have been widely differing opinions and approaches in this regard even among expert pulmonary pathologists.

In this backdrop of diagnostic conundrum, a bold concept was proposed to consider UIP as a stand-alone diagnostic entity, encompassing not only IPF but also other secondary processes, based on the presence of radiologic or histopathologic features of UIP [17]. It was argued that UIP pattern of fibrosis in other ILDs (especially fibrotic HP and CTD-associated ILD) as well as in IPF is associated with unfavorable clinical outcomes [18]. In addition, acute exacerbation may occur in rheumatoid arthritis–associated ILD and fibrotic HP with similarly dismal outcome to that seen in IPF [19,20]. The significant similarities between IPF and other secondary conditions with UIP features in clinical behavior, pathogenic pathways, and the efficacy of anti-fibrotic therapy were cited as the justification for a lumping approach in this proposal. A radiologic study reported that the presence of honeycomb change alone predicted an IPF-like mortality in patients with other conditions (fibrotic HP, CTD-ILD, and unclassifiable ILD), which could support this notion [21].

 https://doi.org/10.4132/jptm.2023.11.17

Concept of PPF: green light for lumping fibrosing ILD diagnoses

There are many types of idiopathic and secondary fibrosing ILDs, in which IPF is considered as the prototype [22]. Non-IPF fibrosing ILDs include other IIPs (e.g., fibrotic NSIP, DIP, and AIP, etc.), autoimmune ILDs (e.g. rheumatoid arthritis-associated ILD), exposure-related ILDs (e.g. HP, occupational exposures, medications), pulmonary Langerhans cell histiocytosis and sarcoidosis, among others [7]. Recently, fibrosing ILDs have been studied as a group, given their clinical, radiological, and histopathological overlap. In this approach, a subset of non-IPF fibrosing ILDs was found to show a very similar clinical phenotype to that of IPF, characterized by progressive worsening of respiratory symptoms, declining lung function, developing acute exacerbation, and resistance to conventional therapy, ultimately resulting in high mortality [23-26]. In 2017, a term "progressive fibrosing ILDs" was first coined to this group of cases but an alternative term "progressive pulmonary fibrosis" (PPF) was endorsed in the 2022 ATS/ERS/JRS/ALAT clinical practice guideline [7,26]. In this 2022 statement, PPF was officially defined as an ILD of known or unknown etiology, other than IPF, with radiologic evidence of pulmonary fibrosis as well as meeting the set of specific clinical/radiological criteria including worsening respiratory symptoms and a certain degree of progression in pulmonary function abnormalities and/or radiological evidence of disease progression, occurring within the past year [7]. In this guideline, PPF is clearly stated as an entity of prognostic significance but not a specific diagnosis per se. The conceptual evolution to PPF over time is illustrated in Fig. 3.

Clinical trials have evaluated the efficacy of antifibrotics approved for IPF in the non-IPF patients who underwent progressive fibrosis, regardless of the type of underlying ILDs. Nintedanib therapy in the INBUILD trial resulted in a significant reduction in the annual decline of FVC in patients with PPF [27]. Pirfenidone therapy in two randomized control trials also showed a reduced FVC decline in some PPF patients [28,29]. Based on the results of these trials, the 2022 ATS clinical practice guidelines gave a conditional recommendation for nintedanib for the treatment of PPF in patients who have failed standard management, but not for pirfenidone given the lack of sufficient evidence [7].

This novel approach to treat ILD based on the disease behavior (i.e., PPF) without consideration of the specific underlying diagnosis will have a broader, potentially deleterious, influence in many aspects of ILD. The ATS guideline on PPF explicitly stated that this new concept of PPF should not discourage clinicians from their rigorous effort to identify the underlying type of ILD before antifibrotic therapy. In reality, however, it is most likely that the incentive of establishing a definitive diagnosis of

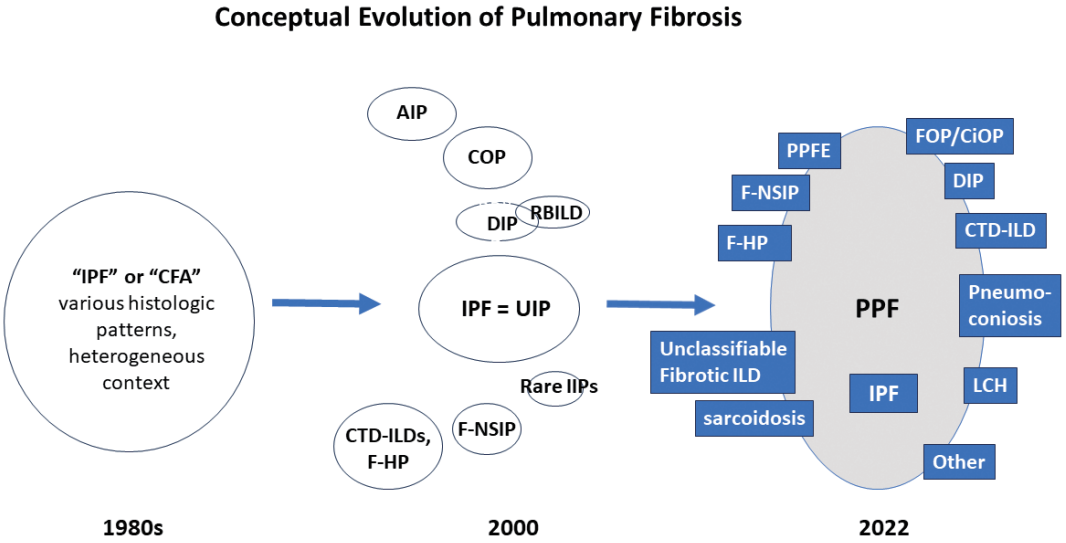

Fig. 3. The idiopathic interstitial pneumonia (IIP) classification established in 2000s is evolved from the less well-defined idiopathic pulmonary fibrosis (IPF) that encompassed various histologic patterns. Progressive pulmonary fibrosis in the current official practice guideline by American Thoracic Society (ATS)/European Respiratory Society (ERS)/Japanese Respiratory Society (JRS)/Latin American Thoracic Association (ALAT) can be the manifestion by many fibrotic lung diseases other than IPF. AIP, acute interstitial pneumonia; CFA, cryptogenic fibrosing alveolitis; CiOP, cicatricial organizing pneumonia; COP, cryptogenic organizing pneumonia; CTD-ILD, connective tissue disease–associated interstitial lung disease; DIP, desquamative interstitial pneumonia; F-HP, fibrotic hypersensitivity pneumonitis; F-NSIP, fibrotic nonspecific interstitial pneumonia; FOP, fibrotic organizing pneumonia; LCH, Langerhans cell histiocytosis; PPFE, pleuroparenchymal fibroelastosis; RBILD, respiratory bronchiolitis interstitial lung disease; UIP, usual interstitial pneumonia.

the underlying ILD would be markedly reduced if not completely vanished. A few studies attempted to analyze the clinical trials data based on specific ILD subgroups within PPF but did not have enough power to provide evidence of benefit in different subgroups [30,31]. The criteria of PPF do not include pathologic findings, but it may be helpful to evaluate any histopathologic findings that correlate with progressive fibrosis. While UIP histopathologic pattern is an obvious leading candidate given its well-known compelling evidence, characterization of other histologic features that could predict the PPF phenotype has yet to be established [17].

Familial pulmonary fibrosis: a clue to decode molecular pathogenesis of fibrosing ILD

Familial cases of ILDs were reported in 1907, which suggested a possibility of genetic factors in ILDs [32]. The concept of familial IPF was first introduced in the 2000 ATS statement with the following definition: at least two members of a primary biological family (parent, child, sibling) with clinical features of IPF and histologic confirmation [3]. Though not explicitly recommended in later ATS statements, the histology requirement in the criteria was eventually dropped in practice, which is in keeping with the trends of bypassing the biopsies and making IPF diagnosis based on HRCT at least in more classic cases of IPF on clinical ground. Familial clustering of non-IPF fibrosing ILDs have also been observed. Other names have been used for this group of diseases, including familial/inherited interstitial lung disease, familial interstitial pneumonia, familial pulmonary fibrosis, and familial IIP, if limited to idiopathic cases. The plethora of terminology has clouded the literature and hampered clearer communication. In this review, the term familial pulmonary fibrosis (FPF) will be used that encompasses all types of pulmonary fibrosis including IPF.

The frequency of FPF may be as high as 20% of patients with pulmonary fibrosis according to the previous studies reported in the literature [33-38]. Among the subtypes of fibrotic ILD, IPF most frequently had a family history of pulmonary fibrosis (20%–25%), followed by chronic HP (14%–17%), and CTD-related ILD (3%–8%) [38-41]. Of note, relatives in the same family may show different subtypes of fibrotic ILD [42,43]. Radiographic screening studies revealed some radiological abnormalities in 15 to 31% of the asymptomatic relatives of patients with known pulmonary fibrosis, suggesting even higher prevalence of FPF than suspected [44-46].

The remarkable advances in molecular technology led to several large-scale, population-based studies on pulmonary fibrosis to identify genetic risk variants that could be associated with crucial pathogenetic mechanisms in pulmonary fibrosis. Two broad categories of the variants associated with pulmonary fibrosis have been recognized based on their frequency in the population: common and rare genetic variants. Common genetic variants typically represent single nucleotide polymorphisms (SNPs) and confer a smaller effect than rare variants as the impact on disease risk tends to be inversely proportional to the frequency of a variant within the population [47]. It has been well accepted that SNPs may contribute to overall risk but not entirely sufficient to cause disease on their own. On the other hand, rare variants often demonstrate cosegregation in FPF kindreds, suggesting a causal relationship.

Linkage analysis and genome-wide association studies have identified numerous common genetic variants associated with IPF. Gain-of-function promoter variant rs35705950 in the promoter region of the *MUC5B* gene is most widely recognized in association with pulmonary fibrosis. A study reported that this genetic variant is identified in 34% of the subjects with familial IIP, 38% of those with sporadic IPF, and 9% of the control subjects [48].

Rare genetic variants in pulmonary fibrosis were mainly implicated in dysfunctional surfactant metabolism and telomere maintenance. Genes involved in abnormal surfactant metabolism include *SFTPC*, *SFTPA1/2*, and *ABCA3* [40]. The pattern of inheritance is autosomal dominant for *SFTPC* and *SFTPA1/2* and autosomal recessive for *ABCA3* [49]. Disease onset has a wide range from infancy to late adulthood in families with a rare surfactant-related gene variant; histologic and radiologic features of ILD are also diverse with the features of UIP, NSIP, and DIP [50-52]. No extrapulmonary manifestations are present in these patients as surfactant production is limited to the lung. The rare genetic variants associated with deranged telomere maintenance account for approximately 25% of FPF kindreds and involve *TERT*, *TERC*, and numerous other genes [53,54]. Unlike the gene variants associated with surfactant dysfunction, these variants of telomere-related genes often cause extrapulmonary systemic manifestations (known as short telomere syndrome or other related terms) [55]. Dyskeratosis congenita (DC) is one of the best known telomeropathy due to homozygous telomere-related gene mutations resulting in extreme telomere shortening. DC causes pulmonary fibrosis (20%) as well as life-threatening bone marrow failure (80%) at pediatric age or in very early adulthood. DC often shows various cutaneous or mucosal manifestations including nail dystrophy, abnormal skin pigmentation, and oral leukoplakia [55,56].

The patients with heterozygous telemere–related gene muta-

 https://doi.org/10.4132/jptm.2023.11.17

tions also often develop pulmonary fibrosis including IPF (50%), fibrotic HP (7%–12%) connective tissue disease–associated ILD (2%–3%), or other IIPs (14%–18%) with similar extrapulmonary manifestations of DC but at an older age than in DC [43,57,58]. Interestingly, about 10% of adult-onset sporadic IPF, chronic HP, and rheumatoid arthritis-related ILD patients have rare telomere-related gene variants [59-62]. Short telomere length is often seen in FPF cases and a frequent finding in sporadic cases of pulmonary fibrosis as compared to control subjects, suggesting a possibility that short telomere length might be a potential cause of pulmonary fibrosis [63].

Despite a remarkable progress in identifying key genetic features associated with FPF (and some sporadic fibrosing ILD cases), characterization of the matching pathologic features in FPF seemed to have lagged behind. Steele et al published a study in 2005 with histopathologic assessment in some of their cases from families with IIPs and found significant heterogeneity within a given family, showing more than one histopathologic subtype of IIP in 45% of family pedigrees [42]. A comprehensive histopathologic study by Leslie et al compiled the findings to differentiate familial and sporadic IIP cases in an effort to characterize the features of familial IIP, primarily focusing on familial IPF [64]. Although most of their patients had some histopathologic features associated with UIP, up to 60% of them did not qualify as UIP, mainly due to lack of the temporal heterogeneity of fibrosis, one of the most important histologic criteria for UIP [64]. Most of these cases ended up in the unclassifiable fibrotic ILD category [64]. Prevailing notion in the past has been that familial and sporadic IPF cases do not have distinguishable clinical or histological features other than earlier onset in familial IPF [6]. However, this 2012 study by Leslie et al. [64] suggested that there may be some histopathologic features differentiating sporadic and familial fibrotic lung diseases. Based on this observation, they concluded that unclassifiable pattern of lung fibrosis should raise a possibility of FPF or familial IPF [64]. They also suggested that less than classic histopathologic features of UIP could still be compatible with familial IPF in an appropriate clinical context [64].

AI in diagnosis of interstitial lung diseases

The application of AI tools on radiologic images for characterization of indeterminate lung nodules, fibrotic lung diseases, and lung cancer risk stratification has been well studied and documented in the literature. As compared to radiology arena, digital pathology (DP) by WSI started more recently and most AI approach has been applied to cancers and biomarker arena of other organs (such as breast and prostate). In the lungs, AI tools have also been more widely applied to cancers than to ILDs, partly due to the current tendency of relying on high-resolution CT and bypassing surgical lung biopsies for diagnosis of ILDs, especially after the 2013 ATS/ERS guidelines.

As there are many clinically as well as morphologically ambiguous cases of ILD, AI-assisted diagnosis may offer a crucial contribution by detecting some features that are not discernable by traditional diagnostic methods. Moreover, AI apporach may resolve some interobserver variability in diagnosing ILDs that has been well-recognized even among the expert pulmonary pathologists. It is inherently subjective to interpret the basic histopathologic parameters for ILD diagnosis (such as architectural distortion or scarring, honeycomb change, traction bronchiectasis, distribution of fibrosis, degree of inflammation, fibroblast foci, presence of granulomas, to name a few). Thus, more objective interpretation and quantitation of these parameters would be ideal by appropriate training and development of AI algorithm. Once AI-assisted diagnostic tool becomes widely available, it may mitigate the challenges encountered by many hospitals without direct access to experienced pathologists who are well versed in ILD diagnoses. Finally, some advanced AI technology (e.g. DL-based AI via unsupervised feature learning) might offer new insights into ILDs by elucidating previously unknown histopathologic features associated with progressive clinical behavior as in PPF cases. Such an approach, however, requires a large number of surgical lung biopsy cases with clinical annotation, which became scarce these days due to the changing practices as elaborated in the earlier sections. Multi-institutional collaboration might be needed to form a consortium for securing sufficient database to develop appropriate AI model.

A complete coverage of AI tools in DP is beyond the scope of the present review and only a brief introduction of basic concepts in the AI approach will be provided, followed by summary of several original studies in the literature on predicting pathologic diagnosis and prognosis of ILDs, or evaluation of histopathologic biomarkers in IPF with AI technology (Table 1).

AI is a broad discipline with multiple approaches to construct a model for a particular task. There are two common ways to extract feature representation for building an AI model: (1) DL-based unsupervised feature learning, (2) hand-crafted approach [65]. Convolutional neural network (CNN) is a type of DL approach suited for low-level tasks such as detecting, identifying, and classification of images. DL-based unsupervised feature learning is favored in low-level tasks such as cell and lung tumor detection and classification. This is useful since visual confirmation of the result is sufficient and does not require interpretation

Table 1. Published original research on interstitial lung diseases with AI-based methods

Study	Purpose of study	Method	Country	No. of cases	Main finding
Makela et al. (2021) [66]	Quantitation of histologic parameters for survival analysis in IPF	Deep CNN	Finland	71 IPF	Increased FF is associated with poor prognosis—interstitial mononuclear infiltrate & intra-alveolar macrophage with longer survival
Uegami et al. (2022) [67]	Prediction of UIP diagnosis	MIXTURE	Japan	231 (UIP+non-UIP) cases; 715 WSI	A model approach to differentiate diseases by AI with collaboration with humans based on expert pathologists' input
Testa et al. (2021) [68]	Pilot study to quantitate fibrosis in HPSPF & IPF	Automated quantitation of fibrosis with "dedicated software"	USA	3 HPSPF & 9 IPF	Their automated image analysis offered accurate, reader-independent pulmonary fibrosis quantitation in HPSPF and IPF groups

AI, artificial intelligence; CNN, convoluted neural network; IPF, idiopathic pulmonary fibrosis; FF, fibroblastic foci; MIXTURE, huMan-In-the loop eXpalainable artificial intelligence Through the Use of REcurrent training; UIP, usual interstitial pneumonia; WSI, whole slide imaging; HPSPF, Hermansky-Pudlak syndrome pulmonary fibrosis.

of selected features. In the hand-crafted approach, relevant features from data are manually selected. The domain knowledge is employed for features engineering, by close collaboration between pathologists and machine learning engineers to construct appropriate AI models. In contrast to DL-based unsupervised feature learning, hand-crafted based models offer some interpretability through incorporating the expertise of subject matter experts. Many high-level tasks such as prognosis or treatment response prediction which require a certain level of interpretability and hence hand-crafted, domain-inspired features may be favored by medical community to construct these models. Integration of DP in clinical workflow across major institutions poses a huge challenge, due to organizational structures, the cost of initial set-up, requirements of advanced security systems in hospitals and demands for storage of big data. Currently, most existing AI tools have been validated on retrospective data, which does not represent the current, real-world scenarios. Validating the algorithms in randomized controlled trials and prospective studies will be a crucial step towards clinical adoption of these AI tools.

Makela et al. [66] reported a study using AI to count fibroblast foci, a known prognostic factor in IPF, and other parameters to evaluate their prognostic significance. In this study, they trained a CNN to quantify fibroblast foci, interstitial mononuclear inflammation, and intra-alveolar macrophages to analyze the association of these parameters with survival [66]. Interstitial mononuclear inflammation and intra-alveolar macrophages were associated longer survival, while increased fibroblast foci were associated with poor prognosis.

Uegami et al. [67] proposed an original method to develop DL models for extracting pathologically significant findings based on expert pathologist's perspective with a small annotation effort. Their method named MIXTURE (huMan-In-the-loop eXplainable artificial intelligence Through the Use of REcurrent training) consisted three steps including (1) creating feature extractors for tiles from whole slide images using self-supervised learning, (2) clustering similar looking tiles based on output features, followed by integration of the pathologically synonymous clusters by pathologists, and (3) creation of DL models to classify tiles into pathological findings by using the integrated clusters as labeled data. They developed three models for different magnification. Their model predicted the diagnosis of UIP with a high accuracy, which was not possible to achieve without the step of integration of findings by pathologists. They proposed this model as the prototype for explainable AI that can collaborate with humans.

Testa et al. [68] reported a study that performed an automated digital quantification of pulmonary fibrosis in human histopathology specimens. They conducted a pilot sutdy to analyze a small number of specimens from patients with Hermansky-Pudlak syndrome pulmonary fibrosis (n = 3) or IPF (n = 9) using digital images of serial lung sections stained with picrosirius red, alcian blue or anti-CD68 antibody. Dedicated software was used to automatically quantify fibrosis, collagen, and macrophage content. Automated fibrosis quantification based on parenchymal tissue density and fibrosis score measurements were compared to the pulmonary function test values or Ashcroft score, a numerical scale with grades from 0 to 8, of the amount of fibrotic tissue in histological samples devised by Ashcroft et al. [69]. A high correlation coefficient was found between some automated quantification measurements and lung function values in the sample groups. They concluded that computerized image analysis can offer accurate, reader-independent pulmonary fibrosis quantification in human histopathology samples for various parameters such as fibrosis, collagen content, and immunostained cells. This approach may enhance the available tools to quantify and study fibrotic ILDs.

https://doi.org/10.4132/jptm.2023.11.17

CONCLUSION

Since Dr. Liebow introduced the diagnosis of UIP/IPF as a type of ILDs more than 50 years ago, histopathologic criteria have been refined and established. Antifibrotic therapy recently became available for UIP/IPF patients and brought modest improvement in its otherwise dismal clinical course. Partly based on the efficacy of antifibrotic therapy in other types of fibrosing ILDs, albeit limited, a proposal of UIP as a stand-alone entity was made to encompass all fibrosing ILDs with UIP pattern under the broad umbrella of UIP to be treated as UIP/IPF patients. Likewise, a concept of PPF that includes many types of fibrosing ILDs was endorsed as a prognostic entity (but not a specific diagnosis) by an international committee that also cited the similar therapeutic approach to that in UIP/IPF as the main reason for creating this category. Common and rare genetic variants identified in fibrosing ILD patients shed light in molecular pathways implicated in sporadic as well as familial cases of fibrosing ILDs. Whole slide imaging and AI might open the door to a new era provided accumulation of big histopathologic database and collective effort in this approach support the progress.

Ethics Statement

Not applicable.

Availability of Data and Material

The datasets generated or analyzed during the study are available from the corresponding author on reasonable request.

Code Availability

Not applicable.

ORCID

Eunhee S. Yi https://orcid.org/0000-0002-7517-6479
Paul Wawryko https://orcid.org/0009-0005-3356-6232
Jay H. Ryu https://orcid.org/0000-0002-9576-2272

Author Contributions

Conceptualization: ESY, JHR. Data curation: ESY, PW. Supervision: ESY. Writing—original draft: ESY, PW. Writing—review & editing: ESY, PW, JHR. Approval of final manuscript: all authors.

Conflicts of Interest

The authors declare that they have no potential conflicts of interest.

Funding Statement

No funding to declare.

References

1. Liebow A, Carrington CB. The interstitial pneumonias. In: Simon M, Potchen EJ, LeMay M, eds. Frontiers of pulmonary radiology. New York: Grune and Stratton, 1969; 102-41.
2. Katzenstein AL, Myers JL. Idiopathic pulmonary fibrosis: clinical relevance of pathologic classification. Am J Respir Crit Care Med 1998; 157: 1301-15.
3. American Thoracic Society. Idiopathic pulmonary fibrosis: diagnosis and treatment. International consensus statement. American Thoracic Society (ATS), and the European Respiratory Society (ERS). Am J Respir Crit Care Med 2000; 161: 646-64.
4. American Thoracic Society; European Respiratory Society. American Thoracic Society/European Respiratory Society international multidisciplinary consensus classification of the idiopathic interstitial pneumonias. This joint statement of the American Thoracic Society (ATS), and the European Respiratory Society (ERS) was adopted by the ATS board of directors, June 2001 and by the ERS Executive Committee, June 2001. Am J Respir Crit Care Med 2002; 165: 277-304.
5. Travis WD, Costabel U, Hansell DM, et al. An official American Thoracic Society/European Respiratory Society statement: Update of the international multidisciplinary classification of the idiopathic interstitial pneumonias. Am J Respir Crit Care Med 2013; 188: 733-48.
6. Raghu G, Collard HR, Egan JJ, et al. An official ATS/ERS/JRS/ALAT statement: idiopathic pulmonary fibrosis: evidence-based guidelines for diagnosis and management. Am J Respir Crit Care Med 2011; 183: 788-824.
7. Raghu G, Remy-Jardin M, Richeldi L, et al. Idiopathic pulmonary fibrosis (an update) and progressive pulmonary fibrosis in adults: an official ATS/ERS/JRS/ALAT clinical practice guideline. Am J Respir Crit Care Med 2022; 205: e18-47.
8. Kim SY, Diggans J, Pankratz D, et al. Classification of usual interstitial pneumonia in patients with interstitial lung disease: assessment of a machine learning approach using high-dimensional transcriptional data. Lancet Respir Med 2015; 3: 473-82.
9. Raghu G, Flaherty KR, Lederer DJ, et al. Use of a molecular classifier to identify usual interstitial pneumonia in conventional transbronchial lung biopsy samples: a prospective validation study. Lancet Respir Med 2019; 7: 487-96.
10. Collard HR, Moore BB, Flaherty KR, et al. Acute exacerbations of idiopathic pulmonary fibrosis. Am J Respir Crit Care Med 2007; 176: 636-43.
11. Azuma A, Nukiwa T, Tsuboi E, et al. Double-blind, placebo-controlled trial of pirfenidone in patients with idiopathic pulmonary fibrosis. Am J Respir Crit Care Med 2005; 171: 1040-7.
12. Taniguchi H, Ebina M, Kondoh Y, et al. Pirfenidone in idiopathic pulmonary fibrosis. Eur Respir J 2010; 35: 821-9.
13. Richeldi L, Costabel U, Selman M, et al. Efficacy of a tyrosine kinase inhibitor in idiopathic pulmonary fibrosis. N Engl J Med 2011; 365: 1079-87.
14. Richeldi L, du Bois RM, Raghu G, et al. Efficacy and safety of nintedanib in idiopathic pulmonary fibrosis. N Engl J Med 2014; 370: 2071-82.
15. Raghu G, Rochwerg B, Zhang Y, et al. An official ATS/ERS/JRS/ALAT clinical practice guideline: treatment of idiopathic pulmonary fibrosis: an update of the 2011 clinical practice guideline. Am J Respir Crit Care Med 2015; 192: e3-19.
16. Raghu G, Remy-Jardin M, Myers JL, et al. Diagnosis of idiopathic pulmonary fibrosis: an official ATS/ERS/JRS/ALAT clinical practice guideline. Am J Respir Crit Care Med 2018; 198: e44-68.
17. Selman M, Pardo A, Wells AU. Usual interstitial pneumonia as a

stand-alone diagnostic entity: the case for a paradigm shift? Lancet Respir Med 2023; 11: 188-96.
18. Hambly N, Farooqi MM, Dvorkin-Gheva A, et al. Prevalence and characteristics of progressive fibrosing interstitial lung disease in a prospective registry. Eur Respir J 2022; 60: 2102571.
19. Hozumi H, Nakamura Y, Johkoh T, et al. Acute exacerbation in rheumatoid arthritis-associated interstitial lung disease: a retrospective case control study. BMJ Open 2013; 3: e003132.
20. Kang J, Kim YJ, Choe J, Chae EJ, Song JW. Acute exacerbation of fibrotic hypersensitivity pneumonitis: incidence and outcomes. Respir Res 2021; 22: 152.
21. Adegunsoye A, Oldham JM, Bellam SK, et al. Computed tomography honeycombing identifies a progressive fibrotic phenotype with increased mortality across diverse interstitial lung diseases. Ann Am Thorac Soc 2019; 16: 580-8.
22. Wijsenbeek M, Cottin V. Spectrum of fibrotic lung diseases. N Engl J Med 2020; 383: 958-68.
23. Cottin V, Wollin L, Fischer A, Quaresma M, Stowasser S, Harari S. Fibrosing interstitial lung diseases: knowns and unknowns. Eur Respir Rev 2019; 28: 180100.
24. Brown KK, Martinez FJ, Walsh SL, et al. The natural history of progressive fibrosing interstitial lung diseases. Eur Respir J 2020; 55: 2000085.
25. Nasser M, Larrieu S, Si-Mohamed S, et al. Progressive fibrosing interstitial lung disease: a clinical cohort (the PROGRESS study). Eur Respir J 2021; 57: 2002718.
26. Flaherty KR, Brown KK, Wells AU, et al. Design of the PF-ILD trial: a double-blind, randomised, placebo-controlled phase III trial of nintedanib in patients with progressive fibrosing interstitial lung disease. BMJ Open Respir Res 2017; 4: e000212.
27. Flaherty KR, Wells AU, Cottin V, et al. Nintedanib in progressive fibrosing interstitial lung diseases. N Engl J Med 2019; 381: 1718-27.
28. Maher TM, Corte TJ, Fischer A, et al. Pirfenidone in patients with unclassifiable progressive fibrosing interstitial lung disease: a double-blind, randomised, placebo-controlled, phase 2 trial. Lancet Respir Med 2020; 8: 147-57.
29. Behr J, Prasse A, Kreuter M, et al. Pirfenidone in patients with progressive fibrotic interstitial lung diseases other than idiopathic pulmonary fibrosis (RELIEF): a double-blind, randomised, placebo-controlled, phase 2b trial. Lancet Respir Med 2021; 9: 476-86.
30. Wells AU, Flaherty KR, Brown KK, et al. Nintedanib in patients with progressive fibrosing interstitial lung diseases-subgroup analyses by interstitial lung disease diagnosis in the INBUILD trial: a randomised, double-blind, placebo-controlled, parallel-group trial. Lancet Respir Med 2020; 8: 453-60.
31. Matteson EL, Kelly C, Distler JH, et al. Nintedanib in patients with autoimmune disease-related progressive fibrosing interstitial lung diseases: subgroup analysis of the INBUILD trial. Arthritis Rheumatol 2022; 74: 1039-47.
32. Sandoz E. Uber zwei falle von fotaler bronchektasie [About two cases of fetal bronchiectasis]. Beitr Pathol Anat 1907; 41: 496-517.
33. Marshall RP, Puddicombe A, Cookson WO, Laurent GJ. Adult familial cryptogenic fibrosing alveolitis in the United Kingdom. Thorax 2000; 55: 143-6.
34. Hodgson U, Laitinen T, Tukiainen P. Nationwide prevalence of sporadic and familial idiopathic pulmonary fibrosis: evidence of founder effect among multiplex families in Finland. Thorax 2002; 57: 338-42.
35. Barlo NP, van Moorsel CH, Ruven HJ, Zanen P, van den Bosch JM, Grutters JC. Surfactant protein-D predicts survival in patients with idiopathic pulmonary fibrosis. Sarcoidosis Vasc Diffuse Lung Dis 2009; 26: 155-61.
36. Garcia-Sancho C, Buendia-Roldan I, Fernandez-Plata MR, et al. Familial pulmonary fibrosis is the strongest risk factor for idiopathic pulmonary fibrosis. Respir Med 2011; 105: 1902-7.
37. Loyd JE. Pulmonary fibrosis in families. Am J Respir Cell Mol Biol 2003; 29: S47-50.
38. Fernandez BA, Fox G, Bhatia R, et al. A Newfoundland cohort of familial and sporadic idiopathic pulmonary fibrosis patients: clinical and genetic features. Respir Res 2012; 13: 64.
39. Ley B, Newton CA, Arnould I, et al. The *MUC5B* promoter polymorphism and telomere length in patients with chronic hypersensitivity pneumonitis: an observational cohort-control study. Lancet Respir Med 2017; 5: 639-47.
40. Newton CA, Oldham JM, Ley B, et al. Telomere length and genetic variant associations with interstitial lung disease progression and survival. Eur Respir J 2019; 53: 1801641.
41. Cutting CC, Bowman WS, Dao N, et al. Family history of pulmonary fibrosis predicts worse survival in patients with interstitial lung disease. Chest 2021; 159: 1913-21.
42. Steele MP, Speer MC, Loyd JE, et al. Clinical and pathologic features of familial interstitial pneumonia. Am J Respir Crit Care Med 2005; 172: 1146-52.
43. Newton CA, Batra K, Torrealba J, et al. Telomere-related lung fibrosis is diagnostically heterogeneous but uniformly progressive. Eur Respir J 2016; 48: 1710-20.
44. Mathai SK, Humphries S, Kropski JA, et al. *MUC5B* variant is associated with visually and quantitatively detected preclinical pulmonary fibrosis. Thorax 2019; 74: 1131-9.
45. Hunninghake GM, Quesada-Arias LD, Carmichael NE, et al. Interstitial lung disease in relatives of patients with pulmonary fibrosis. Am J Respir Crit Care Med 2020; 201: 1240-8.
46. Salisbury ML, Hewlett JC, Ding G, et al. Development and progression of radiologic abnormalities in individuals at risk for familial interstitial lung disease. Am J Respir Crit Care Med 2020; 201: 1230-9.
47. Mathai SK, Newton CA, Schwartz DA, Garcia CK. Pulmonary fibrosis in the era of stratified medicine. Thorax 2016; 71: 1154-60.
48. Seibold MA, Wise AL, Speer MC, et al. A common *MUC5B* promoter polymorphism and pulmonary fibrosis. N Engl J Med 2011; 364: 1503-12.
49. van Moorsel CH, van der Vis JJ, Grutters JC. Genetic disorders of the surfactant system: focus on adult disease. Eur Respir Rev 2021; 30: 200085.
50. Nogee LM, Dunbar AE, 3rd, Wert SE, Askin F, Hamvas A, Whitsett JA. A mutation in the surfactant protein C gene associated with familial interstitial lung disease. N Engl J Med 2001; 344: 573-9.
51. Thomas AQ, Lane K, Phillips J 3rd, et al. Heterozygosity for a surfactant protein C gene mutation associated with usual interstitial pneumonitis and cellular nonspecific interstitial pneumonitis in one kindred. Am J Respir Crit Care Med 2002; 165: 1322-8.
52. van Moorsel CH, Ten Klooster L, van Oosterhout MF, et al. *SFTPA2* mutations in familial and sporadic idiopathic interstitial pneumonia. Am J Respir Crit Care Med 2015; 192: 1249-52.
53. Armanios MY, Chen JJ, Cogan JD, et al. Telomerase mutations in families with idiopathic pulmonary fibrosis. N Engl J Med 2007; 356: 1317-26.

54. Tsakiri KD, Cronkhite JT, Kuan PJ, et al. Adult-onset pulmonary fibrosis caused by mutations in telomerase. Proc Natl Acad Sci U S A 2007; 104: 7552-7.
55. Armanios M. Telomerase and idiopathic pulmonary fibrosis. Mutat Res 2012; 730: 52-8.
56. Savage SA, Alter BP. Dyskeratosis congenita. Hematol Oncol Clin North Am 2009; 23: 215-31.
57. Diaz de Leon A, Cronkhite JT, Yilmaz C, et al. Subclinical lung disease, macrocytosis, and premature graying in kindreds with telomerase (*TERT*) mutations. Chest 2011; 140: 753-63.
58. Borie R, Tabeze L, Thabut G, et al. Prevalence and characteristics of *TERT* and *TERC* mutations in suspected genetic pulmonary fibrosis. Eur Respir J 2016; 48: 1721-31.
59. Juge PA, Borie R, Kannengiesser C, et al. Shared genetic predisposition in rheumatoid arthritis-interstitial lung disease and familial pulmonary fibrosis. Eur Respir J 2017; 49: 1602314.
60. Petrovski S, Todd JL, Durheim MT, et al. An exome sequencing study to assess the role of rare genetic variation in pulmonary fibrosis. Am J Respir Crit Care Med 2017; 196: 82-93.
61. Dressen A, Abbas AR, Cabanski C, et al. Analysis of protein-altering variants in telomerase genes and their association with *MUC5B* common variant status in patients with idiopathic pulmonary fibrosis: a candidate gene sequencing study. Lancet Respir Med 2018; 6: 603-14.
62. Ley B, Torgerson DG, Oldham JM, et al. Rare protein-altering telomere-related gene variants in patients with chronic hypersensitivity pneumonitis. Am J Respir Crit Care Med 2019; 200: 1154-63.
63. Cronkhite JT, Xing C, Raghu G, et al. Telomere shortening in familial and sporadic pulmonary fibrosis. Am J Respir Crit Care Med 2008; 178: 729-37.
64. Leslie KO, Cool CD, Sporn TA, et al. Familial idiopathic interstitial pneumonia: histopathology and survival in 30 patients. Arch Pathol Lab Med 2012; 136: 1366-76.
65. Viswanathan VS, Toro P, Corredor G, Mukhopadhyay S, Madabhushi A. The state of the art for artificial intelligence in lung digital pathology. J Pathol 2022; 257: 413-29.
66. Makela K, Mayranpaa MI, Sihvo HK, et al. Artificial intelligence identifies inflammation and confirms fibroblast foci as prognostic tissue biomarkers in idiopathic pulmonary fibrosis. Hum Pathol 2021; 107: 58-68.
67. Uegami W, Bychkov A, Ozasa M, et al. MIXTURE of human expertise and deep learning-developing an explainable model for predicting pathological diagnosis and survival in patients with interstitial lung disease. Mod Pathol 2022; 35: 1083-91.
68. Testa LC, Jule Y, Lundh L, et al. Automated digital quantification of pulmonary fibrosis in human histopathology specimens. Front Med (Lausanne) 2021; 8: 607720.
69. Ashcroft T, Simpson JM, Timbrell V. Simple method of estimating severity of pulmonary fibrosis on a numerical scale. J Clin Pathol 1988; 41: 467-70.

JPTM
Journal of Pathology and Translational Medicine 2024; 58: 12-21
https://doi.org/10.4132/jptm.2023.11.02

ORIGINAL ARTICLE

Tumor-infiltrating T lymphocytes evaluated using digital image analysis predict the prognosis of patients with diffuse large B-cell lymphoma

Yunjoo Cho[1], Jiyeon Lee[1,2], Bogyeong Han[3], Sang Eun Yoon[4], Seok Jin Kim[4], Won Seog Kim[4], Junhun Cho[1]

[1]Department of Pathology, Samsung Medical Center, Sungkyunkwan University School of Medicine, Seoul;
[2]Department of Pathology, Korea University Guro Hospital, Korea University College of Medicine, Seoul;
[3]Department of Pathology, Seoul National University, Seoul National College of Medicine, Seoul;
[4]Division of Hematology and Oncology, Department of Internal Medicine, Sungkyunkwan University School of Medicine, Seoul, Korea

Background: The implication of the presence of tumor-infiltrating T lymphocytes (TIL-T) in diffuse large B-cell lymphoma (DLBCL) is yet to be elucidated. We aimed to investigate the effect of TIL-T levels on the prognosis of patients with DLBCL. **Methods:** Ninety-six patients with DLBCL were enrolled in the study. The TIL-T ratio was measured using QuPath, a digital pathology software package. The TIL-T ratio was investigated in three foci (highest, intermediate, and lowest) for each case, resulting in TIL-T–Max, TIL-T–Intermediate, and TIL-T–Min. The relationship between the TIL-T ratios and prognosis was investigated. **Results:** When 19% was used as the cutoff value for TIL-T–Max, 72 (75.0%) and 24 (25.0%) patients had high and low TIL-T–Max, respectively. A high TIL-T–Max was significantly associated with lower serum lactate dehydrogenase levels ($p<.001$), with patient group who achieved complete remission after R-CHOP therapy ($p<.001$), and a low-risk revised International Prognostic Index score ($p<.001$). Univariate analysis showed that patients with a low TIL-T–Max had a significantly worse prognosis in overall survival compared to those with a high TIL-T–Max ($p<.001$); this difference remained significant in a multivariate analysis with Cox proportional hazards (hazard ratio, 7.55; 95% confidence interval, 2.54 to 22.42; $p<.001$). **Conclusions:** Patients with DLBCL with a high TIL-T–Max showed significantly better prognosis than those with a low TIL-T–Max, and the TIL-T–Max was an independent indicator of overall survival. These results suggest that evaluating TIL-T ratios using a digital pathology system is useful in predicting the prognosis of patients with DLBCL.

Key Words: Diffuse large B-cell lymphoma; Tumor infiltrating lymphocytes; T lymphocytes; Digital pathology

Received: October 10, 2023 **Revised:** October 30, 2023 **Accepted:** November 1, 2023
Corresponding Author: Junhun Cho, MD, Department of Pathology, Samsung Medical Center, Sungkyunkwan University School of Medicine, 81 Irwon-ro, Gangnam-gu, Seoul 06351, Korea
Tel: +82-2-3410-1891, Fax: +82-2-3410-2831 E-mail: jununius@naver.com

Diffuse large B-cell lymphoma (DLBCL) is the most common malignant lymphoma in adults [1,2]. Currently, the rituximab plus cyclophosphamide, doxorubicin, vincristine, and prednisone (R-CHOP) regimen is used as the first-line chemotherapy for patients with DLBCL. Approximately 70% of the patients achieve long-term remission; however, the remaining patients die as a result of relapse or refractory disease [3-5]. Although immunotherapy is effective for several other solid tumors, only a subset of patients with DLBCL responds to immunotherapy [6,7]. T lymphocytes, macrophages, natural killer cells, stromal cells, blood vessels, and the extracellular matrix act complexly in the mechanism of immunotherapy. Thus, it is important to increase our understanding of the tumor microenvironment (TME) to establish an effective immunotherapeutic strategy [8-12]. In particular, chimeric antigen receptor T-cell (CAR-T) therapy has recently been used to treat patients with DLBCL [13,14], which significantly increases the importance of T lymphocytes in the TME of DLBCL.

Previous studies have speculated that T lymphocytes may be associated with the clinical course of DLBCL. One study demonstrated that a higher percentage of tumor-infiltrating T lymphocytes (TIL-T) was correlated with better patient survival [15]. However, results vary with respect to the effect of CD3-positive T-cell infiltration on patient outcomes [16], and more researchers have reported the prognostic value of a specific subset of TIL-T, namely CD4-positive T cells, in DLBCL [17,18].

pISSN 2383-7837
eISSN 2383-7845

The widespread use of digital pathology systems has made it possible to objectively and accurately evaluate histological analyses performed subjectively by pathologists. In this study, we used immunohistochemistry (IHC) and a digital pathology system to precisely measure TIL-T levels in DLBCL, not otherwise specified (NOS), and investigated its association with patient prognosis. We also revealed that a high TIL-T ratio is an independent favorable prognostic factor in patients with DLBCL NOS.

MATERIALS AND METHODS

Patient selection

Ninety-six consecutive patients diagnosed with DLBCL NOS at Samsung Medical Center, Seoul, Korea, from January to December 2018, were enrolled in this study. Small biopsy and diagnostic resection were performed in 66 and 30 patients, respectively. The patients' clinical and pathological information was evaluated by reviewing their electronic medical records. There were 48 males and 48 females, with a male-to-female ratio of 1:1. The median age of the patients was 61 years (range, 5 to 86 years). According to the Ann Arbor stage, 52 patients (54.2%) were stage I–II and 44 (45.8%) were stage III–IV. The number of cases subtyped by cells of origin (COO) [19] was 32 (33.3%) for the germinal center B-cell (GCB) type and 64 (66.7%) for the non-GCB type. At the time of diagnosis, serum lactate dehydrogenase (LDH) levels were elevated above the normal range in 39 patients (40.6%). All patients initially received R-CHOP chemotherapy, except for five patients who either died or were lost to follow-up before they could be treated. Fifty of the 91 treated patients achieved complete remission (CR) after the standard six course of R-CHOP. Among the 41 patients who did not, nine were only treated with R-CHOP, 17 went on to receive second and/or third-line chemotherapy, and 15 had autologous stem cell transplantation. Based on the revised International Prognostic Index (R-IPI)

Table 1. Various clinical factors in diffuse large B-cell lymphoma, not otherwise specified patients according to TIL-T–Max, TIL-T–Intermediate, and TIL-T–Min

Characteristic	No. of patients (%)	TIL-T–Max			TIL-T–Intermediate			TIL-T–Min		
		High (n=72, 75.0%)	Low (n=24, 25.0%)	p-value	High (n=64, 66.7%)	Low (n=32, 33.3%)	p-value	High (n=36, 37.5%)	Low (n=60, 62.5%)	p-value
Age (yr)				.239			>.999			>.999
≤60	48 (50.0)	39	9		32	16		18	30	
>60	48 (50.0)	33	15		32	16		18	30	
Sex				.630			>.999			>.999
Female	38 (39.6)	30	8		25	13		14	24	
Male	58 (60.4)	42	16		39	19		22	36	
Ann Arbor stage				.098			.096			>.999
Low (I–II)	52 (54.2)	43	9		39	13		20	32	
High (III–IV)	44 (45.8)	29	15		25	19		16	28	
COO				.803			.592			.502
GCB	32 (33.3)	25	7		23	9		14	18	
Non-GCB	64 (66.7)	47	17		41	23		22	42	
Serum LDH level				<.001			.004			.077
Low	57 (59.4)	52	5		45	12		26	31	
High	39 (40.6)	20	19		19	20		10	29	
Treatment				<.001			.002			.246
CR after R-CHOP	50 (52.1)	45	5		41	9		22	28	
Non-CR	46 (47.9)	27	19		23	23		14	32	
R-CHOP only	9									
+2nd and/or 3rd line CTx	17									
+AutoSCT	15									
Pre-treatment	5									
R-IPI				<.001			.040			.202
Low risk (0–2)	63 (65.6)	55	8		47	16		27	36	
High risk (3–5)	33 (34.4)	17	16		17	16		9	24	

TIL-T, tumor-infiltrating T lymphocyte; COO, cells of origin; GCB, germinal center B-cell-like; LDH, lactate dehydrogenase; CR, complete remission; R-CHOP, rituximab plus cyclophosphamide, doxorubicin, vincristine, and prednisone; CTx, chemotherapy; AutoSCT, autologous stem cell transplantation; R-IPI, revised International Prognostic Index.

[20], which takes into consideration the number of negative prognostic factors present at the time of diagnosis (age >60 years, stage III/IV disease, elevated LDH level, Eastern Cooperative Oncology Group performance status ≥2, more than one extranodal site of disease), cases were stratified into low-risk group (0–2 negative factors) and high-risk group (3–5 negative factors). Sixty-three (65.6%) cases were low risk and 33 (34.4%) were high risk. The clinicopathological characteristics of the patients are summarized in Table 1. The median follow-up period was 1,181 days (range, 2 to 1,894 days).

Computational image analysis

IHC for CD3 (Polyconal, Dako, Glostrup, Denmark) and CD20 (clone L26, Dako), performed at the time of diagnosis, was used for TIL-T ratio evaluation. All slides were scanned using a Pannoramic 1000 scanner (3DHistech, Budapest, Hungary). The INFINITT DPS (INFINITT Healthcare, Seoul, Korea) was used as the image-viewing system. Two independent pathologists (Y.C. and J.C.), without prior knowledge of the patients' clinical outcomes, thoroughly evaluated tumor areas with dense B-cell populations, as detected by CD20 IHC. Among the differing densities of CD3-positive lymphocytes, the areas with the highest, lowest, and intermediate densities of CD3-positive cells in each case were manually selected. Areas with the highest and the lowest densities were first identified, then those areas were excluded from determining the intermediate density area. Intermediate density was taken from an area occupying the largest proportion of the tumor with similar level of CD3-positive lymphocyte density. Disagreements were resolved by consensus, and the consensus foci were adopted as final. All the selected areas were then photographed in a 400×400 μm square image. The image files were processed using QuPath software [21]. Cell-detection was conducted using QuPath's built-in "Positive cell detection" to determine the ratio of TIL-T to total cell of each focus (Fig. 1). The TIL-T ratios of the areas with the highest, lowest, and intermediate CD3-positive cell densities were denoted as TIL-T–Max, TIL-T–Min, and TIL-T–Intermediate, respectively.

Statistical analysis

Comparisons between clinical features and TIL-T ratios were

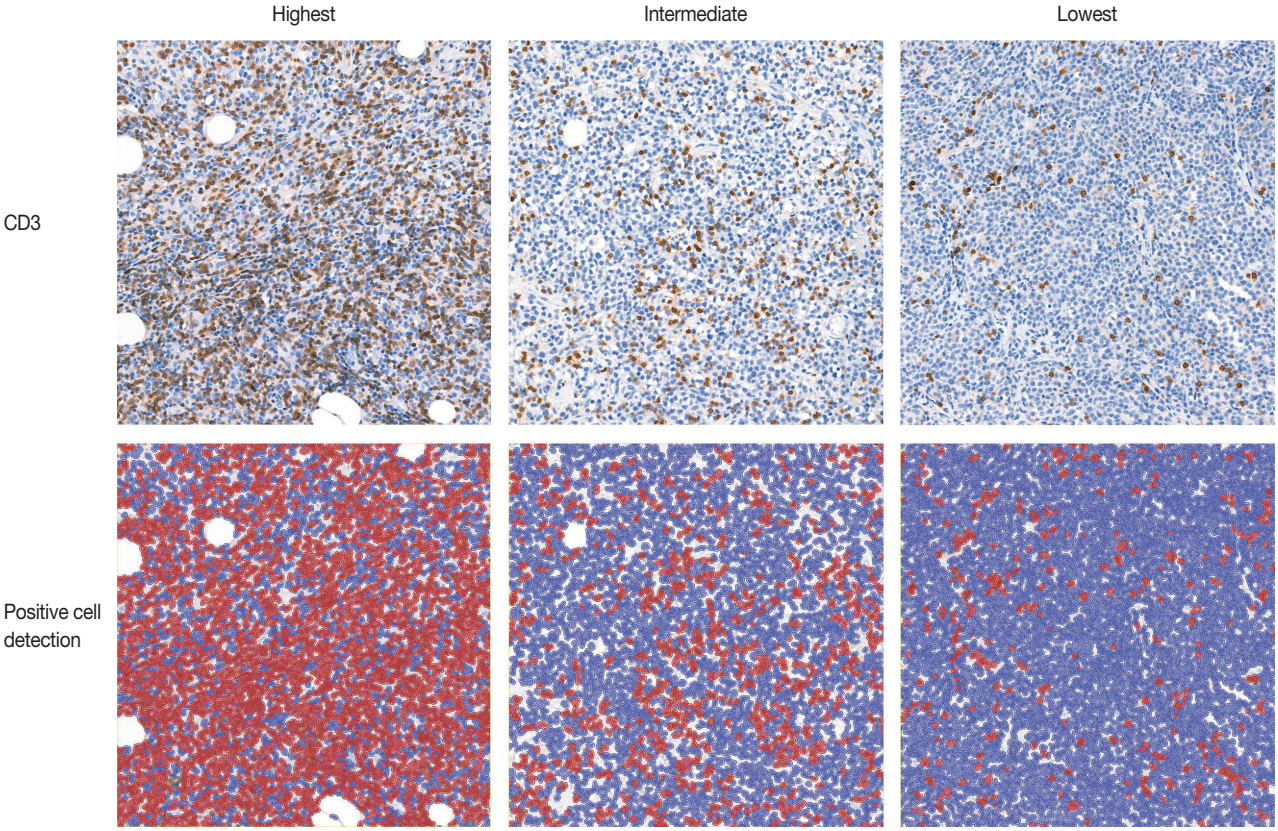

Fig. 1. Representative images of CD3 immunohistochemistry and visualization of positive cell detection analyses by QuPath. Red color denotes positive detected cells, and blue color demonstrates negative cells.

https://doi.org/10.4132/jptm.2023.11.02

performed using Pearson's chi-square test. Overall survival (OS) was defined as the time from the date of diagnosis to death from any cause. Survival distribution was compared using the Kaplan-Meier method and log-rank test. Prognostic variables associated with OS were examined by univariate analysis using the Cox proportional hazards regression model. Only variables significantly associated with survival were included in the multivariate regression analyses. Statistical analyses were performed, and graphics were obtained using R ver. 4.1.3 (https://www.r-project.org). A p-value < .05 was considered statistically significant.

RESULTS

Evaluation of TIL-T ratio and comparison with clinicopathological parameters

TIL-T–Max, TIL-T–Min, and TIL-T–Intermediate were calculated as described above. The receiver operating characteristic curve analysis was used to determine the optimal cutoff value with respect to the OS of patients for each TIL-T ratio (Fig. 2). Cutoff points between high and low TIL-T ratios were 19%, 11%, and 13% for TIL-T–Max, TIL-T–Intermediate, and TIL-T–Min, respectively. With TIL-T–Max as the criterion, 72 (75.0%) had > 19% TIL-T–Max and 24 (25.0%) had < 19% TIL-T–Max; with TIL-T–Intermediate, 64 (66.7%) patients had a high TIL-T- Intermediate and 32 (33.3%) had a low TIL-T–Intermediate; and with TIL-T–Min, 36 (37.5%) had a high TIL-T–Min and 60 (62.5%) had a low TIL-T–Min (Table 1). The mean values for the TIL-T–Max, –Intermediate, and –Min were 41.6 % (range, 0.3% to 98.5%; standard deviation [SD], ± 27.72), 26.3% (range, 0.2% to 97.5%; SD, ± 23.18), and 14.4% (range, 0.1% to 88.8%; SD, ±16.75), respectively. The clinicopathological parameters associated with TIL-T ratios are listed in Table 1. A high TIL-

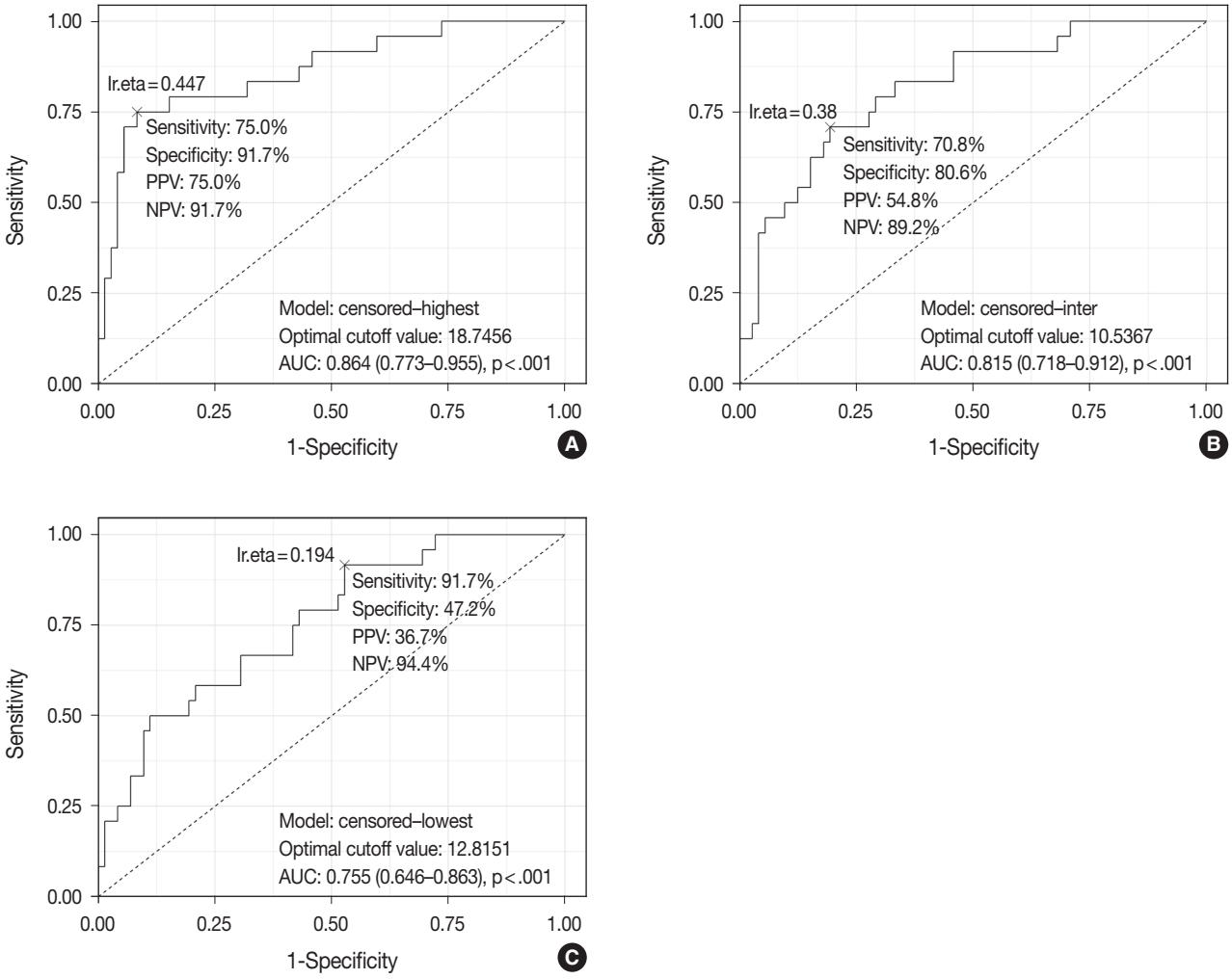

Fig. 2. Receiver operating characteristic curves of tumor-infiltrating T lymphocyte (TIL-T) ratios. The cutoff values of 19%, 11%, and 13% for TIL-T–Max (A), TIL-T–Intermediate (B), and TIL-T–Min (C), respectively, were inferred from theses analyses.

T–Max was significantly associated with serum LDH levels within the normal range (χ^2 = 17.634, degrees of freedom [df] = 1, p < .001), with the group of patients that achieved CR after initial R-CHOP therapy (χ^2 = 10.908, df = 1, p < .001) and with low-risk R-IPI (χ^2 = 12.945, df = 1, p < .001). A high TIL-T–Intermediate was also significantly associated with low serum LDH levels (χ^2 = 8.211, df = 1, p = .004), CR after R-CHOP (χ^2 = 9.647, df = 1, p = .002), and a low risk of R-IPI (χ^2 = 4.208, df = 1, p = .040). The TIL-T–Min was not significantly associated with any of the clinical variables.

Survival analysis

Patients with a high TIL-T–Max showed a significantly longer OS (p < .001) (Fig. 3A). This trend was also observed in the high TIL-T–Intermediate (p < .001) (Fig. 3B) and high TIL-T–Min (p < 0.001) (Fig. 3C). According to the univariate Cox proportional hazards analysis, a shorter OS was significantly associated with a high Ann Arbor stage, and a longer OS was significantly associated with a serum LDH level within the normal range, patients achieving CR after R-CHOP therapy, and low-risk R-IPI (Table 2). Univariate analysis revealed that patients with low TIL-T–Max had a significantly worse prognosis in OS compared to those with high TIL-T–Max (hazard ratio [HR], 15.8; 95% confidence interval [CI], 6.20 to 40.25; p < .001) (Table 2), and those with low TIL-T–Intermediate compared to high TIL-T–Intermediate (HR, 6.91; 95% CI, 2.85 to 16.74; p < .001) (Table 2). This trend was also observed in the TIL-T–Min; patients with a low TIL-T–Min had worse OS than those with a high TIL-T–Min (HR, 7.98; CI, 1.87 to 33.95; p = .005) (Table 2). In multivariate analysis, a low TIL-T–Max was found to be an independent unfavorable prognostic factor in patients with DLBCL NOS (HR, 7.55; 95% CI, 2.54 to 22.42; p < .001). The same trend was also observed in TIL-T–Intermediate (HR, 2.96; 95% CI, 1.17 to 7.53; p = .022) (Table 2, Fig. 4).

DISCUSSION

In this study, we used digital image analysis to evaluate the

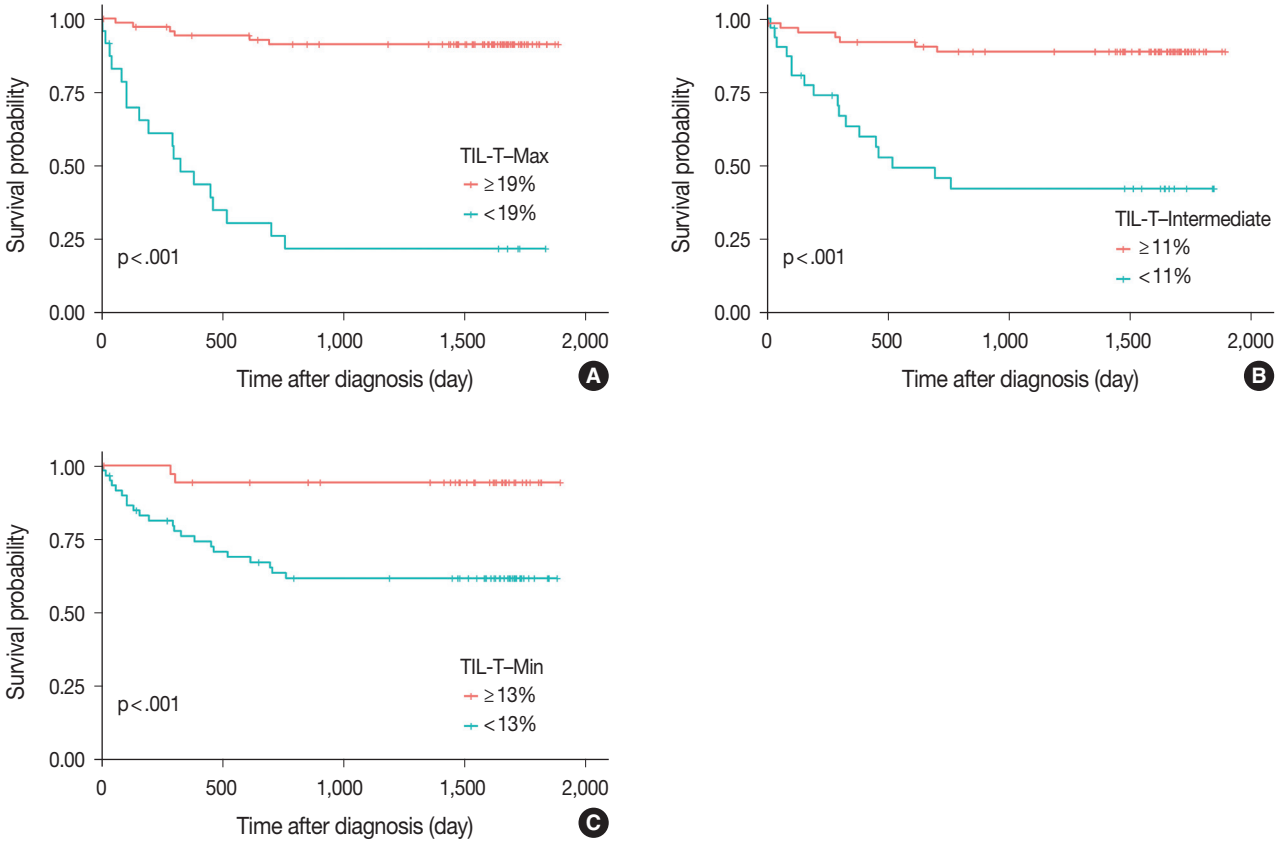

Fig. 3. Prognostic effects of tumor-infiltrating T lymphocyte (TIL-T) ratios in diffuse large B-cell lymphoma, not otherwise specified. The Kaplan-Meier curve demonstrates a longer overall survival in all TIL-T ratios. Significant differences of overall survival in patients were observed in TIL-T–Max (A), TIL-T–Intermediate (B), and TIL-T–Min (C). The p-values were determined by the log-rank test.

https://doi.org/10.4132/jptm.2023.11.02

Table 2. Univariate and multivariate analyses of factors associated with overall survival in 96 diffuse large B-cell lymphoma, not otherwise specified patients

Variable	Comparison/referent	Univariate			Multivariate		
		HR	95% CI	p-value	HR	95% CI	p-value
TIL-T–Max							
Age (yr)	>60/≤60	0.62	0.28–1.40	.251			
Sex	Male/Female	1.42	0.61–3.33	.414			
Ann Arbor stage	III–IV/I–II	4.14	1.64–10.43	.003	1.24	0.42–3.66	.699
Cell-of-origin	Non-GCB/GCB	1.60	0.64–4.03	.318			
Serum LDH level	Low/High	0.18	0.07–0.45	<.001	0.76	0.20–2.77	.675
Treatment	Non-CR/CR after R-CHOP	37.42	5.04–277.70	<.001	23.81	3.13–181.15	.002
R-IPI	Low risk/High risk	0.15	0.06–0.37	<.001	0.50	0.14–1.77	.282
TIL-T–Max	Low/High	15.81	6.20–40.25	<.001	7.55	2.54–22.42	<.001
TIL-T–Intermediate							
Age (yr)	>60/≤60	0.62	0.28–1.40	.251			
Sex	Male/Female	1.42	0.61–3.33	.414			
Ann Arbor stage	III–IV/I–II	4.14	1.64–10.43	.003	0.99	0.34–2.89	.981
Cell-of-origin	Non-GCB/GCB	1.60	0.64–4.03	.318			
Serum LDH level	High/Low	0.18	0.07–0.45	<.001	0.35	0.12–1.06	.065
Treatment	Non-CR/CR after R-CHOP	37.42	5.04–277.70	<.001	26.00	3.44–-196.81	.002
R-IPI	Low risk/High risk	0.15	0.06–0.37	<.001	0.44	0.14–1.44	.175
TIL-T–Intermediate	Low/High	6.91	2.85–16.74	<.001	2.96	1.17–7.53	.022
TIL-T–Min							
Age (yr)	>60/≤60	0.62	0.28–1.40	.251			
Sex	Male/Female	1.42	0.61–3.33	.414			
Ann Arbor stage	III-IV/I-II	4.14	1.64–10.43	.003	1.05	0.33–3.32	.936
Cell-of-origin	Non-GCB/GCB	1.60	0.64–4.03	.318			
Serum LDH level	High/Low	0.18	0.07–0.45	<.001	0.43	0.13–1.36	.151
Treatment	Non-CR/CR after R-CHOP	37.42	5.04–277.70	<.001	25.76	3.40–195.27	.002
R-IPI	Low risk/High risk	0.15	0.06–0.37	<.001	0.47	0.13–1.72	.254
TIL-T–Min	Low/High	7.98	1.87–33.95	.005	3.80	0.82–17.58	.088

HR, hazard ratio; CI, confidence interval; TIL-T, tumor-infiltrating T lymphocyte; GCB, germinal center B-cell-like; LDH, lactate dehydrogenase; CR, complete remission; R-CHOP, rituximab plus cyclophosphamide, doxorubicin, vincristine, and prednisone; R-IPI, revised International Prognostic Index.

exact ratio of TIL-T in patients with DLBCL NOS. Low TIL-T ratios in the TIL-T–Max, TIL-T–Intermediate, and TIL-T–Min were associated with shorter OS and were found to be independent prognostic factors in patients with DLBCL.

Previous studies have focused on the prognostic significance of the total TIL-T ratio in patients with DLBCL. An immunohistochemical study of TIL-T in DLBCL showed no correlation between survival and TIL-T percentage [16]. Another study found that the percentage of CD3+ cells (total T cells) had no impact on DLBCL patient outcomes [18]. However, Xu et al. (2001) [15] found that a TIL-T ratio >20% showed a favorable prognosis compared to a TIL-T ratio <20%. Another study reported that patients with high CD3+ TIL-T levels (>45%) had better event-free survival and OS rates, although CD4+ TIL-T was statistically more relevant than CD3+ TIL-T in predicting patient outcomes [17]. All the studies mentioned above were conducted using flow cytometry analyses of fresh biopsy tissue, except for one by Lippman et al. (1990) [16]. Flow cytometric analysis of the TIL-T ratio in DLBCL specimens may have contributed to these contradictory results. Flow cytometric analysis, a rapid multi-parametric analysis of single cells in solution, lacks morphological correlation. Sampling errors such as the inclusion of normal lymphoid tissue adjacent to the malignant tumor area can influence the sensitivity of flow cytometry and result in reports that are not representative of the actual TME. Also, flow cytometric analysis cannot take into consideration of the differing areas of densities of TIL-Ts in one tumor specimen. In our study, formalin-fixed paraffin-embedded tissue specimens were used for IHC staining, and morphological evaluation of the whole slide was performed to detect the actual focus of T-lymphocyte infiltration among diffuse neoplastic B-cell populations. Moreover, the correlation between the TIL-T ratio and patient outcome was more statistically significant in the TIL-T–Max, suggesting that the clinical behavior of DLBCL may be more

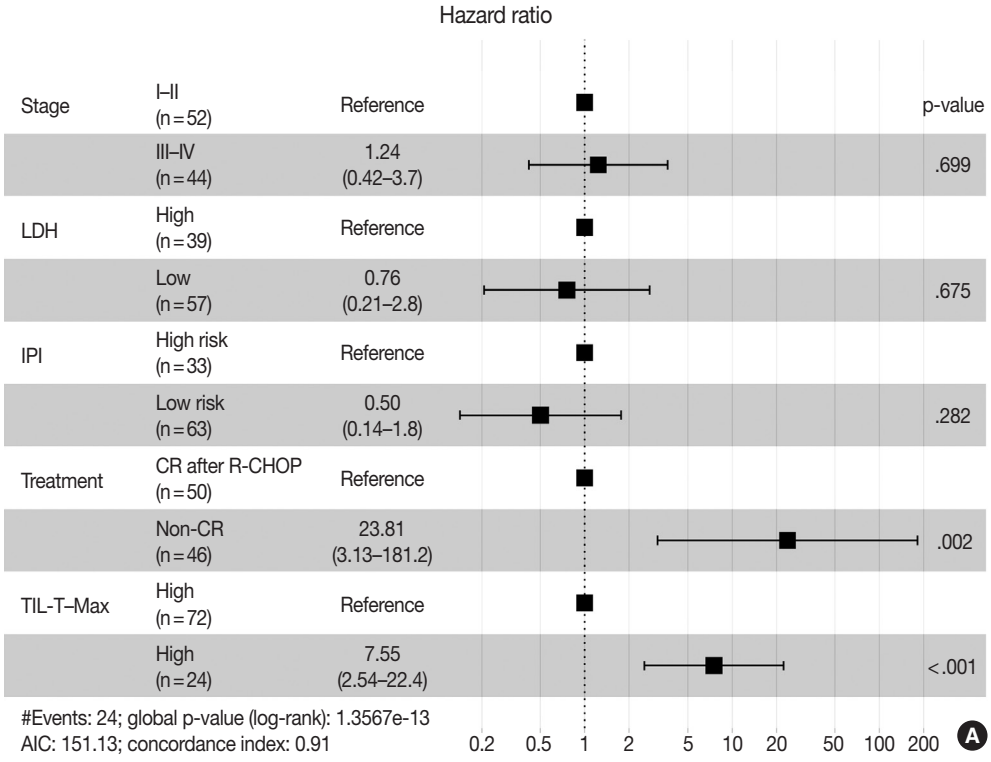

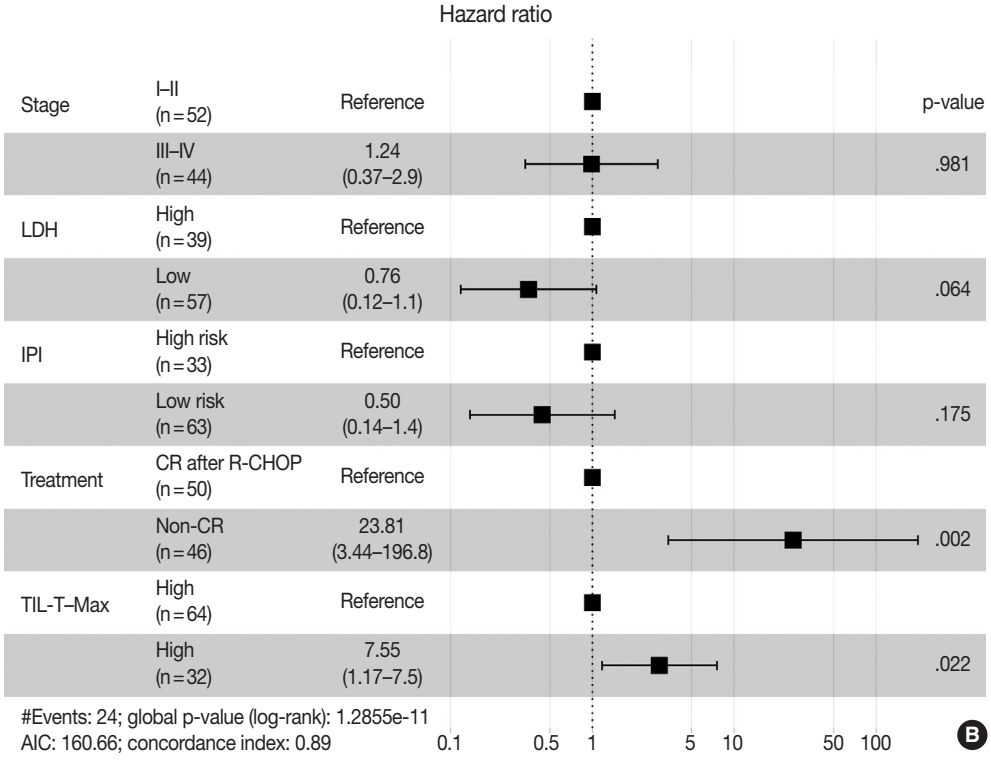

Fig. 4. Associations between survival probability and tumor-infiltrating T lymphocyte (TIL-T) ratios. Hazards ratios are shown separately for TIL-T–Max (A), TIL-T–Intermediate (B), and TIL-T–Min (C). Hazard ratio and p-values were corrected by Ann Arbor stage, serum lactate dehydrogenase (LDH) levels, patient treatment, and the revised International Prognostic Index (R-IPI) score. AIC, Akaike information criterion; CR, complete remission; R-CHOP, rituximab plus cyclophosphamide, doxorubicin, vincristine, and prednisone. (Continued to next page)

https://doi.org/10.4132/jptm.2023.11.02

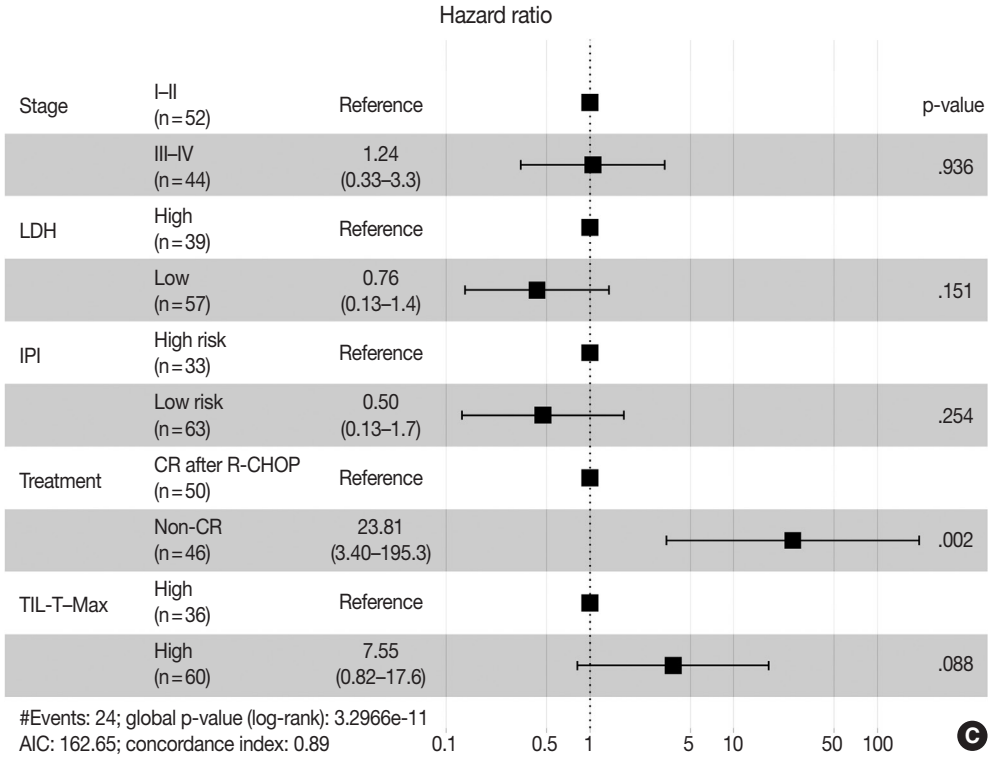

Fig. 4. (Continued from previous page)

accurately reflected by the TIL-T ratio at the densest T lymphocyte infiltration. This finding underscores the importance of histological assessment in determining the TIL-T ratio in patients with DLBCL. TIL-T levels of tumor are mainly determined by the intrinsic immunogenicity of tumor cells. In partial areas of tumors, it is possible that TIL-T levels are lowered by other factors, such as immune checkpoints. Therefore, among various TIL-T levels in tumors, it could be considered that TIL-T–Max is most likely to accurately reflect the intrinsic immunogenic capacity of tumor cells, which may have contributed to a more precise predictions of a patient prognosis. Further study is required to confirm the prognostic value of the TIL-T–Max and to substantiate the hypothesis behind it.

In our results, the high TIL-T ratio group according to the TIL-T–Max showed no correlation with patient age, sex, or COO of tumor. The Ann Arbor stage also showed no statistically significant association with the TIL-T–Max. However, serum LDH levels were significantly elevated in patients with a low TIL-T–Max. This suggests that the degree of TIL-T is determined by the immunogenicity of the tumor cells rather than by the patient's demographic characteristics or the origin of the tumor cells. Tumor immunogenicity is influenced by tumor mutation burden, DNA mismatch repair function, antigen presentation defects, and immune checkpoint genes [22,23]. Therefore, further studies are needed to compare TIL-T levels with the molecular features and expression of immune checkpoint genes in DLBCL. Tumor immunogenicity can affect not only the prognosis of patients, but also their responsiveness to immunotherapy, such as immune checkpoint blockade or CAR-T therapy. Therefore, it is necessary to conduct additional research on the application of the TIL-T ratio criteria presented in our study (a ratio of ≥19% measured in the TIL-T–Max area) for immunotherapy in patients with DLBCL through digital image analysis.

As more pathology departments implement digital reviews, digital image analyses are expected to become more commonplace [24]. It is important to recognize accurate quantification facilitated by artificial intelligence for prognostic and predictive scoring as a diagnostic tool for pathologists. Several studies have shown that digital image analysis is equal to or better than manual scoring by pathologists [25,26]. The application of digital image analysis to assess TIL-T ratios in tissue specimens may help minimize inter- and intra-observer variability, thus contributing to the discovery of accurate cutoff points for TIL-T ratio analysis in the future.

This study has several limitations. First, this study was a retrospective analysis and lacked validation of the cutoff point used

to differentiate between high and low TIL-T levels. Second, molecular analyses of the biological factors that determine the level of TIL-T are lacking. Further studies are required to address these shortcomings, including verification of the results and cutoff values using outside cohorts. Additional subset analyses of different T-cell populations in tissue specimens and the genetic profiles of the different groups of TIL-T ratios may help understand the immunobiology of the TILs in DLBCL.

Patients with DLBCL with high TIL-T ratios showed a significantly better prognosis than those with low TIL-T ratios, and the TIL-T ratio was an independent indicator of OS. These results suggest that TIL-T may play a critical role in DLBCL disease progression and evaluating the level of TIL-T in DLBCL specimens using digital pathology software may be useful in predicting the clinical behavior and response to immunotherapy in patients with DLBCL.

Ethics Statement

All methods were performed in accordance with the Helsinki Declaration, and all protocols of this study were approved by the Institutional Review Board (IRB) of the Samsung Medical Center (IRB file number: SMC 2021-01-093-004). Formal written informed consent was not required with a waiver by the appropriate IRB.

Availability of Data and Material

The datasets generated or analyzed during the study are available from the corresponding author on reasonable request.

Code Availability

Not applicable.

ORCID

Yunjoo Cho https://orcid.org/0000-0003-1309-2015
Jiyeon Lee https://orcid.org/0000-0002-4457-7499
Bogyeong Han https://orcid.org/0000-0003-0391-7415
Sang Eun Yoon https://orcid.org/0000-0002-0379-5297
Seok Jin Kim https://orcid.org/0000-0002-2776-4401
Won Seog Kim https://orcid.org/0000-0002-5400-0466
Junhun Cho https://orcid.org/0000-0002-6089-9340

Author Contributions

Conceptualization: YC, JC. Data acquisition: SEY, SJK, WSK. Data analysis: YC, JL, BH. Writing—original draft: YC. Writing—review & editing: WSK, JC. Approval of final manuscript: all authors.

Conflicts of Interest

The authors declare that they have no potential conflicts of interest.

Funding Statement

No funding to declare.

References

1. Alaggio R, Amador C, Anagnostopoulos I, et al. The 5th edition of the World Health Organization classification of haematolymphoid tumours: lymphoid neoplasms. Leukemia 2022; 36: 1720-48.
2. Campo E, Jaffe ES, Cook JR, et al. The International Consensus Classification of Mature Lymphoid Neoplasms: a report from the Clinical Advisory Committee. Blood 2022; 140: 1229-53.
3. Younes A, Sehn LH, Johnson P, et al. Randomized phase III trial of ibrutinib and rituximab plus cyclophosphamide, doxorubicin, vincristine, and prednisone in non-germinal center B-cell diffuse large B-cell lymphoma. J Clin Oncol 2019; 37: 1285-95.
4. Davies A, Cummin TE, Barrans S, et al. Gene-expression profiling of bortezomib added to standard chemoimmunotherapy for diffuse large B-cell lymphoma (REMoDL-B): an open-label, randomised, phase 3 trial. Lancet Oncol 2019; 20: 649-62.
5. Nowakowski GS, Chiappella A, Gascoyne RD, et al. ROBUST: a phase III study of lenalidomide plus R-CHOP versus placebo plus R-CHOP in previously untreated patients with ABC-type diffuse large B-cell lymphoma. J Clin Oncol 2021; 39: 1317-28.
6. Zhang J, Medeiros LJ, Young KH. Cancer immunotherapy in diffuse large B-cell lymphoma. Front Oncol 2018; 8: 351.
7. Wang L, Li LR, Young KH. New agents and regimens for diffuse large B cell lymphoma. J Hematol Oncol 2020; 13: 175.
8. Nicholas NS, Apollonio B, Ramsay AG. Tumor microenvironment (TME)-driven immune suppression in B cell malignancy. Biochim Biophys Acta 2016; 1863: 471-82.
9. Scott DW, Gascoyne RD. The tumour microenvironment in B cell lymphomas. Nat Rev Cancer 2014; 14: 517-34.
10. Fridman WH, Pages F, Sautes-Fridman C, Galon J. The immune contexture in human tumours: impact on clinical outcome. Nat Rev Cancer 2012; 12: 298-306.
11. Keane C, Vari F, Hertzberg M, et al. Ratios of T-cell immune effectors and checkpoint molecules as prognostic biomarkers in diffuse large B-cell lymphoma: a population-based study. Lancet Haematol 2015; 2: e445-55.
12. Xu-Monette ZY, Xiao M, Au Q, et al. Immune profiling and quantitative analysis decipher the clinical role of immune-checkpoint expression in the tumor immune microenvironment of DLBCL. Cancer Immunol Res 2019; 7: 644-57.
13. Sermer D, Batlevi C, Palomba ML, et al. Outcomes in patients with DLBCL treated with commercial CAR T cells compared with alternate therapies. Blood Adv 2020; 4: 4669-78.
14. Hopfinger G, Jager U, Worel N. CAR-T cell therapy in diffuse large B cell lymphoma: hype and hope. Hemasphere 2019; 3: e185.
15. Xu Y, Kroft SH, McKenna RW, Aquino DB. Prognostic significance of tumour-infiltrating T lymphocytes and T-cell subsets in de novo diffuse large B-cell lymphoma: a multiparameter flow cytometry study. Br J Haematol 2001; 112: 945-9.
16. Lippman SM, Spier CM, Miller TP, Slymen DJ, Rybski JA, Grogan TM. Tumor-infiltrating T-lymphocytes in B-cell diffuse large cell lymphoma related to disease course. Mod Pathol 1990; 3: 361-7.
17. Keane C, Gill D, Vari F, Cross D, Griffiths L, Gandhi M. CD4(+) tumor infiltrating lymphocytes are prognostic and independent of R-IPI in patients with DLBCL receiving R-CHOP chemo-immunotherapy. Am J Hematol 2013; 88: 273-6.
18. Ansell SM, Stenson M, Habermann TM, Jelinek DF, Witzig TE. Cd4+ T-cell immune response to large B-cell non-Hodgkin's lymphoma predicts patient outcome. J Clin Oncol 2001; 19: 720-6.
19. Hans CP, Weisenburger DD, Greiner TC, et al. Confirmation of the molecular classification of diffuse large B-cell lymphoma by immu-

nohistochemistry using a tissue microarray. Blood 2004; 103: 275-82.
20. Sehn LH, Berry B, Chhanabhai M, et al. The revised International Prognostic Index (R-IPI) is a better predictor of outcome than the standard IPI for patients with diffuse large B-cell lymphoma treated with R-CHOP. Blood 2007; 109: 1857-61.
21. Bankhead P, Loughrey MB, Fernandez JA, et al. QuPath: Open source software for digital pathology image analysis. Sci Rep 2017; 7: 16878.
22. Wang S, He Z, Wang X, Li H, Liu XS. Antigen presentation and tumor immunogenicity in cancer immunotherapy response prediction. Elife 2019; 8: e4020.
23. Blankenstein T, Coulie PG, Gilboa E, Jaffee EM. The determinants of tumour immunogenicity. Nat Rev Cancer 2012; 12: 307-13.
24. Mukhopadhyay S, Feldman MD, Abels E, et al. Whole slide imaging versus microscopy for primary diagnosis in surgical pathology: a multicenter blinded randomized noninferiority study of 1992 cases (pivotal study). Am J Surg Pathol 2018; 42: 39-52.
25. Gudlaugsson E, Skaland I, Janssen EA, et al. Comparison of the effect of different techniques for measurement of Ki67 proliferation on reproducibility and prognosis prediction accuracy in breast cancer. Histopathology 2012; 61: 1134-44.
26. Stalhammar G, Robertson S, Wedlund L, et al. Digital image analysis of Ki67 in hot spots is superior to both manual Ki67 and mitotic counts in breast cancer. Histopathology 2018; 72: 974-89.

JPTM
Journal of Pathology and Translational Medicine 2024; 58: 22-28
https://doi.org/10.4132/jptm.2023.11.21

ORIGINAL ARTICLE

Identification of invasive subpopulations using spatial transcriptome analysis in thyroid follicular tumors

Ayana Suzuki[1,2], Satoshi Nojima[1], Shinichiro Tahara[1], Daisuke Motooka[3], Masaharu Kohara[1], Daisuke Okuzaki[3,4], Mitsuyoshi Hirokawa[2], Eiichi Morii[1,4]

[1]Department of Pathology, Graduate School of Medicine, Osaka University, Suita, Osaka;
[2]Department of Diagnostic Pathology and Cytology, Kuma Hospital, Kobe, Hyogo;
[3]Genome Information Research Center, Research Institute for Microbial Diseases, Osaka University, Suita, Osaka;
[4]Institute for Open and Transdisciplinary Research Initiatives, Osaka University, Suita, Osaka, Japan

Background: Follicular tumors include follicular thyroid adenomas and carcinomas; however, it is difficult to distinguish between the two when the cytology or biopsy material is obtained from a portion of the tumor. The presence or absence of invasion in the resected material is used to differentiate between adenomas and carcinomas, which often results in the unnecessary removal of the adenomas. If nodules that may be follicular thyroid carcinomas are identified preoperatively, active surveillance of other nodules as adenomas is possible, which reduces the risk of surgical complications and the expenses incurred during medical treatment. Therefore, we aimed to identify biomarkers in the invasive subpopulation of follicular tumor cells. **Methods:** We performed a spatial transcriptome analysis of a case of follicular thyroid carcinoma and examined the dynamics of CD74 expression in 36 cases. **Results:** We identified a subpopulation in a region close to the invasive area, and this subpopulation expressed high levels of CD74. Immunohistochemically, CD74 was highly expressed in the invasive and peripheral areas of the tumor. **Conclusions:** Although high CD74 expression has been reported in papillary and anaplastic thyroid carcinomas, it has not been analyzed in follicular thyroid carcinomas. Furthermore, the heterogeneity of CD74 expression in thyroid tumors has not yet been reported. The CD74-positive subpopulation identified in this study may be useful in predicting invasion of follicular thyroid carcinomas.

Key Words: Thyroid; Follicular carcinoma; Spatial transcriptome analysis; CD74; Capsular invasion

Received: October 27, 2023 **Revised:** November 21, 2023 **Accepted:** November 21, 2023
Corresponding Author: Ayana Suzuki, MHSc, Department of Diagnostic Pathology and Cytology, Kuma Hospital, Kobe, 8-2-35, Shimoyamate-dori, Chuo-ku, Kobe, Hyogo, 650-0011, Japan
Tel: +81-78-371-3721, Fax: +81-78-371-3645, E-mail: suzuki01@kuma-h.or.jp

Follicular tumors include follicular thyroid adenomas and carcinomas, which are differentiated by the presence of capsular or vascular invasion in the resected materials or metastasis [1]. Owing to the absence of morphological differences between the tumor cells, fine-needle aspiration cytology, in which the contents of the nodule are sampled, and tissue biopsy, in which a portion of the tumor is sampled, cannot differentiate between them preoperatively [2]. Hence, many adenomas are unnecessarily resected [3,4]. If potential follicular thyroid carcinoma nodules are identified preoperatively, active surveillance of adenomas is possible, which could reduce the risk of surgical complications and decrease the cost of medical treatment.

Many studies have reported methods to distinguish follicular thyroid adenomas from carcinomas [5-8]. Some of them require special equipment and techniques for analysis [5,6]. Markers used in immunohistochemistry may be helpful to distinguish between the two using simple methods. Several studies have suggested markers for this purpose; however, no definitive marker worthy of clinical application has yet been found [7-12]. Spatial transcriptome analysis technology for formalin-fixed paraffin-embedded (FFPE) specimens has advanced considerably, and tumor heterogeneity can be detected [13,14]. If invasive tumor subpopulations can be detected by spatial transcriptome analysis of FFPE specimens of follicular thyroid carcinomas, new markers for assessing the invasiveness of follicular thyroid carcinoma may be identified. The eligibility of the target tumors for resection can

pISSN 2383-7837
eISSN 2383-7845

be determined during tissue biopsy and cytology. In this study, we aimed to identify tumor subpopulations composing invasive areas using spatial transcriptome analysis of FFPE specimens containing the invasive area of follicular thyroid carcinoma and to perform immunohistochemical studies based on these results.

MATERIALS AND METHODS

Patients

Between May 2016 and December 2022, 283 follicular thyroid carcinoma nodules were resected at the Kuma Hospital in Japan. Of these, 36 nodules (minimally invasive [n = 18], encapsulated angioinvasive [n = 8], widely invasive [n = 10]) were extracted after excluding those with papillary-like nuclear features, poorly differentiated carcinoma components, and very small invasive areas. A nodule with an invasive area within a 5-mm-diameter circle was subjected to spatial transcriptome analysis, and all cases were subjected to immunohistochemical staining. The clinicopathological features of the enrolled 36 cases are shown in Table 1.

Spatial transcriptome analysis

We performed spatial transcriptome analysis using Visium CytAssist Spatial Gene Expression for FFPE (10x Genomics, Pleasanton, CA, USA). In this analysis, the whole RNA transcriptome of cells in each spot of the specialized slides was obtained from FFPE tissue sections. Each spot contained approximately 10–20 cells, and the RNA transcriptome of these cells revealed the features of RNA expression in each spot. The tissues were sectioned as described in the Visium CytAssist Spatial Gene Expression for FFPE Tissue Preparation Guide (CG000518). Sections were stained with hematoxylin and eosin (H&E), imaged, and de-cover-slipped, followed by H&E de-staining and de-crosslinking. Glass slides with tissue sections were processed using a Visium CytAssist instrument to transfer analytes to a Visium CytAssist Spatial Gene Expression slide with a 0.42 cm^2 capture area. Probe extension and library construction steps followed the standard Visium for the FFPE workflow. Libraries were sequenced using a DNBSEQ-G400 sequencer (BGI) (read 1: 28 bp, read 2: 100 bp). Spatial data were pre-processed and aligned using 10x Genomics Space Ranger v1.3.0 with the reference human genome GRCh38 (refdata-gex-GRCh38-2020-A) to generate raw unique molecular identifier count spot matrices. Dimensionality reduction was performed using classical principal component analysis integrated uniform manifold approximation and projection (UMAP) [15]. Unsupervised clustering of the data spots was performed using Louvain clustering [16] integrated into the BioTuring Lens with a resolution of 0.1. Further downstream analysis and gene expression visualization were conducted using the BBrowser (BioTuring, San Digo, CA, USA).

CD74 immunohistochemical analysis

Immunohistochemical staining was performed using 3-μm-thick FFPE specimens. Anti-CD74 (1:100, LN2, ab9514, Abcam, Cambridge, UK) and anti–thyroid transcription factor-1 (TTF-1; 1:100, SP141, ab227652, Abcam) were used as primary antibodies. Staining was performed using a Dako Autostainer Link 48+ (Dako, Carpinteria, CA, USA), according to the manufacturer's recommendations. The expression of CD74 was assessed using a visual grading system based on staining intensity under light microscopy. High intensity (++), low intensity (+), and no signal (–) were defined as strong, weak, and no staining, respectively. The histological index was calculated using the following formula:

Histological index = 2 × (% cells of high intensity) + 1 × (% cells of low intensity).

The invasive area was defined as a tumor lesion invading or over the capsule or an angioinvasive lesion. The peripheral area of the tumor was defined as the tumor lesion within 1 mm of the tumor border. The tumor central area was defined as the tumor lesion > 1 mm from the border. One pathology assistant (A.S) and one pathologist (E.M) scored the data independently.

RESULTS

Spatial transcriptome analysis

Among the 36 cases of follicular thyroid carcinoma, a nodule with an invasive area within a circle of 5 mm diameter was subjected to spatial transcriptome analysis (Fig. 1A). As tissue samples in the circle could be examined in the spatial transcriptome

Table 1. Clinicopathological features of enrolled cases

	Minimally invasive	Encapsulated angioinvasive	Widely invasive	Total
No.	18	8	10	36
Sex (male:female)	3:15	4:4	2:8	9:27
Age (yr), mean (range)	49.1 (27–83)	43.5 (11–68)	47.3 (12–69)	47.4 (11–83)

analysis, we selected a case in which the invasive and non-invasive areas were involved in the circle. A minimally invasive case was selected for spatial transcriptome analysis. The invasive, peripheral, and central areas were shown in Fig. 1B. Louvain clustering with a resolution of 0.1 showed three clusters, and the H&E staining image merged with the three clusters (Fig. 1C). Dimensionality reduction using classical principal component analysis integrated with UMAP showed that the features of cluster 1 were distinct from those of clusters 2 and 3 (Fig. 1D). Cluster 1 was detected in the invasive area, where clusters 2 or 3 were not found (Fig. 1C, asterisk portion). The BioTuring Lens showed 10 highly expressed genes in each cluster (Table 2). CD74 was highly expressed in cluster 1 but not in clusters 2 or 3. We examined the expression of CD74 with immunohistochemistry in all 36 cases of follicular thyroid carcinoma.

CD74 immunohistochemical analyses

Immunohistochemically, the CD74 staining intensity was heterogeneous. The intensity increased in the invasive and peripheral areas of the tumors (Fig. 2A, B). Since CD74 is expressed in macrophages, double staining for CD74 and TTF-1 was performed to confirm that CD74-positive cells were follicular thyroid carcinoma cells. CD74-positive cells in the invasive and peripheral areas were TTF-1 positive, indicating that CD74

Table 2. Top 10 highly expressed genes in each cluster

Cluster 1	Cluster 2	Cluster 3
CD74	COL9A3	COL9A3
IGHG1	SFRP1	APLP2
IGHG3	APLP2	MT1G
IGHM	CD24	CD24
B2M	GPX3	SFRP1
IGHA1	MT1G	SLC26A7
COL1A1	PDCD4	PDCD4
COL3A1	SLC26A7	GPX3
ACTB	IGFG1	FCGBP
FOS	B2M	APP

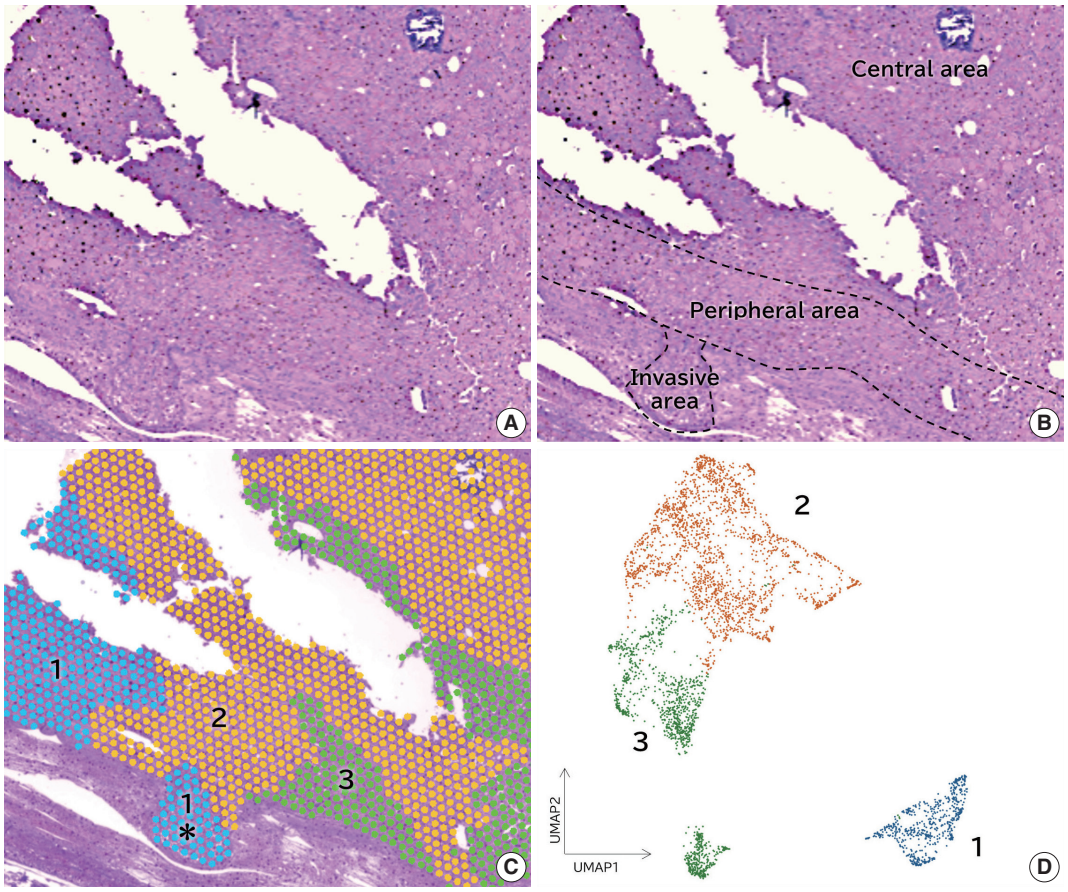

Fig. 1. Spatial transcriptomic analysis of follicular thyroid carcinoma with minimally invasive area. (A) Hematoxylin and eosin staining of examined case. (B) The invasive, peripheral, and central areas are shown. (C) Three clusters are obtained by Louvain clustering with a resolution of 0.1. Invasive area is shown with the asterisk. (D) Features of three clusters obtained by dimensionality reduction through classical principal component analysis integrated uniform manifold approximation and projection (UMAP).

https://doi.org/10.4132/jptm.2023.11.21

positivity was detected in tumor cells located in the invasive and peripheral areas (Fig. 2C, D).

We evaluated the CD74 staining intensity in follicular thyroid carcinoma cells using a histological index (Fig. 3A). The histological index was 98.1 ± 50.6 (mean ± standard deviation) in invasive areas, 96.0 ± 48.5 in peripheral areas, and 65.8 ± 36.2 in central areas (Fig. 3B, C). Significant differences were detected between the invasive and central areas and between the peripheral and central areas ($p < .01$).

DISCUSSION

Follicular thyroid adenomas and carcinomas are collectively treated as follicular tumors. They are difficult to differentiate using fine-needle aspiration cytology [2], and the clinical management is not differentiated [3]. However, because follicular thyroid adenomas, which comprise the majority of follicular tumors, are benign, unnecessary resection is often performed in many cases. Several studies have proposed the use of various markers for distinguishing between follicular thyroid adenomas and carcinomas. Sato et al. [5] reported the utility of p53-binding protein 1 (53BP1) expression in nuclear foci, a marker reflecting the DNA damage response, to distinguish follicular thyroid carcinomas from adenomas. 53BP1 showed high sensitivity (89.3%) and specificity (83.3%), although the interpretation of results required advanced techniques. Suzuki et al. [6] attempted to differentiate between the two tumor types by determining the cell proliferation index reflecting increased nuclear DNA levels using a special flow cytometry device, LC-1000 (Sysmex Corporation, Tokyo, Japan). This method automatically calculates the index; however, a huge initial investment is required. An easier method to incorporate is immunohistochemistry, and antibodies such as ki-67, bax, secreted protein acidic and rich in cysteine, HBME1, Rac1, Galectin-3, and CD61 have been investigated, but none of them is currently in clinical use [7-12].

RNA sequences of microdissected samples are useful for identifying molecular markers; however, they only provide information on the bulk expression of tumor cells in the microdissected area. The most precise investigation of RNA expression is a single-cell RNA sequence; however, this method loses the spatial

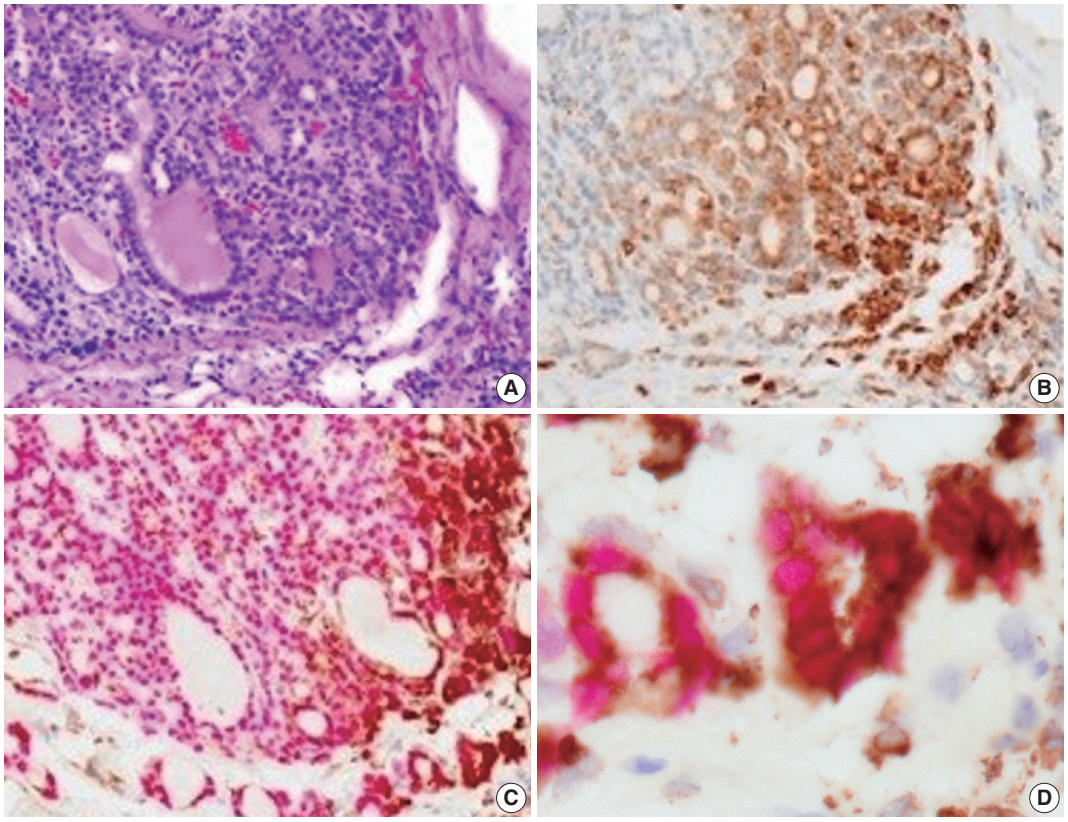

Fig. 2. Immunohistochemical analyses of CD74 in follicular thyroid carcinoma. (A) Hematoxylin and eosin staining. (B) Immunohistochemical staining using anti-CD74 antibody. (C) Double immunohistochemical staining using anti-CD74 (brown) and anti–thyroid transcription factor-1 (red) antibodies. (D) High power field of (C).

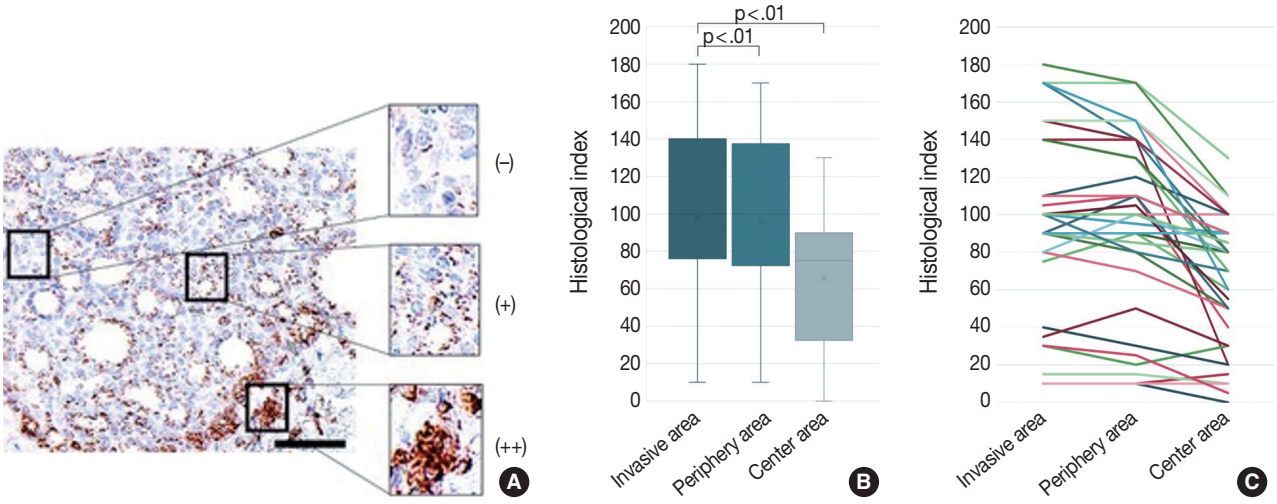

Fig. 3. Evaluation of CD74 staining intensity with histological index. (A) Typical image of CD74 immunohistochemical staining. Staining intensity was divided into three categories; high intensity (++), low intensity (+), and no signal (–) defined as strong, weak, and no staining, respectively. (B) Box plot of CD74 staining intensity in invasive, peripheral, and central areas. Significant differences were detected between the invasive and central areas, and between peripheral and central areas. (C) Line graph of CD74 staining intensity in each case.

information of each individual cell. Spatial transcriptome analysis is a new technique that enables whole-transcriptome analysis without microdissection of FFPE specimens while maintaining morphological information; it has been investigated in a variety of tissues [13,14]. In this study, we performed spatial transcriptome analysis using follicular thyroid carcinoma and identified a subpopulation in the invasive area that was found to express high levels of CD74.

CD74 is known to play an important role in antigen presentation by mediating the construction of major histocompatibility complex class II complexes and intracellular trafficking [17]. CD74 has also been reported to be upregulated in malignant tumors and involved in increased growth and metastatic potential [18-28]. In a study on urothelial bladder carcinomas by Choi et al. [18], urothelial bladder carcinomas with high CD74 expression were characterized by older age, high World Health Organization grade, and advanced stages of TNM classification. In a study on gastrointestinal carcinomas, Gold et al. [26] found that the expression of CD74 in gastrointestinal carcinomas was significantly greater than that in their normal tissue counterparts ($p < .001$ or lower). With regard to thyroid carcinomas, Varinelli et al. [27] and Cheng et al. [28] reported that the CD74 axis plays an important role in the biology of aggressive cases in papillary and anaplastic thyroid carcinomas. In these two studies [27,28], CD74 staining was detected in all tumor cells of aggressive cases, and no heterogeneous staining was reported. To our knowledge, the present study is the first report of CD74 staining in follicular thyroid carcinomas and the heterogeneous staining intensity of CD74 was detected for the first time, suggesting the presence of an invasive subpopulation of follicular tumor cells. In a study by Cheng et al. [28], treatment with anti-CD74 antibody in papillary thyroid carcinoma cell lines inhibited cell growth, colony formation, cell migration and invasion, and vascular endothelial growth factor secretion. Our results suggested that CD74 might play a role in cell invasion and might be a novel therapeutic target for follicular thyroid carcinomas, such as papillary thyroid carcinoma.

Our results demonstrated a significantly higher staining score in the invasive area than in the central area ($p < .01$), suggesting that the CD74-positive subpopulation may be used to predict the invasion of follicular tumors. Although there was no significant difference between the invasive and peripheral areas just below the capsule ($p = .429$), Gold et al. [26] stated that precursor lesions might express the same or higher CD74 levels as the respective cancers, as the activation of survival pathways was particularly important in the early stages of tumorigenesis. It was possible that the positive cells observed immediately below the capsule in our study were near invasion. Although this study was performed on resected material, we expect that immunocytochemical staining for CD74 will be performed in the future on nodules suspected of having follicular tumors on cytological examination or biopsy tissue specimens to determine the possibility of invasion before surgery, which will contribute to reducing unnecessary resection of nodules with a low possibility of invasion.

In this study, we only included follicular thyroid carcinomas with a clear invasion. Future studies are required to examine CD74

https://doi.org/10.4132/jptm.2023.11.21

immunostaining in patients with follicular tumors of uncertain malignant potential [1] with unclear histological status to identify whether they are follicular thyroid adenomas or carcinomas and prospectively observe their prognosis. The correlation between the staining results and prognosis provided a better confirmation of the relationship between CD74 immunostaining and invasion.

Ethics Statement

The study protocol was reviewed and approved by the Institutional Review Board of Kuma Hospital (no. 20230112-2, 12/01/2023) and Osaka University Clinical Research Review Committee (no. 22425, 17/02/2023). This study complied with the 1964 Declaration of Helsinki and its later amendments. All study participants provided informed consent.

Availability of Data and Material

The datasets generated or analyzed during the study are available from the corresponding author on reasonable request.

Code Availability

Not applicable.

ORCID

Ayana Suzuki	https://orcid.org/0000-0002-0827-1580
Satoshi Nojima	https://orcid.org/0000-0002-5124-0026
Shinichiro Tahara	https://orcid.org/0000-0001-6134-3275
Daisuke Motooka	https://orcid.org/0000-0002-4616-9608
Masaharu Kohara	https://orcid.org/0009-0006-7636-5833
Daisuke Okuzaki	https://orcid.org/0000-0002-4552-783X
Mitsuyoshi Hirokawa	https://orcid.org/0000-0001-5558-7142
Eiichi Morii	https://orcid.org/0000-0001-8490-3650

Author Contributions

Conceptualization: SN, EM, AS. Data curation: SN, EM. Formal analysis: SN, AS. Investigation: SN, AS, MK. Methodology: SN, ST, DM, DO, MK. Project administration: SN, EM. Resources: EM. Supervision: SN, EM. Writing—original draft: AS, EM. Writing—review & editing: SN, ST, DM, DO, MH, EM. Approval of the final manuscript: all authors.

Conflicts of Interest

The authors declare that they have no potential conflicts of interest.

Funding Statement

This work was supported by JSPS KAKENHI under Grant Numbers A19H034520, T22K194330 and A23H027000, and by AMED under Grant Number JP21ae0121049.

Acknowledgments

We would like to thank Editage (www.editage.jp) for English language editing.

References

1. World Health Organization. WHO classification of tumours online. Endocrine and neuroendocrine tumours. 5th ed. Thyroid tumours [Internet]. Geneva: World Health Organization, 2022 [cited 2023 Oct 25]. Available from: https://tumourclassification.iarc.who.int/chapters/53.
2. Auger M, Callegari F, Fadda G, Hirokawa M, Rooper L. Follicular neoplasm. In: Ali SZ, VanderLaan PA, eds. The Bethesda system for reporting thyroid cytopathology: definitions, criteria, and explanatory notes. 3rd ed. Cham: Springer, 2023; 81-95.
3. Haugen BR, Alexander EK, Bible KC, et al. 2015 American Thyroid Association management guidelines for adult patients with thyroid nodules and differentiated thyroid cancer: the American Thyroid Association Guidelines Task Force on Thyroid Nodules and Differentiated Thyroid Cancer. Thyroid 2016; 26: 1-133.
4. Hirokawa M, Suzuki A, Kawakami M, Kudo T, Miyauchi A. Criteria for follow-up of thyroid nodules diagnosed as follicular neoplasm without molecular testing: the experience of a high-volume thyroid centre in Japan. Diagn Cytopathol 2022; 50: 223-9.
5. Sato A, Matsuda K, Motoyama T, et al. 53BP1 expression as a biomarker to differentiate thyroid follicular tumors. Endocr Connect 2021; 10: 309-15.
6. Suzuki A, Hirokawa M, Furutate M, Hirai Y, Miyauchi A. LC-1000 Flow cytometry system improves risk stratification of thyroid nodules with suspected follicular neoplasm. JMA J 2022; 5: 124-6.
7. Kim HK, Lee DW, Jin SY, Kim DW. Ki-67 labelling index and bax expression according to the capsular invasion in the follicular neoplasms of the thyroid. Korean J Pathol 2001; 35: 531-5.
8. Kim CY, Cho SJ, Kim MK, Chae YS. SPARC expression in thyroid follicular adenomas and carcinomas. Korean J Pathol 2000; 34: 1016-21.
9. Pujani M, Arora B, Pujani M, Singh SK, Tejwani N. Role of Ki-67 as a proliferative marker in lesions of thyroid. Indian J Cancer 2010; 47: 304-7.
10. Mase T, Funahashi H, Koshikawa T, et al. HBME-1 immunostaining in thyroid tumors especially in follicular neoplasm. Endocr J 2003; 50: 173-7.
11. Agustina H, Ahyati R, Suryanti S, Hernowo BS. The potential diagnostic value of Rac1 immunohistochemistry in follicular thyroid carcinoma. Malays J Pathol 2022; 44: 225-33.
12. Cracolici V, Parilla M, Henriksen KJ, Cipriani NA. An evaluation of CD61 immunohistochemistry in identification of vascular invasion in follicular thyroid neoplasms. Head Neck Pathol 2020; 14: 399-405.
13. Gracia Villacampa E, Larsson L, Mirzazadeh R, et al. Genome-wide spatial expression profiling in formalin-fixed tissues. Cell Genom 2021; 1: 100065.
14. Watanabe R, Miura N, Kurata M, Kitazawa R, Kikugawa T, Saika T. Spatial gene expression analysis reveals characteristic gene expression patterns of de novo neuroendocrine prostate cancer coexisting with androgen receptor pathway prostate cancer. Int J Mol Sci 2023; 24: 8955.
15. McInnes L, Healy J, Saul N, Grossberger L. UMAP: Uniform Manifold Approximation and Projection. J Open Source Softw 2018; 3: 861.
16. Blondel VD, Guillaume JL, Lambiotte R, Lefebvre E. Fast unfolding of communities in large networks. J Stat Mech 2008; 10: P10008.
17. Schroder B. The multifaceted roles of the invariant chain CD74: more than just a chaperone. Biochim Biophys Acta 2016; 1863: 1269-81.
18. Choi JW, Kim Y, Lee JH, Kim YS. CD74 expression is increased in high-grade, invasive urothelial carcinoma of the bladder. Int J Urol 2013; 20: 251-5.
19. Hong WC, Lee DE, Kang HW, et al. CD74 promotes a pro-inflam-

matory tumor microenvironment by inducing S100A8 and S100A9 secretion in pancreatic cancer. Int J Mol Sci 2023; 24: 12993.
20. Xu S, Li X, Tang L, Liu Z, Yang K, Cheng Q. CD74 correlated with malignancies and immune microenvironment in gliomas. Front Mol Biosci 2021; 8: 706949.
21. Zeiner PS, Zinke J, Kowalewski DJ, et al. CD74 regulates complexity of tumor cell HLA class II peptidome in brain metastasis and is a positive prognostic marker for patient survival. Acta Neuropathol Commun 2018; 6: 18.
22. Gai JW, Wahafu W, Song L, et al. Expression of CD74 in bladder cancer and its suppression in association with cancer proliferation, invasion and angiogenesis in HT-1376 cells. Oncol Lett 2018; 15: 7631-8.
23. Wang P, Shi Q, Zuo T, He X, Yu J, Wang W. Expression of cluster of differentiation 74 in gallbladder carcinoma and the correlation with epithelial growth factor receptor levels. Oncol Lett 2016; 11: 2061-6.
24. Liu Z, Chu S, Yao S, et al. CD74 interacts with CD44 and enhances tumorigenesis and metastasis via RHOA-mediated cofilin phosphorylation in human breast cancer cells. Oncotarget 2016; 7: 68303-13.
25. Zhang JT, Zhang J, Wang SR, et al. Spatial downregulation of CD74 signatures may drive invasive component development in part-solid lung adenocarcinoma. iScience 2023; 26: 107699.
26. Gold DV, Stein R, Burton J, Goldenberg DM. Enhanced expression of CD74 in gastrointestinal cancers and benign tissues. Int J Clin Exp Pathol 2010; 4: 1-12.
27. Varinelli L, Caccia D, Volpi CC, et al. 4-IPP, a selective MIF inhibitor, causes mitotic catastrophe in thyroid carcinomas. Endocr Relat Cancer 2015; 22: 759-75.
28. Cheng SP, Liu CL, Chen MJ, et al. CD74 expression and its therapeutic potential in thyroid carcinoma. Endocr Relat Cancer 2015; 22: 179-90.

 https://doi.org/10.4132/jptm.2023.11.21

JPTM
Journal of Pathology and Translational Medicine 2024; 58: 29-34
https://doi.org/10.4132/jptm.2023.12.07

ORIGINAL ARTICLE

Immunohistochemical expression of anaplastic lymphoma kinase in neuroblastoma and its relations with some clinical and histopathological features

Thu Dang Anh Phan[1], Thao Quyen Nguyen[1], Nhi Thuy To[2], Thien Ly Thanh[1], Dat Quoc Ngo[1]

[1]Department of Pathology, University of Medicine and Pharmacy at Ho Chi Minh City, Ho Chi Minh City;
[2]Department of Oncology–Hematology, Children Hospital 2, Ho Chi Minh City, Vietnam

Background: Anaplastic lymphoma kinase (ALK) mutations have been identified as a prominent cause of some familial and sporadic neuroblastoma (NB). ALK expression in NB and its relationship with clinical and histopathological features remains controversial. This study investigated ALK expression and its potential relations with these features in NB. **Methods:** Ninety cases of NB at the Department of Pathology, University of Medicine and Pharmacy at Ho Chi Minh City, Viet Nam from 01/01/2018 to 12/31/2021, were immunohistochemically stained with ALK (D5F3) antibody. The ALK expression and its relations with some clinical and histopathological features were investigated. **Results:** The rate of ALK expression in NB was 91.1%. High ALK expression (over 50% of tumor cells were positive with moderate-strong intensity) accounted for 65.6%, and low ALK expression accounted for 34.4%. All the *MYCN*-amplified NB patients had ALK immunohistochemistry positivity, most cases had high ALK protein expression. The undifferentiated subtype of NB had a lower ALK-positive rate than the poorly differentiated and differentiated subtype. The percentages of ALK positivity were significantly higher in more differentiated histological types of NB (p=.024). There was no relation between ALK expression and: age group, sex, primary tumor location, tumor stage, *MYCN* status, clinical risk, Mitotic-Karyorrhectic Index, prognostic group, necrosis, and calcification. **Conclusions:** ALK was highly expressed in NB. ALK expression was not related to several clinical and histopathological features. More studies are needed to elucidate the association between ALK expression and ALK gene status and to investigate disease progression, especially the oncogenesis of ALK-positive NB.

Key Words: Neuroblastoma; Anaplastic lymphoma kinase

Received: October 23, 2023 **Revised:** November 28, 2023 **Accepted:** December 6, 2023
Corresponding Author: Thao Quyen Nguyen MD, Department of Pathology, University of Medicine and Pharmacy at Ho Chi Minh City, Ho Chi Minh City 70000, Vietnam
Tel: +84-847-554-196, Fax: +84-28-3855-2304, E-mail: quyennguyen1191995@gmail.com

Neuroblastomas (NB) are tumors deriving from the sympathoadrenal lineage - one of the neural crest derivatives. NB represents the most prevalent extracranial solid tumor in children and accounts for 12% of all childhood cancer deaths [1]. The presence of anaplastic lymphoma kinase (*ALK*) mutations in NB has been published since 2008 [2]. Approximately 8% to 10% of NB have *ALK* mutations, and about 25% have *ALK* amplification or overexpression of the ALK protein [3]. Many studies have shown that the *ALK* gene is a significant oncogene in NB, and ALK mutations have been identified in association with familial and sporadic NB [2]. Besides, ALK is a consummate tumor antigen for targeted inhibition, due to its frequent expression in NB and restricted distribution in normal tissue [4]. These results open the door to new therapeutic strategies for treating NB with ALK inhibitors.

Several research groups have reported that ALK overexpression in NB is an adverse prognostic factor, however, the relations between ALK protein expression and clinical and histopathological features of NB are still controversial [2,5-7]. There are many methods to evaluate ALK in NB, in which immunohistochemistry (IHC) is available and capable of routine application. The clone D5F3 showed the highest sensitivity compared to other clones such as ALK 1, and 5A4. The ALK D5F3 antibody is likely the most appropriate antibody for determining ALK protein expression levels in NB, which may be used to predict patient prognosis [8,9].

pISSN 2383-7837
eISSN 2383-7845

In this study, ALK protein expression was studied to investigate potential relations with some clinical and pathological features of NB.

MATERIALS AND METHODS

Patients and specimens

Patients who were histologically diagnosed with NB (Schwannian stroma-poor) (based on International Neuroblastoma Pathology Classification [INPC]) at the Department of Pathology, University of Medicine and Pharmacy at Ho Chi Minh City, Viet Nam from January 2018 to December 2021 were enrolled in this study. All tumor specimens were obtained from the primary or metastatic tumor through surgery or biopsy before starting chemotherapy. The clinical parameters, including age at diagnosis, gender, tumor stages (based on International Neuroblastoma Risk Group Staging System [INRGSS]), primary tumor sites were collected. *MYCN* status (by fluorescence in situ hybridization [FISH]) was retrospectively inquired through record data from the Center for Molecular Biomedicine, University of Medicine and Pharmacy at Ho Chi Minh City. Hematoxylin a eosin slides were assessed for degree of differentiation, Mitotic-Karyorrhectic Index (MKI), and prognostic groups (according to INPC). In addition, tumor necrosis and calcification will also be noted.

Formalin-fixed, paraffin-embedded tumor tissue collected during surgery or biopsy was used. For surgical specimens, a representative area of tumor tissue will be submitted for tissue microarray, and whole biopsied specimens will be collected for IHC staining.

IHC staining

IHC staining was performed on 4-µm-thick sections using VENTANA anti-ALK (clone D5F3, Ventana Medical Systems, Tucson, AZ, USA) rabbit monoclonal primary antibody was used in this study. The IHC staining process was fully automated using a BenchMark XT automated slide stainer (Ventana Medical Systems).

Cytoplasmic and membrane staining with any ratio was considered positive. Negative when absolutely no tumor cells were stained. ALK IHC staining was scored based on the percentage of antibody-reactive neoplastic cells and the intensity as follows: "0" (negative, no stained cells), "1+" (weak expression, < 20% of cells stained), "2+" (heterogeneous weak-moderate expression, around 20%–50% of cells stained), "3+" (heterogeneous moderate-strong expression, > 50% of cell stained), and "4+" (> 75%, strong expression).

Cases with ALK IHC score 3+, and 4+ are considered to have high ALK protein expression (i.e., more than 50% of tumor cells are stained with moderate-strong intensity). The remaining cases were considered to have low ALK protein expression (IHC ALK score 0, 1+, 2+).

Statistical analysis

Pearson's χ^2 test (or Fisher's exact test if the sample size was small) was used to evaluate relationship between pairs of categorical variables. All statistical analyses were performed using STATA ver. 14.2 (Stata Corp., College Station, TX, USA). p-value < .05 were statistically significant.

RESULTS

Patient characteristics

A total of 90 patients were enrolled in this study. The clinical and pathological characteristics of the patients are summarized in Table 1. The median age of patients was 24 months old (15 days old–14 years old), and the group under 18 months old accounted for the majority. The male/female ratio is 1.3:1. In 80 cases tested for FISH *MYCN*, 11.3% had *MYCN* amplification. More than 80% of NB were poorly differentiated subtype, unfavorable histology group accounted for the majority with 57.8% (Table 1).

ALK protein expression

ALK was positive in 91.1% of cases (82/90 cases), in which high ALK expression (3+, 4+) accounted for 65.6% (59/90 cases). The ALK IHC expression is summarized in Table 2.

ALK IHC staining was observed in the cytoplasm or membrane of NB cells and was negative for lymphocytes, endothelium, and normal adrenal gland (Fig. 1). Different intensity of ALK IHC was shown in Fig. 2.

The relation between ALK expression and some clinical and pathological features

Our study showed all cases of differentiating NB were ALK-positive (Table 3). There was significant relation of ALK positivity with NB histological types (undifferentiated NB [9/13, 69.2%] vs. poorly differentiated NB [69/73, 94.5%] vs. differentiating NB [4/4, 100%; p = .024]). All cases with MYCN amplification were positive for ALK IHC, in which high ALK expression accounted for 7/9 cases (77.8%). No other relations between ALK expression and clinical and pathological features were observed (Table 3).

https://doi.org/10.4132/jptm.2023.12.07

Table 1. Characteristics of patients (n=90)

Characteristic	No. (%)
Age (mo)	
<18	43 (47.8)
18–60	31 (34.4)
≥60	16 (17.8)
Sex	
Male	51 (56.7)
Female	39 (43.3)
Primary site	
Retroperitoneum/Adrenal	74 (82.2)/47 (52.2)
Posterior mediastinum	12 (13.3)
Neck	3 (3.3)
Unknown	1 (1.1)
Stage (INRGSS)	
L1	25 (27.8)
L2	26 (28.9)
Ms	2 (2.2)
M	37 (41.1)
MYCN status	
Amplified	9 (11.3)
Non-amplified	71 (88.7)
Degree of differentiation	
Undifferentiated	13 (14.4)
Poorly differentiated	73 (81.1)
Differentiating	4 (4.5)
MKI	
Low	54 (60)
Intermediate	16 (17.8)
High	20 (22.2)
Prognostic group (INPC)	
Favorable	38 (42.2)
Unfavorable	52 (57.8)
Necrosis	
Yes	27 (30.0)
No	63 (70.0)
Calcification	
Yes	22 (24.4)
No	68 (75.6)

INRGSS, International Neuroblastoma Risk Group Staging System; MKI, Mitotic-Karyorrhectic Index; INPC, International Neuroblastoma Pathology Classification.

Table 2. ALK IHC expression

ALK IHC score	No. (%)
Low expression	
0	8 (8.9)
1+	10 (11.1)
2+	13 (14.4)
High expression	
3+	13 (14.4)
4+	46 (51.1)
Total	90 (100)

ALK, anaplastic lymphoma kinase; IHC, immunohistochemistry.

DISCUSSION

Until now, there is no consensus method for evaluating ALK IHC staining in NB, most of the studies were based on the percentage of ALK antibody-reactive neoplastic cells and modified evaluation methods depending on the research groups [2,5,8,10-13]. Several previous studies reported the relation between high ALK expression (> 50% of tumor cells) and poor clinical outcome [2,5,13], so a positive threshold of more than 50% of stained tumor cells was applied in many studies [6,7]. In this study, we applied the modified assessment method according to Passoni et al. [2], and investigated the relations between high/low ALK protein expression with some clinical and histopathological factors. Our study showed that the ALK expression rate was 91.1%, similar to many other studies [2,5,9,10]. ALK protein is a single-chain transmembrane protein comprised of three regions: extracellular domain, transmembrane region, and intracellular domain [4], so ALK IHC showed cytoplasmic/membranous expression. ALK protein is expressed on the surface of most NB cells, and its expression is uncommon in normal tissue [4,9]. This makes ALK an ideal target for cancer therapy, whether the NBs exhibit ALK mutations [4,9].

In this study, ALK expression was not related to clinical features including age, sex, stage, or *MYCN* status. A previous study reported that the incidence of ALK expression increased correspondingly with more advanced tumor stages (p = .001) [7]. In another study by Passoni et al. [2], ALK protein expression was significantly up-regulated in advanced/metastatic NB, however, our study showed that ALK expression was not related to the disease stage [2]. This discrepancy may be attributed to differences in the staging system used in the two studies (INRGSS vs. International Neuroblastoma Staging System [INSS]), and the ALK antibody clone (D5F3 vs. 5A4, ALK1, SP8, each antibody binds to a different epitope, which may explain why they have different sensitivities [14]).

Our study revealed that all cases with *MYCN* amplification were positive for ALK IHC (Table 3), in which high ALK expression accounted for 7/9 cases (77.8%). Similar to our results, Lee et al. evaluated ALK expression on 70 NBs and reported that all seven cases with *MYCN* amplification were positive for ALK IHC (over 50% tumor cells expressed) [7]. In another study by Wang et al. [6], NBs with *MYCN* amplification or gain were more likely to be ALK-positive than tumors with normal *MYCN* status (p < .05) [6]. Yan et al. [8] found a strong relationship between ALK D5F3 IHC and the number of copies of the *MYCN* gene on NB. Schonherr et al. [15] reported that ALK activity was

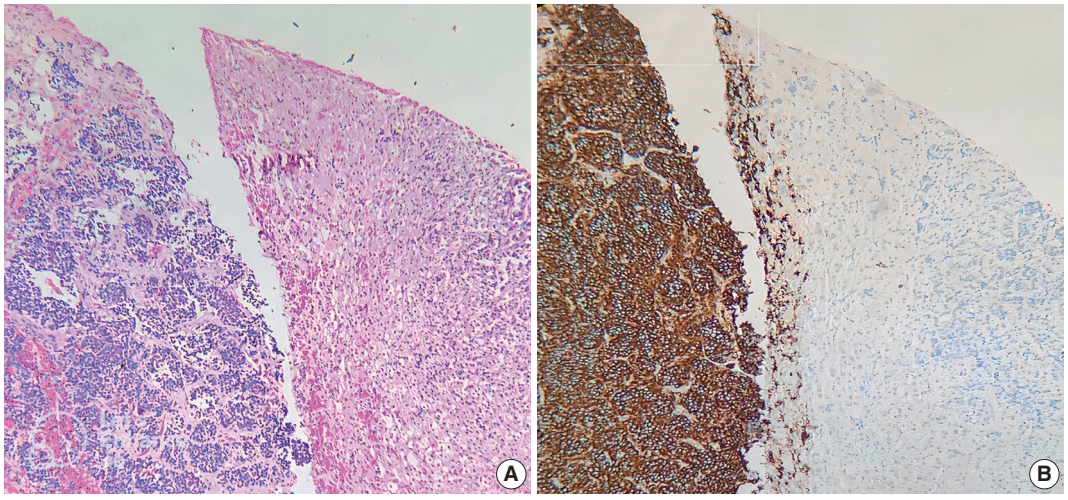

Fig. 1. (A) Neuroblastoma (left side) and normal adrenal gland (right side). (B) Strong immunohistochemistry staining of anaplastic lymphoma kinase (ALK) in tumor cells (left side), no ALK staining is found in normal adrenal tissue (right side).

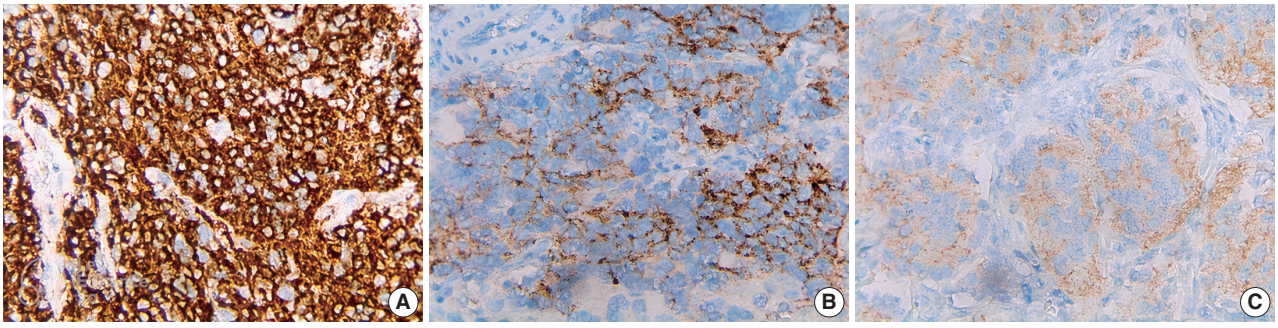

Fig. 2. (A) Immunohistochemistry (IHC) staining for anaplastic lymphoma kinase (ALK) in neuroblastoma (NB) showed strong, homogeneous cytoplasmic or membraned staining. (B) Moderate ALK IHC staining in NB. (C) Weak, heterogenous ALK IHC staining in NB.

very important in *MYCN* transcription initiation, and *MYCN* gene transcription was eliminated by using a specific ALK inhibitor. From our observations combined with several reports that high ALK expression in NB is predictive of treatment response to ALK inhibitors [2,9], we speculate that *MYCN*-amplified NB patients may benefit from ALK inhibitors treatment if high levels of ALK expression are present.

We noted higher percentages of ALK positivity in more differentiated histological types of NB ($p = .024$). However, there was no statistically significant correlation between ALK IHC score and NB histological types ($p = .143$), similar to another study [10]. ALK expression is found in neural crest cells during early development, and the involvement of ALK activation in neural crest cell migration and proliferation has been shown [16]. However, how ALK helps neural crest cells to develop in humans is poorly understood [17]. In our study, up to 4/13 cases (30.8%) of undifferentiated NB were negative for ALK IHC. As ALK protein expression was not associated with *ALK* mutations in most cases (half or more of NBs have strong ALK protein expression, but only about 10% of NBs harbor *ALK* aberrations) [2,5,8], so further molecular biology tests are needed to determine if these ALK IHC-negative cases have the *ALK* gene mutations. The D5F3 IHC test is highly concordance with ALK-FISH and approved by the U.S. Food and Drug Administration for detecting *ALK* rearrangements in non-small cell lung carcinoma; however, the discrepancy between these two tests has also been reported [18]. In addition, in the group of pulmonary neuroendocrine tumors, many studies have shown that there is a mismatch between ALK protein expression and *ALK* alterations [19-22]. Nakamura et al. [19] indicated that the immunopositivity is probably of a wild-type ALK, which may be due to epigenetic regulation or protein overstabilization. Although there are no *ALK* alterations detected by FISH, cases of lung cancer overexpressing ALK protein that respond positively to ALK inhibitors were announced [23,24]. Similar to NB, ALK-positive tumors may still respond to ALK inhibitor drugs even if tumors

https://doi.org/10.4132/jptm.2023.12.07

Table 3. The relation between ALK expression and some clinical and pathological features

Variable	No. of cases	IHC ALK-positive	IHC ALK-negative	p-value	Low ALK expression	High ALK expression	p-value
Age (mo)				.704[a]			.928[b]
<18	43	40 (93.0)	3 (7.0)		14 (32.6)	29 (67.4)	
18–60	31	28 (90.3)	3 (9.7)		11 (35.5)	20 (64.5)	
≥60	16	14 (87.5)	2 (12.5)		6 (37.5)	10 (62.5)	
Sex				.723[a]			.124[b]
Male	51	47 (92.2)	4 (7.8)		21 (41.2)	30 (58.8)	
Female	39	35 (89.7)	4 (10.3)		10 (25.6)	29 (74.4)	
Stage (INRGSS)				>.99[a]			.631[a]
L1	25	23 (92.0)	2 (8.0)		7 (28.0)	18 (72.0)	
L2	26	24 (92.3)	2 (7.7)		11 (42.3)	15 (57.7)	
Ms	2	2 (100)	0		1 (50.0)	1 (50.0)	
M	37	33 (89.2)	4 (10.8)		12 (32.4)	25 (67.6)	
MYCN				>.99[a]			.471[a]
Amplified	9	9 (100)	0		2 (22.2)	7 (77.8)	
Non-amplified	71	64 (90.2)	7 (9.8)		28 (39.4)	43 (60.6)	
Differentiation				.024[a]			.143[a]
Undifferentiation	13	9 (69.2)	4 (30.8)		7 (53.9)	6 (46.1)	
Poorly differentiation	73	69 (94.5)	4 (5.5)		22 (30.1)	51 (69.9)	
Differentiating	4	4 (100)	0		2 (50.0)	2 (50.0)	
MKI				.682[a]			.230[b]
Low	51	45 (88.2)	6 (11.8)		21 (41.2)	30 (58.8)	
Intermediate	19	18 (94.7)	1 (5.3)		6 (31.6)	13 (68.4)	
High	20	19 (95)	1 (5.0)		4 (20.0)	16 (80.0)	
Prognostic group				>.99[a]			.682[b]
Favorable	38	35 (92.1)	3 (7.9)		14 (36.8)	24 (63.2)	
Unfavorable	52	47 (90.4)	5 (9.6)		17 (32.7)	35 (67.3)	
Necrosis				.234[a]			.735[b]
Yes	27	23 (85.2)	4 (14.8)		10 (37.0)	17 (63.0)	
No	63	59 (93.7)	4 (6.3)		21 (33.3)	42 (66.7)	
Calcification				.674[a]			.211[b]
Yes	22	21 (95.5)	1 (4.5)		10 (45.4)	12 (54.6)	
No	68	61 (89.7)	7 (10.3)		21 (30.9)	47 (69.1)	

Values are presented as number (%).
ALK, anaplastic lymphoma kinase; IHC, immunohistochemistry; INRGSS, International Neuroblastoma Risk Group Staging System; MKI, Mitotic-Karyorrhectic Index.
[a]Fisher's exact test; [b]χ^2 test.

lack *ALK* mutations [5,9], therefore, ALK-negative undifferentiated NB cases may be an indicator of unresponsiveness to ALK inhibitors. Until now, many generations of ALK inhibitors have been created and included in research. Overcoming the limitations of the pioneering ALK inhibitor crizotinib, several novel designed generations of ALK inhibitors and the combinatory therapy with either pathway inhibitors or other agents against other targets are also of interest [25,26]. The definitive efficacy of ALK inhibitors in NB remains to be elucidated upon the conclusion of ongoing clinical trials within the next few years [25].

In summary, this study highlights the characteristics of ALK expression in NB by applying both approaches to evaluating ALK expression in NB and clarifies the reason for the difference in the results of previous studies. ALK expression was not related to several clinical and histopathological features. Our study revealed a significant relation between ALK positivity with NB histological types, and all cases with *MYCN* amplification were positive for ALK, speculating that *MYCN*-amplified NB patients may benefit from ALK inhibitors. Since the role of ALK in neural crest development is still unclear, further studies are needed to elucidate the association between ALK expression and *ALK* gene status and to investigate disease progression, especially the oncogenesis of ALK-positive NB.

Ethics Statement

This study was conducted in accordance with the guidelines of the Declaration of Helsinki and approved by the Institutional Review Board of Bio-

medical Research of University of Medicine and Pharmacy at Ho Chi Minh City (IRB No. 174/HDDD-DHYD; on February 21, 2022). Informed consent was obtained from all individual participants included in the study.

Availability of Data and Material

The datasets generated or analyzed during the study are available from the corresponding author on reasonable request.

Code Availability

Not applicable.

ORCID

Thu Dang Anh Phan https://orcid.org/0000-0002-4062-0904
Thao Quyen Nguyen https://orcid.org/0009-0004-2391-1613
Nhi Thuy To https://orcid.org/0009-0006-6727-0242
Thien Ly Thanh https://orcid.org/0009-0006-7773-1321
Dat Quoc Ngo https://orcid.org/0000-0003-1461-0216

Author Contributions

Conceptualization: TDAP, TQN, DQN. Data curation: TDAP, TQN, TLT, NTT. Formal analysis: TDAP, TQN. Funding acquisition: TDAP, TLT. Investigation: TQN, TDAP, NTT, TLT. Resources: TDAP, NTT. Methodology: TDAP, TQN. Supervision: DQN. Writing—original draft: TQN, TDAP. Writing—review & editing: TDAP, TQN, DQN. Approval of final manuscript: all authors.

Conflicts of Interest

The authors declare that they have no potential conflicts of interest.

Funding Statement

This study was funded by grants from the University of Medicine and Pharmacy at Ho Chi Minh City.

References

1. Maris JM, Hogarty MD, Bagatell R, Cohn SL. Neuroblastoma. Lancet 2007; 369: 2106-20.
2. Passoni L, Longo L, Collini P, et al. Mutation-independent anaplastic lymphoma kinase overexpression in poor prognosis neuroblastoma patients. Cancer Res 2009; 69: 7338-46.
3. Pugh TJ, Morozova O, Attiyeh EF, et al. The genetic landscape of high-risk neuroblastoma. Nat Genet 2013; 45: 279-84.
4. Carpenter EL, Haglund EA, Mace EM, et al. Antibody targeting of anaplastic lymphoma kinase induces cytotoxicity of human neuroblastoma. Oncogene 2012; 31: 4859-67.
5. Duijkers FA, Gaal J, Meijerink JP, et al. High anaplastic lymphoma kinase immunohistochemical staining in neuroblastoma and ganglioneuroblastoma is an independent predictor of poor outcome. Am J Pathol 2012; 180: 1223-31.
6. Wang M, Zhou C, Sun Q, et al. *ALK* amplification and protein expression predict inferior prognosis in neuroblastomas. Exp Mol Pathol 2013; 95: 124-30.
7. Lee JW, Park SH, Kang HJ, Park KD, Shin HY, Ahn HS. ALK protein expression is related to neuroblastoma aggressiveness but is not independent prognostic factor. Cancer Res Treat 2018; 50: 495-505.
8. Yan B, Kuick CH, Lim M, et al. Platform comparison for evaluation of ALK protein immunohistochemical expression, genomic copy number and hotspot mutation status in neuroblastomas. PLoS One 2014; 9: e106575.
9. Sano R, Krytska K, Larmour CE, et al. An antibody-drug conjugate directed to the ALK receptor demonstrates efficacy in preclinical models of neuroblastoma. Sci Transl Med 2019; 11: eaau9732.
10. Aygun Z, Batur S, Emre S, Celkan T, Ozman O, Comunoglu N. Frequency of ALK and GD2 expression in neuroblastoma. Fetal Pediatr Pathol 2019; 38: 326-34.
11. Chang HH, Lu MY, Yang YL, et al. The prognostic roles of and correlation between ALK and MYCN protein expression in neuroblastoma. J Clin Pathol 2020; 73: 154-61.
12. De Brouwer S, De Preter K, Kumps C, et al. Meta-analysis of neuroblastomas reveals a skewed *ALK* mutation spectrum in tumors with MYCN amplification. Clin Cancer Res 2010; 16: 4353-62.
13. Uryu K, Nishimura R, Kataoka K, et al. Identification of the genetic and clinical characteristics of neuroblastomas using genome-wide analysis. Oncotarget 2017; 8: 107513-29.
14. Kim EK, Kim S. ALK gene copy number gain and immunohistochemical expression status using three antibodies in neuroblastoma. Pediatr Dev Pathol 2017; 20: 133-41.
15. Schonherr C, Ruuth K, Kamaraj S, et al. Anaplastic lymphoma kinase (ALK) regulates initiation of transcription of MYCN in neuroblastoma cells. Oncogene 2012; 31: 5193-200.
16. Wulf AM, Moreno MM, Paka C, Rampasekova A, Liu KJ. Defining pathological activities of ALK in neuroblastoma, a neural crest-derived cancer. Int J Mol Sci 2021; 22: 11718.
17. Nakazawa A. Biological categories of neuroblastoma based on the international neuroblastoma pathology classification for treatment stratification. Pathol Int 2021; 71: 232-44.
18. Ilie MI, Bence C, Hofman V, et al. Discrepancies between FISH and immunohistochemistry for assessment of the ALK status are associated with ALK 'borderline'-positive rearrangements or a high copy number: a potential major issue for anti-ALK therapeutic strategies. Ann Oncol 2015; 26: 238-44.
19. Nakamura H, Tsuta K, Yoshida A, et al. Aberrant anaplastic lymphoma kinase expression in high-grade pulmonary neuroendocrine carcinoma. J Clin Pathol 2013; 66: 705-7.
20. Akhoundova D, Haberecker M, Fritsch R, et al. Targeting ALK in neuroendocrine tumors of the lung. Front Oncol 2022; 12: 911294.
21. Leal JL, Peters G, Szaumkessel M, et al. *NTRK* and *ALK* rearrangements in malignant pleural mesothelioma, pulmonary neuroendocrine tumours and non-small cell lung cancer. Lung Cancer 2020; 146: 154-9.
22. Zheng Q, Zheng M, Jin Y, et al. *ALK*-rearrangement neuroendocrine carcinoma of the lung: a comprehensive study of a rare case series and review of literature. Onco Targets Ther 2018; 11: 4991-8.
23. Sun JM, Choi YL, Won JK, et al. A dramatic response to crizotinib in a non-small-cell lung cancer patient with IHC-positive and FISH-negative ALK. J Thorac Oncol 2012; 7: e36-8.
24. van der Wekken AJ, Pelgrim R, t Hart N, et al. Dichotomous ALK-IHC is a better predictor for ALK inhibition outcome than traditional ALK-FISH in advanced non-small cell lung cancer. Clin Cancer Res 2017; 23: 4251-8.
25. Brenner AK, Gunnes MW. Therapeutic targeting of the anaplastic lymphoma kinase (ALK) in neuroblastoma: a comprehensive update. Pharmaceutics 2021; 13: 1427.
26. Kozuma Y, Toyokawa G, Seto T. ALK testing methods: is there a winner or loser? Expert Rev Anticancer Ther 2019; 19: 237-44.

JPTM
Journal of Pathology and Translational Medicine 2024; 58: 35-39
https://doi.org/10.4132/jptm.2023.11.14

CASE STUDY

Primary leiomyosarcoma of the bone: a case report

Ala Abu-Dayeh, Samir Alhyassat

Anatomic Pathology Division, Hamad Medical Corporation, Doha, Qatar

Primary leiomyosarcoma of the bone is rare. Histologically, it resembles leiomyosarcoma of soft tissue. Given the rarity of this entity, its diagnosis should be made only after clinical studies and workup have excluded metastasis from other sites. Herein, we describe an additional case of primary bone leiomyosarcoma. We report a 32-year-old female patient, who presented with right knee pain and was found to have a right distal femur mass by imaging studies. Biopsy showed a neoplasm composed of fascicles of spindle cells, arranged in different patterns, with significant pleomorphism. The tumor cells were positive for smooth muscle actin, focally positive for desmin and H-caldesmon. No other masses in the body were detected by imaging studies. The diagnosis of leiomyosarcoma of the bone was rendered. Given the broad diagnostic differential of primary bone leiomyosarcoma, it is important to be aware of this rare bone tumor phenotype and of its histomorphologic and immunohistochemical features for an accurate diagnosis.

Key Words: Bone; Sarcoma; Leiomyosarcoma; Case report

Received: June 17, 2023 **Revised:** November 4, 2023 **Accepted:** November 14, 2023
Corresponding Author: Ala Abu-Dayeh, MD, Anatomic Pathology Division, Hamad Medical Corporation, Ahmed Bin Ali St., AlRumaileh, Doha, Qatar
Tel: +974-30940603, E-mail: Alaaabudayeh@hotmail.com, AAbudayeh@hamad.qa

Primary bone leiomyosarcoma accounts for less than 0.7% of primary malignant bone neoplasms [1]. It has no known etiology, though a few cases have been associated with previous radiation therapy or Epstein-Barr virus (EBV) infection [2]. It most commonly arises from the distal femur [3]. Histologically, it resembles leiomyosarcoma of soft tissue. Immunohistochemical findings demonstrate diffuse positivity for smooth muscle actin (SMA), desmin, and H-caldesmon [2]. Given the rarity of primary bone leiomyosarcoma, its diagnosis should always be made only after thorough clinical studies and workup have excluded metastasis from other sites.

The main differential diagnoses of primary bone leiomyosarcoma include osteosarcoma, chondrosarcoma, myxofibrosarcoma, and synovial sarcoma among others [4]. Few cases of primary bone leiomyosarcoma have been reported in the literature [5-7], therefore, the information regarding its clinical and histological features, biological behavior, prognosis, and treatment modalities is still limited. Herein, we describe an additional case of primary bone leiomyosarcoma, to further increase our understanding of this rare tumor and to help avoid potential diagnostic pitfalls. Increasing awareness of this rare tumor is also important to improve prognosis and guide treatment.

CASE REPORT

A 32-year-old, medically-free female patient presented with right knee pain of 10-day duration. The pain worsened at night and with physical activities. Physical examination was unremarkable. X-ray revealed a right distal femur intraosseous metaphyseal central lytic lesion with cortical thinning and soft tissue extension. Magnetic resonance imaging showed a well-defined central destructive lesion, completely replacing the medullary cavity of the distal third of the right femoral shaft for a 10 cm span in craniocaudal dimension, reaching the anterior aspect of both femoral condyles and the posterior aspect of the intercondylar fossa with multiple areas of cortical bone destruction (Fig. 1). The patient underwent a core needle biopsy of the right distal femur lesion.

Histopathologic findings

Gross examination revealed multiple tan-pink irregular friable focally hemorrhagic soft tissue fragments, measuring 2.5×1.7×0.4 cm in aggregate. Microscopic examination demonstrated fascicles of spindle and epithelioid cells with plump, blunt-ended nuclei, occasional subnuclear vacuoles, and moderate brightly

pISSN 2383-7837
eISSN 2383-7845

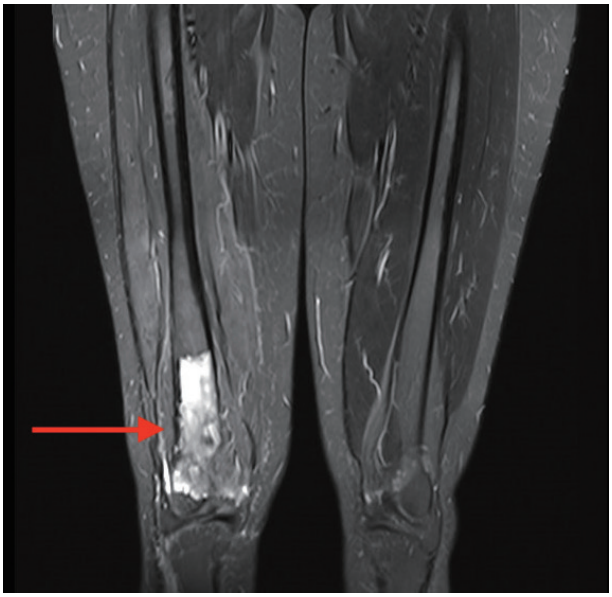

Fig. 1. Magnetic resonance imaging shows an intraosseous metaphyseal central lytic lesion (red arrow), completely replacing the medullary cavity of the distal third of the right femoral shaft for a 10 cm span in craniocaudal dimension with multiple areas of cortical bone destruction.

eosinophilic cytoplasm. There was significant pleomorphism in the form of hyperchromasia, high nucleus-to-cytoplasmic ratio, and irregular nuclear contours, arranged in intersecting, storiform, and haphazard patterns (Fig. 2A, B). Other cells showed vesicular nuclei and prominent nucleoli. Multinucleated giant cells were also identified. The background was sclerotic. Fat lobules infiltrated by the atypical cells were also seen (Fig. 2C). Mitotic activity was 5 per 10 high-power fields.

Immunohistochemical findings

On immunohistochemical stains, performed by machine, the tumor cells were positive for SMA (ready-to-use, Dako, Glostrup, Denmark) "shown in Fig. 2D", focally positive for desmin (ready-to-use, Dako) (Fig. 2E), H-caldesmon (ready-to-use, Dako) (Fig. 2F), CD10 (ready-to-use, Dako), CD68 (ready-to-use, Dako) and SATB2 (prediluted, Cell Marque, Rocklin, CA, USA), and negative for cytokeratin (CK) AE1/AE3 (ready-to-use, Dako), CK MNF 116 (1:50, Dako), CDK4 (prediluted, Cell Marque), MDM2 (prediluted, Cell Marque), Melan-A (ready-to-use, Dako), S100 (ready-to-use, Dako), SOX-10 (prediluted, Cell Marque), estrogen receptor (ER; ready-to-use, Dako) (Fig. 2G), progesterone receptor (PR; ready-to-use, Dako), CD31 (ready-to-use, Dako), CD34 (ready-to-use, Dako), and myogenin (ready-to-use, Dako). S100 (ready-to-use, Dako) was positive in the adipocytes. Ki-67 (ready-to-use, Dako) proliferation index was high.

Final diagnosis and clinical course

The diagnosis of high-grade sarcoma, most consistent with leiomyosarcoma of the bone, was rendered. The patient had no previous gynecological history. Imaging studies revealed no uterine masses (Fig. 3) or soft tissue masses, and no lung or bony metastatic lesions. The patient underwent wide excision of the right distal femur. The gross examination of the resected specimen revealed an intramedullary irregular tan-white ill-defined infiltrative lesion measuring 9.2×6.3×3.2 cm. The final diagnosis on the excision specimen concurred with the biopsy diagnosis. The TNM stage was pT2 N0. The patient will be followed up by the oncology team on a regular basis.

DISCUSSION

Leiomyosarcomas are aggressive malignant soft tissue tumors arising from smooth muscle cells. They are common among soft tissue sarcomas, comprising approximately 25% of all sarcomas [8]. Primary bone leiomyosarcoma is a rare tumor, accounting for less than 0.7% of primary malignant bone neoplasms [1]. It was first described by Evans and Sanerkin in 1965 [5], and is slightly more common in males, with its incidence peaking at the fifth decade of life [2]. It mostly occurs at the distal femur followed by the proximal tibia and proximal humerus [3]. A small number of cases have been found to be associated with previous radiation therapy or EBV infection [2]. The most common symptom of primary bone leiomyosarcoma is pain, followed by the presence of a palpable mass and a pathologic fracture [9]. On radiographic examination, it usually presents as an intraosseous aggressive lytic lesion with a permeative pattern of osseous destruction [10]. The outline of low-grade lesions shows regular cortical destruction and is demarcated by a sclerotic rim whereas high-grade lesions have an ill-defined outline and lack a sclerotic rim. On gross examination, the lesions vary in size and have gray-tan creamy appearance with foci of necrosis and cystic degeneration [9]. Histologically, it resembles leiomyosarcoma of soft tissue with intersecting fascicles and bundles of pleomorphic spindle cells. The cells are characterized by eosinophilic cytoplasm and cigar-shaped nuclei with blunted ends. High-grade leiomyosarcomas are associated with marked pleomorphism, necrosis, and significant mitotic activity. Immunohistochemical findings demonstrate diffuse positivity for SMA, desmin, and H-caldesmon [2].

The cellular origin of primary bone leiomyosarcoma remains controversial. A vascular smooth muscle cell origin has been sug-

https://doi.org/10.4132/jptm.2023.11.14

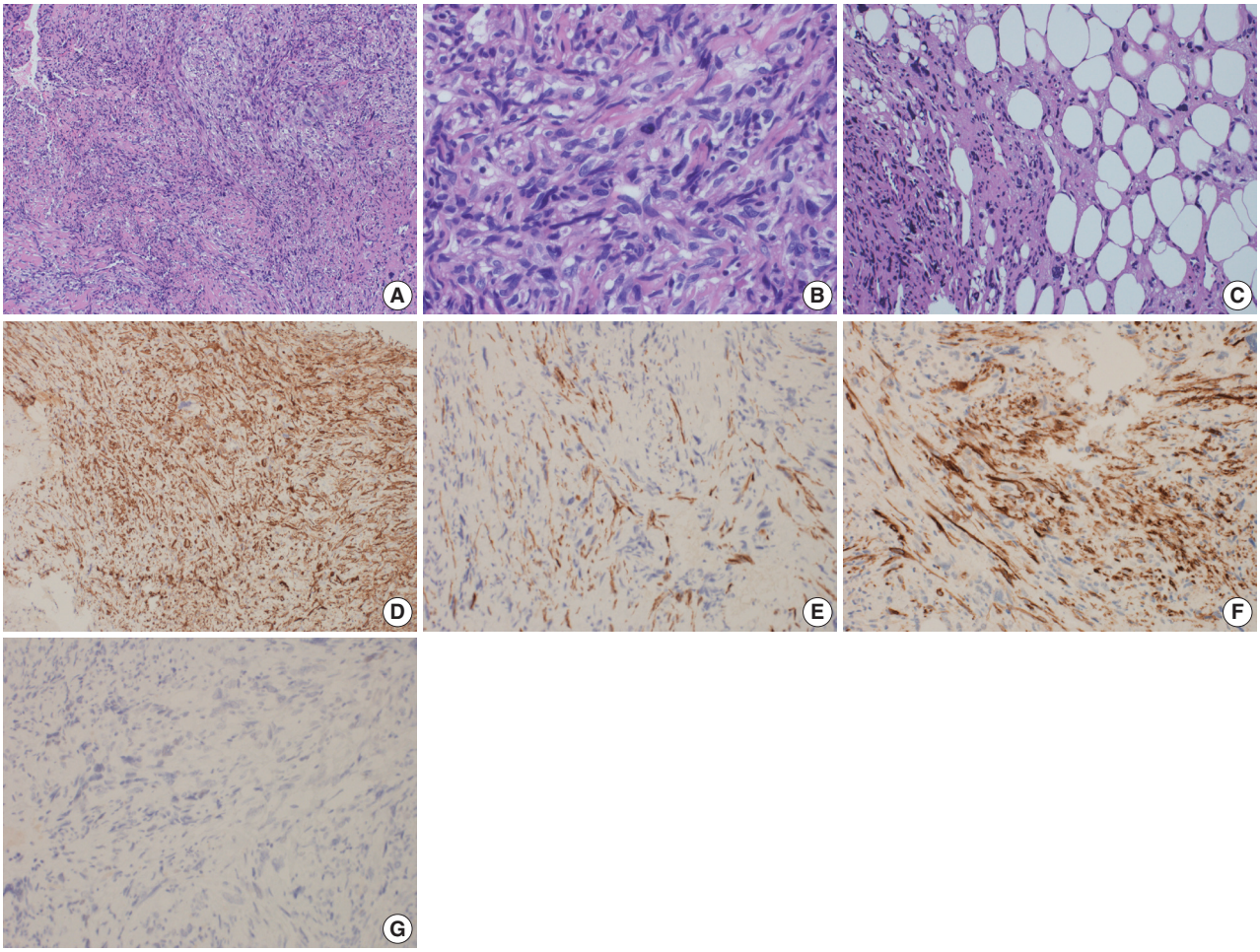

Fig. 2. Microscopic and immunohistochemical features of primary bone leiomyosarcoma. (A) Photomicrograph shows fascicles of pleomorphic spindle and epithelioid cells arranged in fascicular, storiform, and haphazard patterns. (B) High-power view demonstrates cellular pleomorphism in the form of hyperchromasia, high nucleus-to-cytoplasmic ratios, and irregular nuclear contours. Some cells show vesicular nuclei and prominent nucleoli. (C) Photomicrograph shows fat lobules infiltrated by tumor cells. (D) The tumor cells are positive for smooth muscle actin. (E) The tumor cells show focal reactivity for Desmin. (F) The tumor cells show focal reactivity for H-caldesmon. (G) The tumor cells are negative for estrogen receptor.

gested due to the high vascularity of some of these lesions, while others have suggested that it can originate from multipotential mesenchymal stem cells capable of undergoing smooth muscle differentiation [11,12].

Given the rarity of primary bone leiomyosarcoma, metastasis from other sites should always be carefully excluded through clinical examination and imaging studies. In female patients, positivity for ER or PR immunostains hints toward a primary uterine origin [13]. In our case, the patient was medically free and had no previous history of leiomyosarcoma and her physical examination and pan–computed tomography findings were unremarkable. Based on this, the diagnosis of primary bone leiomyosarcoma was rendered.

In 1997, a case series on thirty-three patients with primary bone osteosarcoma was conducted [9]. In this study, they found that the patient's age at diagnosis ranged from 13 to 77 years (average 44.4) with a male-to-female ratio of 1:1. The long bones were mostly affected, with distal femur and proximal tibia predominantly involved. Post-radiation bone leiomyosarcoma occurred in 15% of the patients, and seventy-five percent of the cases were high-grade with worse prognosis [9]. A recent case series was conducted on twenty-two patients with primary bone leiomyosarcoma. Researchers found that the patient's age at diagnosis ranged from 17 to 73 years (average 45.5), and there was a slight male predominance. The lower limb was the most affected site. In this study, they reported 90.9% of the cases as high-grade, with distant metastasis reported in 40.9% of the patients and an overall survival rate of 59.1% in 5 years [14].

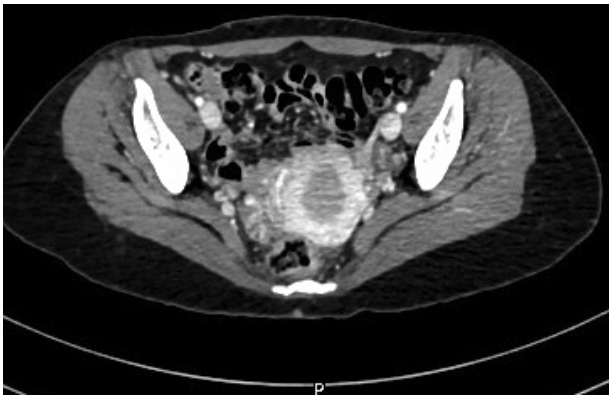

Fig. 3. A computerized tomography scan of the pelvis reveals no uterine lesions.

Compared to the previous studies, our case involves a 32-year-old female patient with no previous medical history or exposure to radiation. The tumor was located at the right distal femur. The patient has not developed local recurrence or metastasis since the time of diagnosis and treatment.

The main differential diagnoses of primary bone leiomyosarcoma include osteosarcoma, chondrosarcoma, myxofibrosarcoma, synovial sarcoma, malignant peripheral nerve sheath tumor (MPNST), fibrosarcoma, undifferentiated pleomorphic sarcoma and metastatic carcinoma [4]. The lack of malignant osteoid can help in excluding osteosarcoma, though this may be difficult in fibroblastic osteosarcomas since osteoid is focally present in such cases. Osteosarcomas may express desmin which will immunophenotypically overlap with leiomyosarcomas. Therefore, osteosarcomas should be carefully excluded after good radiological investigation and extensive sampling [4]. The lack of malignant cartilage production rules out chondrosarcoma. Synovial sarcoma usually demonstrates monotonous spindled cells with scant amphophilic cytoplasm, has a specific chromosomal translocation t(X;18) (p11;q11) and usually expresses TLE1, epithelial membrane antigen, and keratins. Features favoring leiomyosarcoma against MPNST include blunt-ended cigar-shaped nuclei with bright eosinophilic cytoplasm, positivity for SMA, H-caldesmon, and desmin. The diagnosis of fibrosarcoma and undifferentiated pleomorphic sarcoma is made by exclusion of other entities as they lack specific immunohistochemical and genetic markers [2,4]. Metastatic carcinomas express epithelial markers and lack myogenic markers. Lack of well-differentiated liposarcomatous component, MDM2 and CDK4 immunostains expression, and 12q13-15 amplification rules out dedifferentiated liposarcoma.

Data regarding the treatment modalities and prognosis of primary bone leiomyosarcoma is still limited due to its low prevalence. In one study, researchers reported that half of the patients with primary bone leiomyosarcoma developed metastases within one year of diagnosis [15].

In summary, we describe an additional case of primary bone leiomyosarcoma, which adds on more data about this rare category of bone tumors. In our case, the patient was medically free, had no previous history of leiomyosarcoma and no previous gynecological history, and had no uterine or soft tissue masses, along with the negative results of ER and PR in the tumor, which excludes the possibility of metastatic leiomyosarcoma from the uterus. Given the broad diagnostic differential of primary bone leiomyosarcoma, it is important to be aware of this rare bone tumor phenotype and its histomorphological and immunohistochemical features for accurate diagnosis.

Ethics Statement

The Institutional Review Board at Hamad Medical Corporation approved publication of this article under the number (MRC-04-22-670). Informed consent from the participant has been waived by Institutional Review Board.

Availability of Data and Material

The datasets generated or analyzed during the study are available from the corresponding author on reasonable request.

Code Availability

Not applicable.

ORCID

Ala Abu-Dayeh https://orcid.org/0000-0002-8728-7352
Samir Alhyassat https://orcid.org/0000-0003-2905-8495

Author Contributions

Conceptualization: SH. Data curation: AAD. Formal analysis: AAD. Investigation: AAD. Methodology: AAD. Supervision: SH. Validation: SH. Writing—original draft: AAD. Writing—review & editing: AAD, SH. Approval of final manuscript: all authors.

Conflicts of Interest

The authors declare that they have no potential conflicts of interest.

Funding Statement

No funding to declare.

References

1. Siegel RL, Miller KD, Jemal A. Cancer statistics, 2016. CA Cancer J Clin 2016; 66: 7-30.
2. Antonescu CR. WHO classification of tumours of soft tissue and bone. 5th ed. Lyon: IARC Press, 2020.
3. Brewer P, Sumathi V, Grimer RJ, et al. Primary leiomyosarcoma of bone: analysis of prognosis. Sarcoma 2012; 2012: 636849.
4. Palmerini E, Righi A, Staals EL. Rare primary malignant bone sarcomas. Cancers (Basel) 2020; 12: 3092.

5. Evans DM, Sanerkin NG. Primary leiomyosarcoma of bone. J Pathol Bacteriol 1965; 90: 348-50.
6. Khoddami M, Bedard YC, Bell RS, Kandel RA. Primary leiomyosarcoma of bone: report of seven cases and review of the literature. Arch Pathol Lab Med 1996; 120: 671-5.
7. Wang GY, Lucas DR. Primary leiomyosarcoma of bone: review and update. Arch Pathol Lab Med 2019; 143: 1332-7.
8. Mangla A, Yadav U. Leiomyosarcoma. In: StatPearls. Treasure Island: StatPearls Publishing, 2023.
9. Antonescu CR, Erlandson RA, Huvos AG. Primary leiomyosarcoma of bone: a clinicopathologic, immunohistochemical, and ultrastructural study of 33 patients and a literature review. Am J Surg Pathol 1997; 21: 1281-94.
10. Sundaram M, Akduman I, White LM, McDonald DJ, Kandel R, Janney C. Primary leiomyosarcoma of bone. AJR Am J Roentgenol 1999; 172: 771-6.
11. von Hochstetter AR, Eberle H, Ruttner JR. Primary leiomyosarcoma of extragnathic bones: case report and review of literature. Cancer 1984; 53: 2194-200.
12. Lo TH, van Rooij WJ, Teepen JL, Verhagen IT. Primary leiomyosarcoma of the spine. Neuroradiology 1995; 37: 465-7.
13. Myers JL, Arocho J, Bernreuter W, Dunham W, Mazur MT. Leiomyosarcoma of bone: a clinicopathologic, immunohistochemical, and ultrastructural study of five cases. Cancer 1991; 67: 1051-6.
14. Zumarraga JP, Arouca MM, Baptista AM, Caiero MT, Rubio DE, de Camargo OP. Primary leiomyosarcoma of bone: clinicopathologic and prognostic factors analysis in a single institution. Acta Ortop Bras 2019; 27: 152-5.
15. Adelani MA, Schultenover SJ, Holt GE, Cates JM. Primary leiomyosarcoma of extragnathic bone: clinicopathologic features and reevaluation of prognosis. Arch Pathol Lab Med 2009; 133: 1448-56.

JPTM
Journal of Pathology and Translational Medicine 2024; 58: 40-42
https://doi.org/10.4132/jptm.2023.11.05

LETTER TO THE EDITOR

Comment on "A stepwise approach to fine needle aspiration cytology of lymph nodes"

Elisabetta Maffei, Valeria Ciliberti, Pio Zeppa, Alessandro Caputo

Department of Pathology, University Hospital of Salerno, Salerno, Italy

Dear Editor,

We read with great interest the article "A stepwise approach to fine needle aspiration cytology of lymph nodes" by Chong et al. [1], recently published in *J Pathol Transl Med*. The Authors proposed a morphological stepwise algorithm, separate but complementary to the Sydney system, for the cytological diagnosis of lymphadenopathies [2]. In the proposed algorithm the basic diagnostic criteria are structured in a stepwise approach for cytological diagnosis of adenopathy. Regarding the diagnostic classification the Authors basically agree with the Sydney system [2] but they state that *"…the epithelial or lymphomatous nature of the lesion is not clearly separated into different categories and is not emphasized due to the ambiguity of the lymph node features on FNAC. In other words, even though a diagnosis was made on a certain case using the Sydney system, it is still unclear whether the case is lymphoid or metastatic."* We disagree with this observation because when a case is atypical, suspicious, or malignant, the Sydney System strongly encourages to report the nature (lymphoid/metastatic) of the nosologic entity. This is also in keeping with clinical practice, since no hematocytopathologist would ever omit such information from a report. Even in cases in which the cytomorphology is insufficient to distinguish between a lymphoid or metastatic malignancy, a comment will be added to state this.

One additional important point is that the stepwise system proposed by the authors is purely morphological and does not consider ancillary techniques. While the two-level structure of the Sydney System was intentionally conceived to be applicable even in settings where ancillary testing is unavailable, it is important to note that cytopathologists should strive to perform ancillary techniques whenever possible, for three reasons. First, it helps limit atypical and suspicious cases and categorize them in a definite category instead (benign or malignant) [3]. Second, it helps to further subclassify the nosological process responsible for the lymphadenopathy (e.g., "malignant, lymphoma" can become "malignant, follicular B-cell lymphoma" after flow cytometry; "malignant, metastasis" can become "malignant, breast cancer metastasis" after immunocytochemistry; and "benign, granulomatous" can become "benign, tuberculous lymphadenopathy" after polymerase chain reaction). Third, in some cases a fully actionable diagnosis, including prognostic and predictive biomarkers, can be performed on lymph node fine needle aspiration cytology (LN-FNAC). For example, after harvesting non–small-cell lung cancer material from a nodal metastasis, it is possible to employ cytologic material to guide targeted therapy [4].

In fact, the relatively high risk of malignancy (ROM) registered for the category atypical (atypical, undermined significance–atypical lymphoid uncertain significance, AUS-ALUS) by Gupta et al. [5] was the highest among similar series which applied the Sydney System to LN-FNAC [3], mainly because no ancillary techniques were utilized. This high ROM was foreseen by the authors of the Sydney System because some differential diagnoses, such as that between florid reactive hyperplasia and follicular lymphoma or other low-grade non-Hodgkin lymphoma, can be difficult or almost impossible using only cytomorphological criteria (Fig. 1). This differential diagnosis by FNAC, other than in lymphadenopathies, is crucial in extranodal lymphoproliferative processes in which diagnostic excision or invasive biopsies might be useless or even harmful [6,7]. Focusing on the proposed algorithm, we do not believe that only cytomorphological criteria will reduce the incidence of this diagnostic category and its ROM. On the other hand, ancillary techniques (flow cytometry, immunohistochemistry or molecular testing) combined

Received: August 31, 2023 **Accepted:** November 5, 2023

Corresponding Author: Alessandro Caputo, MD
Department of Pathology, University Hospital of Salerno, 84131 Salerno, Italy
Tel: +39-089672840, Fax: +39-089672841, E-mail: alcap94@gmail.com

pISSN 2383-7837
eISSN 2383-7845

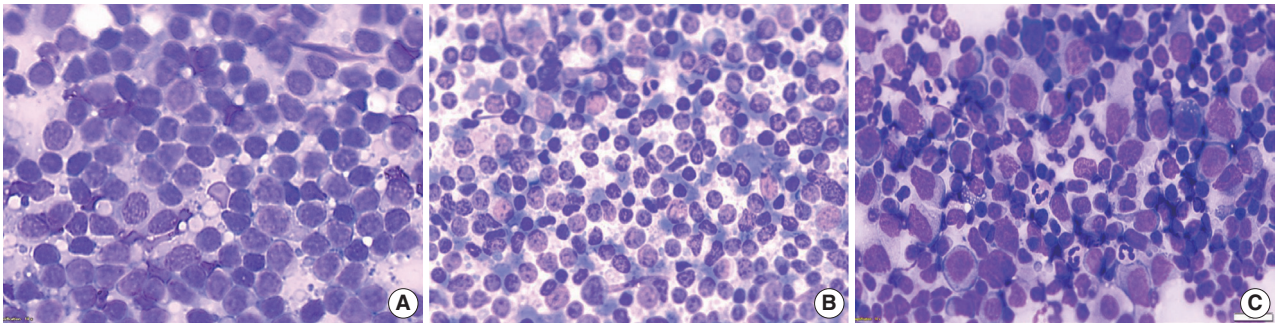

Fig. 1. Three cases of atypical lymphoid cells solved by ancillary techniques. (A) Cervical lymph node fine needle aspiration cytology (LN-FNAC) in a 38-year-old woman. (B) Axillary LN-FNAC in a 62-year-old woman. (C) Cervical lymph node FNAC in a 28-year-old man. Cases A and C were found to be polyclonal on flow cytometry; additionally, in case C, Epstein-Barr virus (EBV)–encoded RNA stain positivity demonstrated EBV infection. Both the lymph nodes shrunk at follow-up. In case B, flow cytometry showed kappa light chain restriction and CD5/CD19 co-expression. Cytological and phenotypical features were indicative of a diffuse, small lymphocytic lymphoma. Histological control demonstrated a small lymphocytic lymphoma/chronic lymphocytic leukemia (A–C, Diff-Quik stain).

with clinical data and cytological features, can discriminate these entities in many cases. For this reason, the Sydney System [2] strongly suggests the application of ancillary techniques in these cases because cytological criteria alone cannot discriminate between entities included with similar cytological patterns. Moreover, repetition of LN-FNAC in AUS-ALUS cases, after six-eight weeks may show dramatically changed cytological features in case of reactive hyperplasia. The authors [1] also state that *"the L3 category, which includes AUS and ALUS, is a good example. It is often quite challenging to discriminate a certain lesion as lymphoid or epithelial in origin"* and that the Sydney System includes *"cases in which the FNAC features favor certain diseases, the cases should be described specifically as "AUS, favor poorly differentiated carcinoma,"* This sentence is not reported in the Sydney system text in which suspicious lymphoma and metastases are included in the category suspicious, which has a higher ROM and different clinical implications than the atypical category. Regarding some specific entities (progressive transformation of germinal centers, Kikuchi-Fujimoto disease, Rosai-Dorfman disease, or others) there is relatively little FNAC experience on their cytological features and few case reports or small series are available in the literature to foresee their diagnostic category (AUS-ALUS or suspicious) and corresponding ROM. We are aware that the ROM of diagnostic categories largely depends on technical issues, different clinical contexts, local epidemiology, and on the reproducibility of diagnostic criteria. For this purpose, a recent experience on LN-FNAC digital slides has been performed producing quite encouraging results [8]. In conclusion we think that the algorithm proposed by Chong et al. [1] matches with the Sydney system which will be reproduced in five diagnostic categories and two diagnostic levels also by the near to be published *WHO Reporting System for Lymph Node, Spleen, and Thymus Cytopathology*.

Ethics Statement

Not applicable.

Availability of Data and Material

Data sharing not applicable to this article as no datasets were generated or analyzed during the study.

Code Availability

Not applicable.

ORCID

Elisabetta Maffei https://orcid.org/0009-0000-4761-6855
Valeria Ciliberti https://orcid.org/0009-0000-3234-6020
Pio Zeppa https://orcid.org/0000-0001-7358-5925
Alessandro Caputo https://orcid.org/0000-0001-5139-3869

Author Contributions

Conceptualization: PZ, AC. Supervision: PZ, AC. Visualization: VC, EM. Writing—original draft: EM, PZ. Writing—review & editing: EM, VC, PZ, AC. Approval of final manuscript: all authors.

Conflicts of Interest

The authors declare that they have no potential conflicts of interest.

Funding Statement

No funding to declare.

References

1. Chong Y, Park G, Cha HJ, et al. A stepwise approach to fine needle aspiration cytology of lymph nodes. J Pathol Transl Med 2023; 57: 196-207.
2. Al-Abbadi MA, Barroca H, Bode-Lesniewska B, et al. A proposal for the performance, classification, and reporting of lymph node

fine-needle aspiration cytopathology: the Sydney system. Acta Cytol 2020; 64: 306-22.
3. Caputo A, Ciliberti V, D'Antonio A, et al. Real-world experience with the Sydney System on 1458 cases of lymph node fine needle aspiration cytology. Cytopathology 2022; 33: 166-75.
4. D'Ardia A, Caputo A, Fumo R, et al. Advanced non-small cell lung cancer: rapid evaluation of EGFR status on fine-needle cytology samples using Idylla. Pathol Res Pract 2021; 224: 153547.
5. Gupta P, Gupta N, Kumar P, et al. Assessment of risk of malignancy by application of the proposed Sydney system for classification and reporting lymph node cytopathology. Cancer Cytopathol 2021; 129: 701-18.
6. Caleo A, Vigliar E, Vitale M, et al. Cytological diagnosis of thyroid nodules in Hashimoto thyroiditis in elderly patients. BMC Surg 2013; 13 Suppl 2: S41.
7. Vigliar E, Cozzolino I, Fernandez LV, et al. Fine-needle cytology and flow cytometry assessment of reactive and lymphoproliferative processes of the breast. Acta Cytol 2012; 56: 130-8.
8. Caputo A, Fraggetta F, Cretella P, et al. Digital Examination of LYmph node CYtopathology Using the Sydney system (DELYCYUS): an international, multi-institutional study. Cancer Cytopathol 2023; 131: 679-92.

 https://doi.org/10.4132/jptm.2023.11.05

JPTM
Journal of Pathology and Translational Medicine 2024; 58: 43-44
https://doi.org/10.4132/jptm.2023.12.04

LETTER TO THE EDITOR

Response to comment on "A stepwise approach to fine needle aspiration cytology of lymph nodes"

Yosep Chong[1], Gyeongsin Park[1], Hee Jeong Cha[2], Hyun-Jung Kim[3], Chang Suk Kang[4], Jamshid Abdul-Ghafar[1], Seung-Sook Lee[5]

[1]Department of Hospital Pathology, College of Medicine, The Catholic University of Korea, Seoul;
[2]Department of Pathology, Ulsan University Hospital, University of Ulsan College of Medicine, Ulsan;
[3]Department of Pathology, Inje University Sanggye Paik Hospital, Seoul;
[4]Department of Pathology, Samkwang Medical Laboratories, Seoul;
[5]Department of Pathology, Korea Institute of Radiological and Medical Sciences, Seoul, Korea

To the Editor,

We read Caputo et al.'s letter [1] regarding our recently published review, "A Stepwise Approach to Fine Needle Aspiration Cytology of Lymph Nodes," with great interest and we really appreciate to their keen observation and critique to our review [2]. Their critique of our publication focuses on three primary issues: (1) The Sydney system's strong recommendation for reporting the nosologic entity's nature (lymphoid/metastatic) [3]. (2) Our proposed stepwise system's exclusive focus on morphology, overlooking ancillary techniques like flow cytometry and polymerase chain reaction. (3) The heightened risk of malignancy in the AUS-ALUS (atypical, undermined significance–atypical lymphoid uncertain significance) category, as highlighted in Gupta et al.'s study [4], attributed mainly to the non-use of ancillary techniques.

While we align with the Sydney system's recommendation to identify the nosologic entity and integrate ancillary tests in the diagnostic process, our approach in the review was broader. In Fig. 10's diagnostic algorithm, we referenced "sufficient features for malignancy," intending to encompass all feasible test findings, including morphology, immunocytology, and molecular tests. This was not explicitly stated, but it was implied [2].

Our focus initially was on the morphological features of lymph node fine needle aspiration cytology (FNAC), acknowledging that ancillary tests are not always accessible. In Korea, for instance, excisional biopsy on lymph nodes post-FNAC is common, with most ancillary testing conducted on histologic sections. This preference stems from the rapid and cost-effective nature of excisional biopsies specifically in Korean medical environment. Korean clinicians and patients often opt for confirmatory diagnoses involving more comprehensive sample analyses.

Rapid advancements in molecular pathology have undoubtedly enhanced lymphoma understanding and treatment. However, many countries still struggle to fully incorporate these tests in cytodiagnostics and it sometimes causes subsequent confusion during the diagnostic process in the clinical practice. The study by Gupta et al. [4], also applying the Sydney system, reflects this limitation in India, as ancillary techniques were scarcely employed. Recent detailed molecular research on lymphoid neoplasms has divided the academic community, resulting in the development of two distinct classification systems on histologic diagnosis: the 5th edition of the World Health Organization classification (WHO-HAEM5) and the International Consensus Classification (ICC), which brings many confusions to the practicing pathologists in the daily practice [5]. On the other hand, the Sydney system for cytologic diagnosis, in our view, is versatile, accommodating both contexts where molecular pathology is feasible and scenarios reliant solely on morphological evaluation [3,6].

We concur with Caputo et al.'s observations [1] and aimed our review to enrich the diagnostic process, focusing on morphological details. Our comprehensive algorithm, incorporating various morphological features, seeks to streamline and improve diagnostic accuracy. In scenarios where specimen quantity limits further testing, or when additional molecular tests are impractical due to cost, infrastructure, or even sociocultural constraints,

Received: November 27, 2023 **Accepted:** December 4, 2023

Corresponding Author: Yosep Chong, MD, PhD
Department of Hospital Pathology, Uijeongbu St. Mary's Hospital, College of Medicine, The Catholic University of Korea, 271 Cheonbo-ro, Uijeongbu 11765, Korea
Tel: +82-32-820-3160, Fax: +82-32-820-3877, E-mail: ychong@catholic.ac.kr

pISSN 2383-7837
eISSN 2383-7845

our approach offers direct support to cytopathologists. Hopefully, further validation studies on the Sydney System using real cases of lymph node FNAC in Korea or Asian population should be followed for the reconfirmation of the clinical efficacy as proven in previous studies [4,6]. Looking forward, we anticipate that advancements in digital cytopathology and artificial intelligence image analysis will enhance cancer diagnosis, subtype differentiation, and molecular mutation prediction in near future, as Caputo et al. also suggested [7-9].

Ethics Statement

Not applicable.

Availability of Data and Material

The datasets generated or analyzed during the study are available from the corresponding author on reasonable request.

Code Availability

Not applicable.

ORCID

Yosep Chong https://orcid.org/0000-0001-8615-3064
Gyeongsin Park https://orcid.org/0000-0002-9727-5566
Hee Jeong Cha https://orcid.org/0000-0001-8744-5747
Hyung-Jung Kim https://orcid.org/0000-0002-6617-4578
Jamshid Abdul-Ghafar https://orcid.org/0000-0002-6575-8870

Author Contributions

Conceptualization: YC, GP, HJC, HJK, CSK, SSL. Supervision: GP, SSL. Visualization: YC. Writing—original draft: YC. Writing—review & editing: YC, GP, HJC, HJK, CSK, SSL. Approval of final manuscript: all authors.

Conflicts of Interest

Y.C., a contributing editor of the *Journal of Pathology and Translational Medicine*, was not involved in the editorial evaluation or decision to publish this article. All remaining authors have declared no conflicts of interest.

Funding Statement

No funding to declare.

References

1. Maffei E, Ciliberti V, Zeppa P, Caputo A. Comment on "A stepwise approach to fine needle aspiration cytology of lymph nodes". J Pathol Transl Med 2024; 58: 40-2.
2. Chong Y, Park G, Cha HJ, et al. A stepwise approach to fine needle aspiration cytology of lymph nodes. J Pathol Transl Med 2023; 57: 196-207.
3. Al-Abbadi MA, Barroca H, Bode-Lesniewska B, et al. A proposal for the performance, classification, and reporting of lymph node fine-needle aspiration cytopathology: the Sydney system. Acta Cytol 2020; 64: 306-22.
4. Gupta P, Gupta N, Kumar P, et al. Assessment of risk of malignancy by application of the proposed Sydney system for classification and reporting lymph node cytopathology. Cancer Cytopathol 2021; 129: 701-18.
5. Falini B, Martino G, Lazzi S. A comparison of the International Consensus and 5th World Health Organization classifications of mature B-cell lymphomas. Leukemia 2023; 37: 18-34.
6. Caputo A, Ciliberti V, D'Antonio A, et al. Real-world experience with the Sydney System on 1458 cases of lymph node fine needle aspiration cytology. Cytopathology 2022; 33: 166-75.
7. Caputo A, Fraggetta F, Cretella P, et al. Digital examination of LYmph node CYtopathology Using the Sydney system (DELYCYUS): an international, multi-institutional study. Cancer Cytopathol 2023; 131: 679-92.
8. Thakur N, Alam MR, Abdul-Ghafar J, Chong Y. Recent application of artificial intelligence in non-gynecological cancer cytopathology: a systematic review. Cancers (Basel) 2022; 14: 3529.
9. Park HS, Chong Y, Lee Y, et al. Deep learning-based computational cytopathologic diagnosis of metastatic breast carcinoma in pleural fluid. Cells 2023; 12: 1847.

JPTM
Journal of Pathology and Translational Medicine 2024; 58: 45-48
https://doi.org/10.4132/jptm.2023.12.11

NEWSLETTER

pISSN 2383-7837 / eISSN 2383-7845

PathologyOutlines.com

What's new in genitourinary pathology 2023: WHO 5th edition updates for urinary tract, prostate, testis, and penis

Bonnie Choy, MD[1], Maria Tretiakova, MD, PhD[2], Debra L. Zynger, MS, MD[3]

[1]Department of Pathology Northwestern University Feinberg School of Medicine, Chicago, IL, USA
[2]Department of Laboratory Medicine and Pathology, University of Washington, Seattle, WA, USA
[3]Department of Pathology, The Ohio State University Wexner Medical Center, Columbus, OH, USA

Received: August 15, 2023
Accepted: December 11, 2023
Corresponding Author:
Debra L. Zynger, MS, MD
Department of Pathology, The Ohio State University Wexner Medical Center, Columbus, OH, USA
E-mail: debra.zynger@osumc.edu

ORCID
Bonnie Choy
https://orcid.org/0000-0002-3670-3715
Maria Tretiakova
https://orcid.org/0000-0002-0819-9638
Debra L. Zynger
https://orcid.org/0000-0003-1038-5699

This article has been published jointly, with consent, in both Journal of Pathology and Translational Medicine and PathologyOutlines.com.

Abstract

The 5th edition WHO Classification of Urinary and Male Genital Tumours (2022) introduced many significant changes relevant to urologic daily practice, mainly to renal tumors which was covered in the What's New newsletter in September 2022. In this newsletter, we summarize the notable changes to bladder, prostate, testis, and penis based on the 5th edition of the WHO.

URINARY TRACT

Inverted urothelial papilloma

- This is reserved for almost exclusively inverted lesions and continues to be in a separate section.
- Use of the descriptor "inverted" in other papillary tumors with inverted histology (non-invasive papillary urothelial carcinoma and papillary urothelial neoplasm of low malignant potential) is discussed within each respective section in the WHO.

Non-invasive papillary urothelial carcinoma, low-grade

- Papillary urothelial hyperplasia and urothelial proliferation with undetermined malignant potential (tented architecture with short, non-branching papillae covered by mildly atypical urothelium) are no longer regarded as distinct entities but are considered **early** low-grade non-invasive papillary carcinoma.

Non-invasive papillary urothelial carcinoma, high-grade

- To address grade heterogeneity, there are now new proposed criteria for reporting papillary tumors.
  - A tumor with ≥ 5% high-grade component is diagnosed as "high-grade".
  - A tumor with < 5% high-grade component is diagnosed as "**low-grade with < 5% high-grade component**".

Urothelial carcinoma in situ

- Urothelial dysplasia is no longer discussed in its own section but continues to be used as a diagnostic term for lesions that fall short of carcinoma in situ, despite the lack of reproducible criteria.

Invasive urothelial carcinoma

- Presence of *TERT* promoter mutations can help to: 1) distinguish urothelial carcinoma from a non-neoplastic proliferative process and 2) establish urothelial origin.
- Advanced urothelial carcinoma with *FGFR3* alterations may be eligible for treatment with anti-FGFR agents, while mutations in *ERCC2* and other DNA damage repair genes may determine those likely to benefit from cisplatin-based chemotherapy.
- Predictors of response to immune checkpoint inhibitors include PDL1 expression in tumor and host immune cells, tumor mutation burden, and microsatellite instability/mismatch repair defect status.
- Terminology is standardized to charac-

terize genetic alterations as "variants," distinct morphologies as "histologic patterns," and unique morphologies with prognostic significance as tumor "subtypes."
- Muscle-invasive bladder carcinoma is divided into 6 molecular subgroups with differing prognosis: luminal-papillary (24%), luminal non-specified (8%), luminal-unstable (15%), stroma-rich (15%), basal-squamous (35%), and neuroendocrine-like (3%).

PROSTATE

Prostatic intraepithelial neoplasia

- Low-grade prostatic intraepithelial neoplasia has no increased risk of cancer detection and it is not possible to reliably differentiate from benign glandular hyperplasia; thus it was removed as a reportable entity.

Intraductal carcinoma of the prostate (IDC-P)

- The cribriform growth pattern of high-grade prostatic intraepithelial neoplasia (HGPIN) is no longer regarded as a distinct entity but rather a spectrum of intraductal proliferation that falls between HGPIN and IDC-P; it is increasingly being referred to as **atypical intraductal proliferation** (AIP), although there is no consensus on the best terminology.
- IDC-P may represent two distinct entities: 1) the majority are late events associated with invasive high-grade carcinoma spreading into non-neoplastic prostatic ducts and acini and 2) a small subset which arises from a HGPIN precursor and may represent carcinoma in situ.
- The presence of IDC-P should be reported but whether to incorporate areas of IDC-P into Gleason grading remains controversial, with diverging recommendations by leading societies.

Prostatic acinar adenocarcinoma

- **PIN-like carcinoma** is now discussed as a subtype of acinar adenocarcinoma (Fig. 1). It generally has favorable behavior and has the recent distinctive molecular finding of frequent activating mutations in the RAF/RAS pathway.
- Prostate cancers harboring homologous recombination repair defects may respond to poly (ADP-ribose) polymerase (PARP) inhibition, while those with mismatch repair defects may respond to immune checkpoint inhibitors.

Adenoid cystic (basal cell) carcinoma of the prostate

- Adenoid cystic carcinoma of the prostate is now the preferred diagnostic term, renamed from basal cell carcinoma, to avoid confusion with the skin tumor.

TESTIS

Noninvasive germ cell neoplasia

- Gonadoblastoma has been moved from the category called "tumor containing both germ cell and sex cord-stromal elements" into the category "noninvasive germ cell neoplasia".

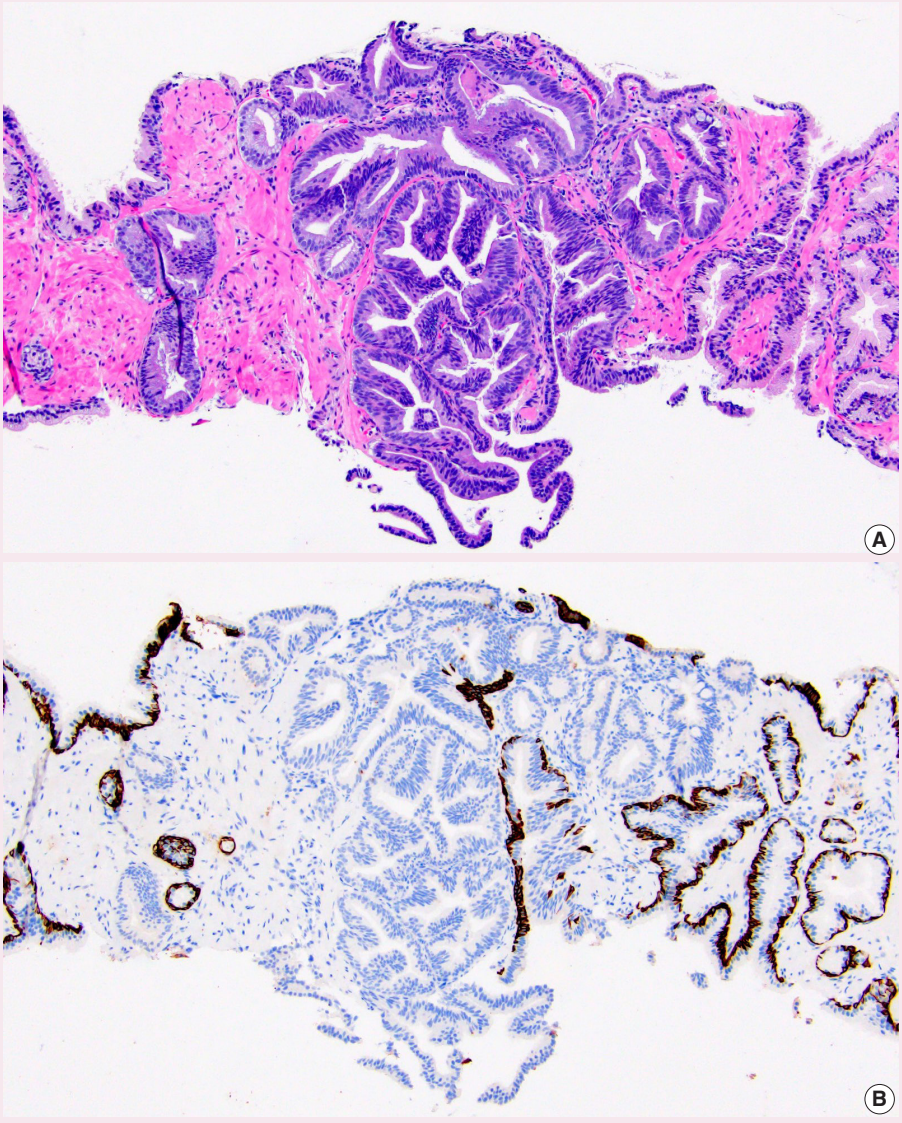

Fig. 1. PIN-like prostatic adenocarcinoma. A. It is comprised of large discrete glands with flat or tufted pseudostratified epithelium. B. Immunostaining with HMWCK highlights lack of basal cells in PIN-like carcinoma focus.

Germ cell tumors derived from germ cell neoplasia in situ

- Teratoma is regarded as containing a somatic-type malignancy if the component that resembles a neoplasm has overgrowth of at least a 5 mm focus (consistent with the previous definition of 1 field at 4x magnification).
- Somatic malignancy composed of immature neuroectoderm was formerly referred to as primitive neuroectodermal tumor (PNET) but has been renamed to **teratoma with embryonic-type neuroectodermal tumor** (Fig. 2). This helps avoid confusion with the unrelated tumor, Ewing sarcoma.

Germ cell tumors unrelated to germ cell neoplasia in situ

- Well-differentiated neuroendocrine tumor is renamed testicular neuroendocrine tumor, prepubertal-type.

Sex cord stromal tumors

- The recently proposed Leydig cell tumor Scaled Score (LeSS), in which Leydig cell tumor is classified as high or low risk based on size, mitoses, necrosis, infiltrative pattern, and vascular invasion, is mentioned in the WHO but is noted to require further validation (Fig. 3).
- Leydig cell tumor can be FH deficient and this may merit FH testing, particularly in high risk tumors in which mutations may occur more frequently.
- Sertoliform cystadenoma of the rete testis has been moved from being classified as an adenoma within the tumors of the collecting duct and rete testis, to being a part of Sertoli cell tumor.
- The signet ring pattern of Sertoli cell tumor is now listed as a separate tumor called **signet ring stromal tumor** (Fig. 4). It is composed of signet ring cells which do not contain mucin, is positive for vimentin and β-catenin, and is negative for inhibin. These tumors appear to have indolent behavior.
- **Myoid gonadal stromal tumor** has been changed from a provisional entity to a confirmed entity. This tumor features densely packed, bland spindle cells positive for SMA and S100. Reported tumors have indolent behavior.

Paratesticular mesothelial tumors

- Well-differentiated papillary mesothelioma is renamed to well-differentiated papillary mesothelial tumor.

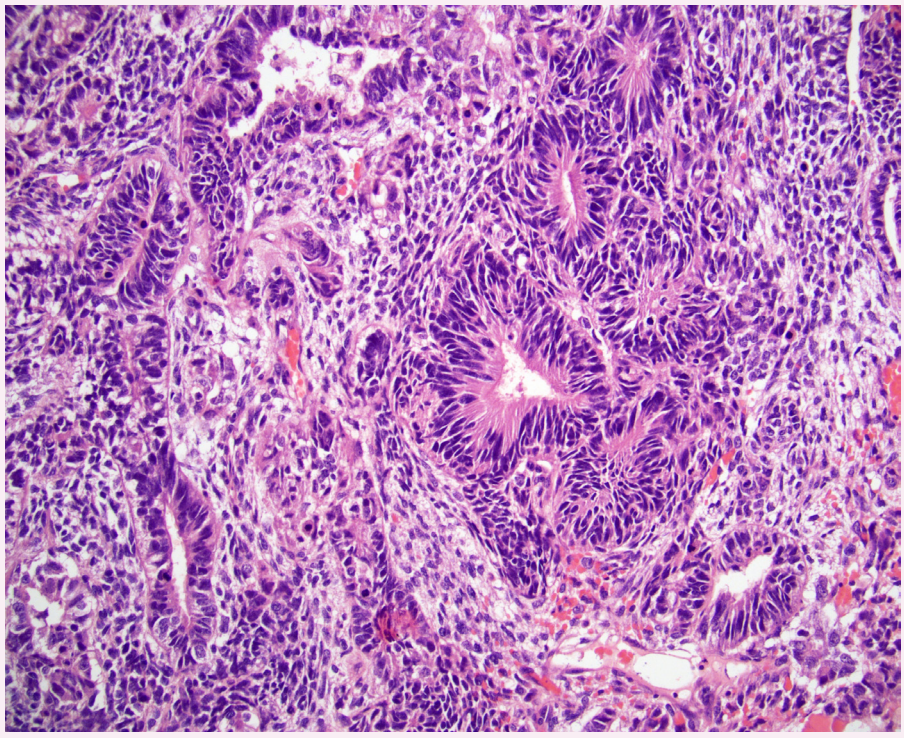

Fig. 2. Teratoma with embryonic-type neuroectodermal tumor. The area with exclusive somatic malignancy spanned over 3 cm.

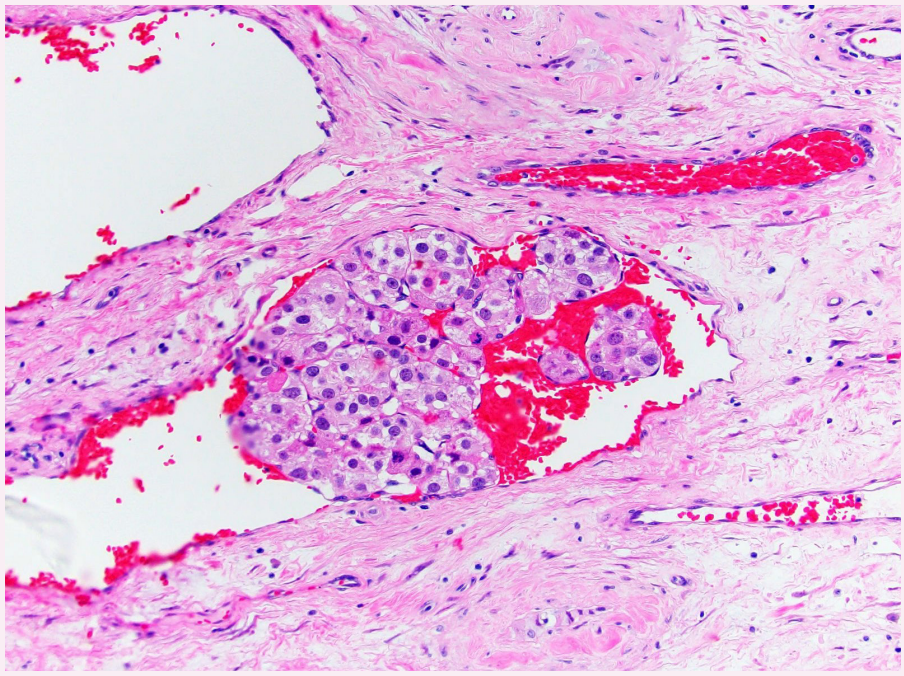

Fig. 3. Leydig cell tumor with lymphovascular invasion, categorized as high risk by LeSS.

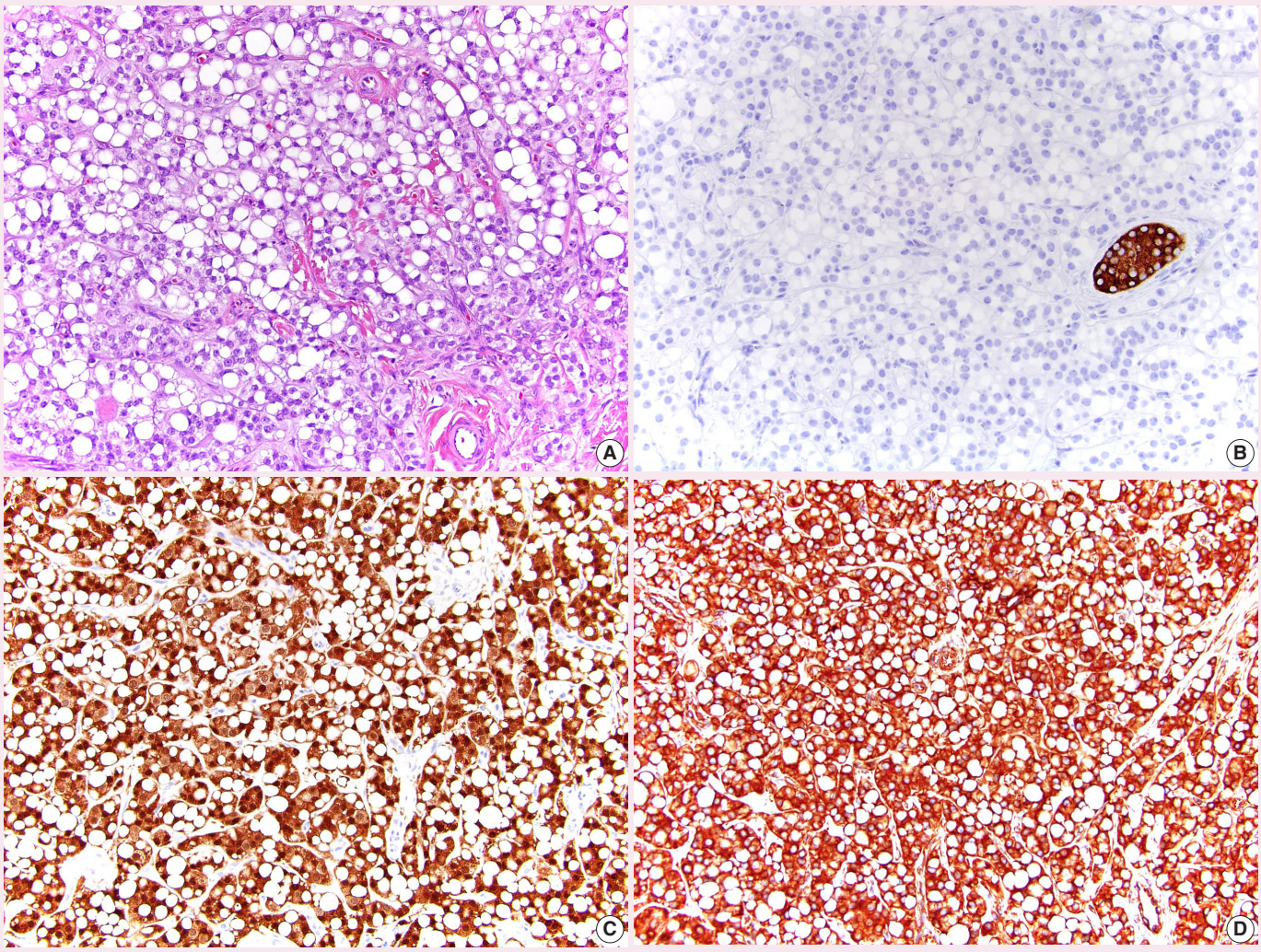

Fig. 4. Signet ring stromal tumor. A. The tumor has large cytoplasmic vacuoles. B. Inhibin is negative. C. β-catenin has diffuse nuclear and cytoplasmic expression. D. Vimentin is diffusely positive.

PENIS

- The terminology for squamous cell carcinoma groupings has been changed from non-HPV-related to HPV-independent and from HPV-related to HPV-associated.
- Papillary basaloid carcinoma, warty basaloid carcinoma, pseudohyperplastic carcinoma, pseudoglandular carcinoma, carcinoma cuniculatum, and mixed squamous cell carcinoma have been removed as distinct subtypes.
- Pseudohyperplastic and pseudoglandular patterns are now a part of squamous cell carcinoma, usual type.
- Carcinoma cuniculatum pattern is now a part of verrucous carcinoma.

Meet the Authors

Dr. Choy has been an author for PathologyOutlines since 2020 and a part of the editorial board since 2021 as the Prostate and Cytopathology subspecialty section editor. She is currently an Assistant Professor and Associate Program Director of the Pathology Residency and Cytopathology Fellowship at Northwestern University where she practices GU Pathology and Cytopathology.

Dr. Tretiakova has been an author for PathologyOutlines since 2015, part of the PathologyOutlines editorial board since 2019, and Deputy Editor in Chief for GU Pathology since 2021. She is currently a Professor and Director of the GU Fellowship and Immunohistochemistry Laboratories at the University of Washington where she primarily practices GU Pathology.

Dr. Zynger has been an author for PathologyOutlines since 2013, a part of the editorial board since 2013, and is the subspecialty section editor for Adrenal, Penis, and Testis. She is currently a Professor and Director of Urologic Pathology at The Ohio State University where she primarily practices GU Pathology.